AD-A185 129 FINAL REPORT ON CONTRACT F49620-85-C-0026 VOLUME 1(U) 1/1
PRINCETON UNIV NJ DEPT OF MECHANICAL AND AEROSPACE
ENGINEERING S A ORSZAG MAY 87 AFOSR-TR-87-1349-VOL-1
UNCLASSIFIED F49620-85-C-0026 F/G 20/4 NL

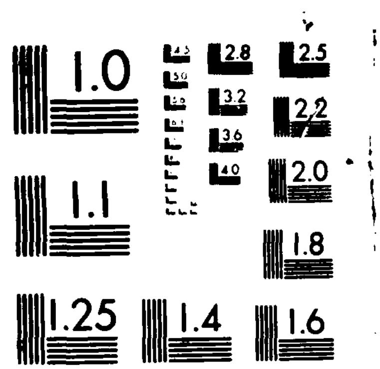

MICROCOPY RESOLUTION TEST CHART
NATIONAL BUREAU OF STANDARDS 1963 A

FINAL REPORT ON
AFOSR CONTRACT F49620-85-C-0026

Steven A. Orszag, Principal Investigator
Department of Mechanical and Aerospace Engineering
Princeton University
Princeton, NJ 08544

Volume 1

DEI SVB NVMINE VIGET

PRINCETON UNIVERSITY

UNCLASSIFIED

SECURITY CLASSIFICATION OF THIS PAGE

REPORT DOCUMENTATION PAGE

1a. REPORT SECURITY CLASSIFICATION: Unclassified	1b. RESTRICTIVE MARKINGS
2a. SECURITY CLASSIFICATION AUTHORITY	3. DISTRIBUTION/AVAILABILITY OF REPORT: Approved for Public Release; distribution is unlimited
2b. DECLASSIFICATION/DOWNGRADING SCHEDULE	
4. PERFORMING ORGANIZATION REPORT NUMBER(S)	5. MONITORING ORGANIZATION REPORT NUMBER(S): AFOSR-TR- 87-1340
6a. NAME OF PERFORMING ORGANIZATION: Princeton University; 6b. OFFICE SYMBOL (If applicable)	7a. NAME OF MONITORING ORGANIZATION: AFOSR/NA
6c. ADDRESS (City, State and ZIP Code): Princeton University, Princeton, NJ 08544	7b. ADDRESS (City, State and ZIP Code): Building 410 Bolling AFB DC 20332-6448
8a. NAME OF FUNDING/SPONSORING ORGANIZATION: AFOSR/NA; 8b. OFFICE SYMBOL (If applicable)	9. PROCUREMENT INSTRUMENT IDENTIFICATION NUMBER: F49620-85-C-0026
8c. ADDRESS (City, State and ZIP Code): BK1410 Bolling Air Force Base, Washington, DC 20332-6448	10. SOURCE OF FUNDING NOS.: PROGRAM ELEMENT NO. 61102F; PROJECT NO. 2307; TASK NO. A2; WORK UNIT NO.
11. TITLE (Include Security Classification): Final Report on Contract F49620-85-C-0026 Vol. I	
12. PERSONAL AUTHOR(S): Steven A. Orszag	
13a. TYPE OF REPORT: Final Report; 13b. TIME COVERED: FROM 10/1/84 TO 11/30/86	14. DATE OF REPORT (Yr., Mo., Day): May, 1987; 15. PAGE COUNT
16. SUPPLEMENTARY NOTATION	
17. COSATI CODES: FIELD / GROUP / SUB. GR.	18. SUBJECT TERMS (Continue on reverse if necessary and identify by block number): Turbulence, Numerical Simulation

19. ABSTRACT (Continue on reverse if necessary and identify by block number)

This report consists of papers that summarize work done on this research project. The major results include: 1) The development and application of the renormalization group method to the calculation of fundamental constants of turbulence, the construction of turbulence transport models, and large-eddy simulations; 2) The application of RNG methods to turbulent heat transfer through the entire range of experimentally accessible Reynolds numbers; 3) The discovery that high Reynolds number turbulent flows tend to act as if they had weak nonlinearities, at least when viewed in terms of suitable 'quasi-particles'; 4) The further analysis of secondary instability mechanisms in free shear flows, including the role of these instabilities in chaotic, 3-D free shear flows; 5) The further development of numerical simulations of turbulent spots in wall bounded shear flows; 6) The study of cellular automata for the solution of fluid mechanical problems; 7) The clarification of the relationship between the hyperscale instability of anisotropic small-scale flow structures to long-wavelength perturbations and the cellular automaton description →

20. DISTRIBUTION/AVAILABILITY OF ABSTRACT: UNCLASSIFIED/UNLIMITED ☒ SAME AS RPT. ☒ DTIC USERS ☐	21. ABSTRACT SECURITY CLASSIFICATION: Unclassified
22a. NAME OF RESPONSIBLE INDIVIDUAL: Dr James M McMichael	22b. TELEPHONE NUMBER (Include Area Code): (202) 767-4936; 22c. OFFICE SYMBOL: AFOSR/NA

DD FORM 1473, 83 APR — EDITION OF 1 JAN 73 IS OBSOLETE.

SECURITY CLASSIFICATION OF THIS PAGE

UNCLASSIFIED

ABSTRACT, continued from other side

of fluids; 8) The development of efficient methods to analyze the structure of strange attractors in the description of dynamical systems; 9) The analysis of hyperscale instability as a mechanism for destabilization of coherent flow structures.

2

FINAL REPORT ON
~~AFOSR~~ CONTRACT F49620-85-C-0026

Steven A. Orszag, Principal Investigator
Department of Mechanical and Aerospace Engineering
Princeton University
Princeton, NJ 08544

Volume 1

FINAL REPORT ON AFOSR CONTRACT F49620-85-C-0026

Steven A. Orszag, Principal Investigator
Department of Mechanical and Aerospace Engineering
Princeton University
Princeton, NJ 08544

In the attached papers, we summarize work done on this research project. The major results include:

1. Development and application of the renormalization group method to the calculation of fundamental constants of turbulence, the construction of turbulence transport models, and large-eddy simulations.

2. The application of RNG methods to turbulent heat transfer through the entire range of experimentally accessible Reynolds numbers.

3. The discovery that high Reynolds number turbulent flows tend to act as if they had weak nonlinearities, at least when viewed in terms of suitable 'quasi-particles.' This discovery suggests that turbulence acts as if there were a significant scale separation in the flows, even though turbulence does not appear to have such scale separation. These ideas seem to provide some justification for eddy transport ideas that have proven so useful in engineering descriptions of turbulence.

4. The further analysis of secondary instability mechanisms in free shear flows, including the role of these instabilities in chaotic, three-dimensional free shear flows.

5. The further development of numerical simulations of turbulent spots in wall bounded shear flows.

6. The study of cellular automata for the solution of fluid mechanical problems. In particular, a realistic assessment of the utility of these new methods for complex high Reynolds number flow problems has been given.

7. The clarification of the relationship between the hyperscale instability of anisotropic small-scale flow structures to long-wavelength perturbations and the cellular automaton description of fluids.

8. The development of efficient methods to analyze the structure of strange attractors in the description of dynamical systems. This includes both the computation of Lyapunov exponents and the computation of dimensions of attractors.

9. The analysis of hyperscale instability as a mechanism for destabilization of coherent flow structures.

Further details are given in the attached papers.

List of Papers

Analogy between Hyperscale Transport and Cellular Automaton Hydrodynamics, Phys. Fluids 29, 2025-2027 (1986).

S.A. Orszag, R.B. Pelz and B.J. Bayly, Secondary Instabilities, Coherent Structures and Turbulence, in Supercomputers and Fluid Dynamics, (ed. by K. Kuwahara, R. Mendez, S. A. Orszag), Springer (1986).

S.A. Orszag and V. Yakhot, Reynolds Number Scaling of Cellular Automaton Hydrodynamics, Phys. Rev. Lett. 56, 1693-1696 (1986).

V. Yakhot and S.A. Orszag, Renormalization Group Analysis of Turbulence. I. Basic Theory. J. Sci. Comp. 1, 3-51 (1986).

V. Yakhot and S.A. Orszag, Renormalization Group Analysis of Turbulence. Phys. Rev. Lett. 57 14, 1722-1724 (1986).

V. Yakhot, S.A. Orszag, and A. Yakhot, Heat Transfer in Turbulent Fluids. I. Pipe Flow. Intl. J. Heat and Mass Transfer 30, 15 (1987).

E.T. Bullister and S.A. Orszag, Numerical Simulation of Turbulent Spots in Channel and Boundary Layer Flows. J. Sci. Comp., in press.

R.W. Metcalfe, S.A. Orszag, M.E. Brachet, S. Menon, and J.J. Riley, Secondary Instability of a Temporally Growing Mixing Layer. J. Fluid Mech., in press.

V. Yakhot, S.A. Orszag, A. Yakhot, R. Panda, U. Frisch, and R.H. Kraichnan, Weak Interactions and Local Order in Strong Turbulence, Phys. Rev. Let. (1986) submitted.

V. Yakhot and S.A. Orszag, Relation Between the Kolmogorov and Batchelor Constants, Phys. Fluids **30**, 3 (1986).

I. Goldhirsch, S.A. Orszag, and B.K. Maulik, An Efficient Method for Computing Leading Eigenvalues and Eigenvectors of Large Asymmetric Matrices, J. Sci. Comp., in press (1987).

M.E. Brachet, R.W. Metcalfe, S.A. Orszag and J.J. Riley, Secondary Instability of Free Shear Flows. In Progress and Supercomputing in Computational Fluid Dynamics, (ed. by E. M. Murman and S. S. Abarbanel), Birkhauser, Boston, 1985.

B.J. Bayly and V. Yakhot, Positive- and Negative-Effective-Viscosity Phenomena in Isotropic and Anisotropic Beltrami Flows, Phys. Rev. **A34**, 381 (1986).

The purpose of this Letters section is to provide rapid dissemination of important new results in the fields regularly covered by The Physics of Fluids. Results of extended research should not be presented as a series of letters in place of comprehensive articles. Letters cannot exceed four printed pages in length, including space allowed for title, figures, tables, references and an abstract limited to about 100 words.

Analogy between hyperscale transport and cellular automaton fluid dynamics

Victor Yakhot, Bruce J. Bayly, and Steven A. Orszag
Applied and Computational Mathematics, Princeton University, Princeton, New Jersey 08544

(Received 24 February 1986; accepted 16 April 1986)

It is argued that the dynamics of a very large scale (hyperscale) flow superposed on the stationary small-scale flow maintained by a force $\mathbf{f}(\mathbf{x})$ is analogous to the cellular automaton hydrodynamics on a lattice having the same spatial symmetry as the force $\mathbf{f}$.

While real fluids consist of discrete particles, they can be regarded as continuous media at scales that are much larger than the typical intermolecular distance, and, on these scales, they can be described by the equations of continuum hydrodynamics. These equations are quite insensitive to the details of the molecular dynamics; the microscopic interactions affect only the viscosity coefficient. Microscopically dissimilar fluids can be described by the Navier–Stokes equations, although the microscopic properties of different fluids may be reflected in a very wide range of viscosity coefficients.

The lack of dependence of the hydrodynamics on the microscopic properties of the fluids is the basis for the recent interest in discrete approximations to molecular dynamics or Cellular automata (CA's).[1-4] Cellular automata are discretely and locally linked, finite state machines. The "molecules" in a CA fluid move in discrete steps over the lattice sites and interact according to a well defined set of rules that typically conserve momentum and the total number of particles. The hydrodynamic behavior of the CA fluid is given by the evolution of the average macroscopic properties of the system ("slow" modes). Some limitations of CA hydrodynamics have been discussed in Ref. 5.

The first lattice model of a fluid was introduced by Hardy, de Passis, and Pomeau (HPP).[1] Recently, new models, which are modifications of the HPP ideas, have led to simulations of two-dimensional fluid motions that appear to be compatible with experimental data.[2-4] Hydrodynamic equations for such a CA fluid can be derived using techniques based on the Chapman–Enskog expansion, as in the kinetic theory of gases. It has been found that the form of the continuum equations for a given CA fluid depends strongly on the symmetry properties of the lattice. In particular, the HPP lattice gas model based on the two-dimensional square lattice leads to anisotropic viscosity and anisotropic nonlinear terms in the resulting continuum dynamics. However, a regular hexagonal lattice, again in two dimensions, introduced by Frisch, Hasslacher, and Pomeau[2] is symmetric enough to produce the Navier–Stokes equations with isotropic viscosity and nonlinear terms. It has been pointed out by Wolfram[6] that in three dimensions none of the space-filling crystallographic lattices have sufficient symmetry to guarantee the isotropy of the corresonding hydrodynamic equations. However, icosahedral symmetry would produce isotropic viscosity and nonlinear terms.[6] Unfortunately, no periodic lattice has such symmetry (with the possible exception of some recently conjectured quasicrystal structures).[7]

Hydrodynamic equations are derived from the microscopic equations of motion by averaging over small scales. It is natural to pose the following problem: Let us consider a viscous fluid driven by a force which generates a stationary field v^l on the small-scale l. The equation of motion for the perturbation v^L defined on scales L which are much larger than the scale l of the basic flow can be derived by averaging over the small-scale velocity field v^l. The resulting equations describe *hyperscale hydrodynamics*. To see that this problem arises quite naturally, let us imagine a system of microscopic particles driven by an external force $\mathbf{f}$. The molecules participate in two kinds of motion, one related to thermodynamic noise and the other caused by the external force. Filtering out the smallest (thermodynamic) scales, one derives the Navier–Stokes equation subject to the external force. If we also average over the scales corresponding to the force $\mathbf{f}$, the resulting equation will not necessarily be the Navier–Stokes equation, but will rather be an equation describing the large-scale (hyperscale) motion that does not explicitly include the external force.

Some examples of hyperscale dynamics have been considered in Ref. 8. It has been shown that a system of square vortices (eddies) gives rise to the equation of motion for the velocity perturbation at large scales with an anisotropic viscosity:

$$\nu_\phi = \nu(1 + \tfrac{3}{8}\,\mathrm{Re}^2 - \tfrac{1}{2}\,\mathrm{Re}^2 \sin 2\phi), \tag{1}$$

where ν_ϕ is the effective viscosity in the direction $(\cos\phi, \sin\phi)$. In this and all subsequent equations, Re denotes the Reynolds number of the small-scale flow; the formulas quoted are the lowest-order nontrivial results of a hierarchy of successive smoothing approximations.[8] A plane parallel system of eddies also leads to an anisotropic viscosity.[8] How-

 0031-9171/86/072025-03$01.90

ever, a system of triangular vortices having hexagonal symmetry (invariance under rotation by 60°) generates an isotropic viscosity coefficient for the hyperscale motion:

$$\nu_1 = \nu(1 + \tfrac{3}{4}\,\mathrm{Re}^2). \tag{2}$$

The analogy with cellular automata is striking: in two dimensions only the triangular lattice and triangular set of vortices produce an isotropic equation for the large-scale velocity fluctuations. Moreover, it has been shown by Sivashinsky[10] that hyperscale hydrodynamics is not Galilean invariant because the averaged Navier–Stokes equation with the forcing term is not. The same holds for the CA hydrodynamics: It has been pointed out[2] that the continuum equations following from cellular automaton models are not Galilean invariant as a result of the discrete lattice underlying the model.

The dynamics of hyperscale flows superposed on small-scale flows in three dimensions have been studied in Refs. 9 and 11. The analogs of steady cellular flows in two dimensions are the family of so-called Beltrami flows in three dimensions, defined by finite Fourier sums of the form

$$\mathbf{v}(\mathbf{x}) = \sum_{\mathbf{Q}\in S} A(\mathbf{Q})(\mathbf{n} + i\mathbf{Q}\times\mathbf{n})e^{i\mathbf{Q}\cdot\mathbf{x}/l}. \tag{3}$$

Here S is a finite set of unit-magnitude vectors $\mathbf{Q}$, $\mathbf{n}$ is a unit vector perpendicular to $\mathbf{Q}$, and the complex amplitudes $A(\mathbf{Q})$ satisfy the reality condition $A(-\mathbf{Q}) = A^*(\mathbf{Q})$. These flows, like two-dimensional cellular flows, are exact steady solutions of the inviscid fluid equations, and can be maintained in viscous fluid by the action of an externally imposed body force.

The form of the equation of motion for hyperscale flow on the small-scale flow (3) involves the fourth-rank tensor[9,11]

$$N_{ijkl} = \sum_{\mathbf{Q}\in S} |A(\mathbf{Q})|^2(\delta_{ik}\delta_{jl} - 2\delta_{ik}Q_jQ_l - \delta_{jl}Q_iQ_k - 2\delta_{ij}Q_kQ_l + 4Q_iQ_jQ_kQ_l),$$

which is isotropic only if

$$\sum_{\mathbf{Q}\in S} |A(\mathbf{Q})|^2 Q_iQ_j = \lambda\delta_{ij},$$

$$\sum_{\mathbf{Q}\in S} |A(\mathbf{Q})|^2 Q_iQ_jQ_kQ_l = \mu(\delta_{ij}\delta_{kl} + \delta_{il}\delta_{kj} + \delta_{ik}\delta_{jl}),$$

for some constants λ and μ. Clearly, the more vectors $\mathbf{Q}$ we have in S, the better our chances of being able to select amplitudes $A(\mathbf{Q})$ of the corresponding components so as to obtain an isotropic tensor N. We shall give some examples to illustrate the connection between the underlying small-scale flow structures and the resulting hyperscale dynamics.

The simplest Beltrami flow in the family (3) has only two Fourier components with the wave vectors $\pm\mathbf{Q}_0 = (\pm 1,0,0)$ and amplitudes $A(\pm\mathbf{Q}_0) = c/2$; $\mathbf{v}' = c\,(0, \cos x/l, -\sin x/l)$. A hyperscale perturbation with the wave vector $(0,k,0)$ then obeys the equation of motion

$$\dot v_1 = -\nu k^2(1 - \tfrac{1}{2}\mathrm{Re}^2)v_1, \quad \dot v_2 \equiv 0,$$

$$\dot v_3 = -\nu k^2(1 + \tfrac{1}{2}\mathrm{Re}^2)v_3.$$

The effective viscosity for the v_1 component is negative, and the hyperscale flow is therefore unstable, if the small-scale Reynolds number $\mathrm{Re} \equiv cl/\nu$ exceeds $\sqrt{2}$.

The so-called ABC flow is obtained when S consists of six wave vectors located at the vertices of an octahedron:

$$S = \{\mathbf{Q}\} = \left\{\begin{pmatrix}\pm 1\\0\\0\end{pmatrix}\begin{pmatrix}0\\\pm 1\\0\end{pmatrix}\begin{pmatrix}0\\0\\\pm 1\end{pmatrix}\right\}, \tag{4}$$

with all amplitudes having the same modulus $|A(\mathbf{Q})| = c/\sqrt{12}$, where c is again the rms fluid velocity. Now the hyperscale equation takes the form

$$\frac{\partial}{\partial t}v_a = -\nu k^2[\delta_{ab} + \mathrm{Re}^2 M_{ab}(\hat{\mathbf{k}})]v_b,$$

where M is a matrix that depends only on the unit vector $\hat{\mathbf{k}}$ in the direction of $\mathbf{k}$. The eigenvalues of M are all greater than or equal to zero, with equality occurring only if $\hat{\mathbf{k}}$ lies in one of the coordinate planes. The hyperscale flow is therefore stable although still somewhat anisotropic.

A more complex flow with similar structure to the ABC flow can be obtained by augmenting the wave vector set by

$$S^1 = \left\{\begin{pmatrix}\pm\frac{2}{3}\\[2pt]\pm\frac{2}{3}\\[2pt]\pm\frac{1}{3}\end{pmatrix}\begin{pmatrix}\pm\frac{1}{3}\\[2pt]\pm\frac{2}{3}\\[2pt]\pm\frac{2}{3}\end{pmatrix}\begin{pmatrix}\pm\frac{2}{3}\\[2pt]\pm\frac{1}{3}\\[2pt]\pm\frac{2}{3}\end{pmatrix}\right\} \tag{5}$$

and assigning the corresponding Fourier modes amplitudes $A(\mathbf{Q}) = \lambda(c/\sqrt{12})$, $\mathbf{Q}\in S^1$. Here λ is a parameter: setting $\lambda = 0$ recovers the ABC flow with its anisotropic equation of motion, but if λ is raised to the special value of $9/(156)^{1/2}$ then the conditions for isotropy of the tensor N_{ijkl} are satisfied, and we obtain an isotropic equation of motion for the hyperscale modes. This example illustrates the fact that a small-scale flow can be constructed to have different large-scale properties from a discrete lattice gas with the same spatial symmetry group.

Going on to more and more symmetric flows, it turns out that *icosahedral* or *dodecahedral* symmetry in the small-scale flow gives exact isotropy to the hyperscale dynamics. For example, the wave vector set for the icosahedral flow is

$$S = \left\{\frac{1}{s}\begin{pmatrix}\pm 1\\\pm\tau\\0\end{pmatrix},\ \frac{1}{s}\begin{pmatrix}0\\\pm 1\\\pm\tau\end{pmatrix},\ \frac{1}{s}\begin{pmatrix}\pm\tau\\0\\\pm 1\end{pmatrix}\right\}, \tag{6}$$

where τ is the golden ratio $(1+\sqrt{5})/2$ and $s = (5+\sqrt{5})/2$. It is easily checked that the tensor N_{ijkl} is isotropic for this flow, provided that the amplitudes of the modes are all chosen equal. The hyperscale properties of the icosahedral flow appear to be indistinguishable from those of the exactly isotropic flow obtained as the limiting case of flows with more and more Fourier components distributed uniformly on the unit sphere.

It is interesting to observe that not only does the momentum equation for the hyperscale modes take the classical form, but so does the hyperscale diffusion equation. The tensor that enters the correction for the effective diffusivity in

the lowest smoothing approximation[8,9] is the sum of the "projection tensors"

$$T_{ij} = \sum_{Q \in S} (\delta_{ij} - Q_i Q_j),$$

which is isotropic for all the aforementioned flows except the simple flow with only two Fourier components. Indeed, it has been demonstrated independently of the smoothing theory that a passive contaminant disperses diffusively in the icosahedral and augmented cubic flows. Simulations of particle dispersion in these flows demonstrate that, for large times, almost all particles migrate away from their starting point with a finite effective diffusivity.

The analogy between the CA and hyperscale hydrodynamic descriptions of the fluids goes even further. The equations for the large-scale velocity field derived in Refs. 7–10 are based on the neglect of the higher-order nonlinear terms generated by the scale elimination procedure and thus they are valid when the ratio $v^L \ll v^l$. The same holds for the CA hydrodynamics:[2] the Navier–Stokes equation is an approximation valid only when the Mach number $\mathrm{Ma} = v/v_{th} \ll 1$, where v_{th} is the velocity of the particles on the lattice.

Based on the analogy between hyperscale hydrodynamics and the CA description of the fluids, we argue that lattice gas models are equivalent to the Navier–Stokes equation with an external force having the symmetry of the lattice.

[1] J. Hardy, O. de Pazzis, and Y. Pomeau, Phys. Rev. A 13, 1949 (1976).
[2] U. Frisch, B. Hasslacher, and Y. Pomeau, Phys. Rev. Lett. 56, 1505 (1986).
[3] S. Wolfram, submitted to Phys. Rev. Lett.
[4] D. d'Humieres, Y. Pomeau, and P. Lallemand, Mech. Fluids (in press).
[5] S. A. Orszag and V. Yakhot, Phys. Rev. Lett. 56, 1693 (1986).
[6] S. Wolfram (private communication).
[7] d'Humieres, Lallemand, and Frisch have recently observed that the 3-D projection of the 4-D Bravais 24-hedral lattice leads to isotropic 3-D fluid dynamics at low Mach numbers.
[8] G. Sivashinsky and V. Yakhot, Phys. Fluids 28, 1040 (1985).
[9] B. Bayly and V. Yakhot, submitted to Phys. Rev. A.
[10] G. Sivashinsky, Physica D 17, 243 (1985).
[11] V. Yakhot and G. Sivashinsky, submitted to Phys. Fluids.

Long waves in a canal with a porous plate located at a step

Peder A. Tyvand
Department of Physics and Meteorology, Agricultural University of Norway, N-1432 Aas-NLH, Norway

(Received 19 February 1986; accepted 10 April 1986)

A linear shallow water theory of waves in a canal is considered. The energy dissipated by a porous plate located at a step where both the depth and width of the canal changes abruptly is calculated. It is found that a broadening of the canal, combined with a plate with optimal properties, is an efficient way of dissipating wave energy. It is also possible to have a strong wave damping without any reflection.

Lamb[1] gave the reflection and transmission coefficients for long waves at a step in a canal. Both the width and depth of the canal may change abruptly at the step. The detailed analysis of Bartholomeusz[2] verified that Lamb's solution is correct to the leading order in a long-wave expansion (see also Mei[3]). We will generalize Lamb's solution to the case of a thin porous plate located at the step, and discuss the dissipation of wave energy. Thereby the recent work of Chwang and Dong[4] is extended.

We consider a straight horizontal canal of uniform depth h_1 and width b_1 for $x < 0$, where x is a coordinate along the canal. For $x > 0$ the depth is h_2 and the width b_2. At the step ($x = 0$) there is a thin vertical porous plate of thickness d and permeability K. The kinematic viscosity of the fluid is ν, but the flow outside the plate is assumed inviscid. The flow inside the porous plate is assumed to be governed by Darcy's law, which may be stated as

$$u = (Kg/\nu d)(y_1 - y_2), \qquad (1)$$

valid in the long-wave limit. Here g is the gravitational acceleration, y_1 and y_2 are the surface elevations on each side of the plate, and u is the average horizontal velocity in the section covered by the plate:

$$\begin{aligned} u &= u_1 / \min(1, b_2/b_1)\min(1, h_2/h_1) \\ &= u_2 \times \min(b_1/b_2, 1)\min(h_1/h_2, 1)\,. \end{aligned} \qquad (2)$$

Here u_1 and u_2 are the average horizontal velocities next to the plate, for $x < 0$ and $x > 0$, respectively.

Following Lamb,[1] we calculate the transmission coefficient T_1 and the reflection coefficient R_1 for waves incident from $x < 0$:

$$T_1 = 2/(G^{-1} + 1 + r)\,, \qquad (3)$$

$$R_1 = (G^{-1} + 1 - r)/(G^{-1} + 1 + r)\,. \qquad (4)$$

In Eqs. (3) and (4) we have introduced the dimensionless parameters

$$G = (K/\nu d)c_2 \min(b_1/b_2, 1)\min(h_1/h_2, 1) \qquad (5)$$

SECONDARY INSTABILITIES, COHERENT STRUCTURES AND TURBULENCE

Steven A. Orszag, Richard B. Pelz and Bruce J. Bayly
Applied and Computational Mathematics
Princeton University, Princeton, 08544

Abstract

In this paper, we review recent progress on several problems of transition and t bulence. First, we explore the role of secondary instabilities in transition to turbulence both wall bounded and free shear flows. It is shown how the competition between second instabilities and classical inviscid inflectional instabilities is important in determining the e *lution of free shear flows*. An outline of a general theory of inviscid instability is giv Then, we explore recent ideas on the *force-free* nature of coherent flow structures in t bulence. The role of viscosity in generating small-scale features of turbulence is discussed t both the Taylor-Green vortex and for two-dimensional turbulence. Finally, we survey rec ideas on the application of renormalization group methods to turbulence transport mod These methods *yield fundamental relationships* between *various* types of turbulent flow qu tities *and should be useful for* the development of transport models in complex geometr with complicated physics, like chemical reactions and buoyant heat transfer.

1. Introduction

Numerical solutions of the Navier-Stokes equations have now been used with mu success in the analysis and simulation of transition and turbulence in fluid flows. Analy refers to the use of numerical solutions to isolate dynamical mechanisms and thus to simpli and organize our understanding of these complex flows. For analysis, computation offers tl advantage over classical theory in that it allows the solution of rather general nonlinear pro lems in complicated geometries. Retaining the essence of complex phenomena like transiti and turbulence seems to yield equations that are just too complicated for classical analyti techniques. However, numerical methods seem to fit the problem well and it has been pos ble to use large-scale computations to obtain insights into these problems.

On the other hand, simulation involves the generation of complex flows on the compu er as a "numerical wind tunnel". Here computation offers the advantage over classical exper mental methods that complete flow field data is available as part of the numerical soluti *and the solution can, at least in principle, be probed without disturbing the flow.*

In this paper, we review progress on some problems of transition and turbulence th have been made possible by access to supercomputers. In Sec. 2, we discuss the role of s *called secondary instabilities in transition in wall-bounded shear flows. In the classical pip* and channel flows, classical linear, viscous instabilities are much too feeble to explain th robust processes of transition to turbulence. However, secondary instability provides a prot type of the kinds of instability that can exist in these flows and that can lead directly to

...ordered chaotic flow states and eventually to turbulence.

In Sec. 3, we contrast the secondary instability of wall-bounded shear flows with those of free-shear flows. The major difference is that free-shear flows are inflectional so they can support strong inviscid linear instabilities. The result is a competition, often delicate, between several classes of strong instabilities. The resulting flow evolution depends sensitively on initial and boundary conditions.

In Sec. 4, we describe some recent results on the structure of eddies in turbulence ...ows. It is found that, away from walls, much of turbulent flows are nearly force free or Beltrami in character. Some putative ideas on the stability of these flows are described.

Then, in Sec. 5, we survey new numerical tests of theories of two-dimensional turbulence. In the evolution of high Reynolds number chaotic flows, vortex layers develop and ...alesce in time, giving rise to qualitatively distinct spectral features.

Finally, in Sec. 6, we review recent ideas applying renormalization group (RNG) methods to the generation of transport approximations for turbulent flows. These methods should be useful for the development of transport approximations to turbulence problems with both geometrical and physical complexity (as with chemical reactions, buoyancy, etc.).

. Transition in wall-bounded shear flows

The classical problem of transition to turbulence in shear flows is to determine the nature of the breakdown of a laminar flow to turbulence. Two prototype wall bounded flows are plane channel flow and boundary layer flow. The boundary layer case represents a situation intermediate between the essentially bounded channel flows and the completely free shear flows which will be discussed in the next section. In addition to their importance in their own right, these flows are instructive as prototypes of a large class of more complex flows whose behavior is nonetheless governed by essentially the same physical processes. Indeed, the main importance of the study of transition in simple, wall bounded shear flows lies in the elucidation of the basic physical mechanisms by which all the more complex flows that are seen in ...e real world become turbulent.

The classical theory [1] of the stability of steady flows was initiated by Rayleigh, Kelvin, and Helmholtz roughly a century ago. On the basis of linearized stability analysis, Rayleigh demonstrated that any planar shear flow which does not possess an inflection point is ...essarily stable, *assuming purely inviscid flow. The inflection-point theorem is manifestly* ...lated by the instability of plane Poiseuille flow (parabolic profile) and plane Couette flow (linear profile), and it was realized that even in the most highly inviscid flows, viscosity may ...t exert a controlling influence on the stability of the flow. Incorporating viscous effects into ...e linear stability theory led to the study of the Orr Sommerfeld equation [1], which was the ...ntral theme of transition theory for much of this century.

The stability analyses for the Orr Sommerfeld equation generally concluded that the ...ost dangerous instabilities were two-dimensional waves (Squire's theorem), that the critical ...ynolds number for plane Poiseuille flow was ≈5772, and that Couette flow appeared to be ...able for all Reynolds numbers. These conclusions are in poor agreement with experience for ...d flows, in which transition appears in both Poiseuille and Couette flows at a Reynolds number of about 1000. Furthermore, the growth rates predicted by the Orr Sommerfeld ...es are very small on the *convective timescale of the flow* [2], *the latter being the times-*

cale observed for the breakdown process, and the breakdown has a complex three dimensional nature, in contrast to the two-dimensionality *of the fastest-growing Orr-Sommerfeld mode's* onset.

The crucial elements of the fast (convective timescale) transition are its nonlinear and three dimensional characteristics. The Orr Sommerfeld analysis for linear, two-dimensional disturbances to plane Poiseuille flow has been extended into the nonlinear regime by means of expansions in powers of the wave amplitude, and by direct simulations of the full nonlinear two-dimensional equations [2]. These analyses show that there exist steady finite amplitude wave disturbances which can exist in the flow at Reynolds numbers much less than the critical value from linear theory. However, such flows (see Figure 1) are stable to two-dimensional disturbances, and it is necessary to take account of three-dimensional effects in order to explain the violent changes the flow suffers during transition.

Although the steady finite-amplitude waves are stable to two-dimensional disturbances, it turns out that they are strongly unstable (on a convective time scale) to three dimensional perturbations [2]. This conclusion has been demonstrated by two distinct methods of analysis. First, the formal stability problem may be solved by finding the eigenvalue with largest real part of the Navier-Stokes equations linearized about the steady wave. Because of the two-dimensional, non parallel nature of the basic flow for this *secondary instability* analysis, the stability matrix is often too large and unwieldy for application of the usual matrix eigenvalue routines. Special methods [3] have been developed for efficiently finding the most dangerous eigenmodes of systems like these. Results from this type of calculation are shown in Figure 2, which shows the maximum instability growth-rate as a function of the Reynolds number and the amplitude of the two-dimensional wave. The smallest Reynolds number at which there can exist a three dimensional instability is seen to be slightly below 1000, which is in agreement with experimental observations of the point at which Poiseuille flow undergoes transition. The results of the eigenvalue analysis are corroborated [2] by performing a direct simulation of the full equations, using as initial conditions the two-dimensional wave 'seeded' with a very small amount of random three-dimensional noise. The disturbance rapidly becomes dominated by the fastest-growing mode, whose structure and growth- rate can be easily observed.

Because the three-dimensional instability grows on the convective rather than the viscous timescale, it seems likely that it is essentially an inviscid phenomenon, whose dynamics are only slightly affected by a small viscosity; in contrast, the Orr Sommerfeld instability which has a viscous growth rate is essentially viscous. A theoretical understanding [6] of the phenomenon may be pursued by developing an inviscid stability theory analogous to the classical theory for plane, parallel shear flows. Although the stability problem is now much more complicated, the basic physical interpretations of the Rayleigh, Fjortoft, and Howard *theorems* as statements of momentum conservation, energy conservation, and phase matching, respectively, remain valid. These theorems supply conditions on the flow that must be satisfied if an instability is to occur, and have important implications for the stability of complex three dimensional helical flows (see Sec. 4) in addition to these two-dimensional waves.

Unlike the two-dimensional waves, the three dimensional instability does not seem to saturate at some finite amplitude. Numerical studies [1] of the nonlinear evolution of the three dimensional instability show that the flow quickly develops the characteristic one spike structure that is typically observed in experiments [5] (see Figure 3). Subsequently, the flow becomes more and more disordered and, finally, turbulent.

The three dimensional instability is not just a characteristic of plane Poiseuille flow. *Three dimensional instabilities* with the same general behavior are found in boundary layer [illegible]

plane Couette flow, pipe flow, and even in free shear layers. The particular nature of three-dimensional secondary instability in free shear layers will be discussed in the next section.

3. Transition in Free Shear Flows

Inflectional free shear flows, like mixing layers and jets, are inviscidly unstable to two-dimensional disturbances. Squire's theorem implies that these instabilities are strongest when two-dimensional; when these two-dimensional instabilities evolve in time, they saturate into ordered laminar flow states characterized by large scale vortical flow structures. These vortical flows may themselves be unstable to subharmonic (pairing) instabilities, in which two (or more) vortices are paired and generate a new large-scale vortex motion [7].

We have found that the pairing process is *the* process that is responsible for positive transport coefficients (like eddy viscosity coefficients) in evolving two-dimensional shear flows [8]. In the direct numerical solution of the Navier Stokes equations (using a spectral code), the periodicity length in the streamwise direction controls the number of allowed vortex pairings (i.e., if the primary vortex has wavelength λ and the flow domain has periodicity length 4λ imposed on it, then just two vortex pairings are allowed). For a limited number of allowed pairings, the results show that the Reynolds stresses remain positive while the pairing process continues, but then, when pairing stops, the Reynolds stress changes sign and energy is transferred from the perturbation field back into the mean flow. Since the eddy viscosity, ν_{eddy}, is related to the Reynolds stress, $-\overline{u' v'}$, by

$$-\overline{u' v'} = \nu_{eddy} \frac{\partial \overline{U}}{\partial z}, \qquad (1)$$

It follows that the eddy viscosity is negative when pairing is artificially suppressed by the numerical boundary conditions.

Three dimensional secondary instability also occurs in free shear flows [9] but, in contrast to non-inflectional, inviscidly stable flows, this secondary instability no longer dominates the laminar instabilities. Indeed, the relative strength of pairing modes and the three-dimensional secondary modes depends strongly on the parameters of the flow [8]. However, the three dimensional secondary instability is effective at much smaller spanwise scales than is the primary inviscid instability and seems to lead directly to chaos rather than ordered laminar flow states [8]. The secondary instability seems to persist to scales smaller by a factor of order $\sqrt{R}$ than the scale of the shear layer (which determines the scale of the shortest wavelength classical instability). It has also been found [8] that growth of the three-dimensional modes occurs mainly by energy transfer from the mean flow with the primary vortex acting as a 'catalyst', as in wall bounded flows. The three-dimensional instability only disappears when viscous dissipation grows to balance transfer out of the mean flow (i.e., at wavenumbers of order $\frac{1}{\sqrt{R}}$).

When pairing modes and secondary instability modes compete, the resulting flow evolution is quite sensitive to details of initial conditions. It has been shown [8] that when three-dimensional modes dominate pairing modes, the three dimensional components grow to finite amplitude and lead to small scale three dimensional chaos. On the other hand, when pairing modes reach finite amplitudes, the positive transport coefficients they generate are so efficient at extracting energy from the mean flow that the growth of three dimensional modes is suppressed. When pairing is stopped, the reversal of sign of the transport coefficients quickly

leads to rapid growth of the three-dimensional small scale secondary instabilities. This interaction process between Reynolds stresses and modal growth was first observed numerical and seems to provide an explanation of the experimentally observed tendency of certain fr shear flows to remain essentially two-dimensional at large Reynolds numbers. A corollary this analysis of free shear flow transition is that small scale mixing may be enhan (suppressed) by suppression (enhancement) of pairing modes (e.g., by action of suital splitter plates in mixing layers).

As the three-dimensional modes achieve finite amplitude, they tend to form spiral fl structures. In Fig. 4, we show the region of large vorticity in an evolving mixing layer fl undergoing secondary instability. It is apparent that there are regions of large streamwi vorticity that connect large two dimensional primary vortex 'rollers'. The flow seems to to one in which the vorticity rotates from an orientation perpendicular to the flow directi in the primary vortex state to one in which the vorticity and velocity are nearly parallel the finite-amplitude pre-turbulent flow. This result will be explored in Sec. 4.

4. Coherent Structures and Turbulence

In this section, we shall discuss some recent ideas on the description and dynamics organized flow structures in turbulent flows. Results are taken exclusively from recent hi resolution, numerical simulations [10,11] in which detailed pictures of complete flow fields a possible.

It is believed that if coherent structures exist in turbulent flows, they will be helical structure [12,13]. Indeed, for a structure to exist for a reasonable amount of time it must tain a large portion of its energy. The term responsible for the cascade of energy into high wavenumbers (dissipation) is $v \times \omega$ which is at a relative *minimum when v and ω are align* Hence it is reasonable to expect that the structure will be helical in nature. Furthermore, t normalized helicity density, $v \cdot \omega / (|v| \, |\omega|)$, which is the cosine of the angle θ between and ω, should be useful in locating coherent structures.

A helical coherent structure will not participate in the dynamical energy cascade. Th may be one of the main reasons for the anisotropy of large scale motions as well as for dep tures from the Kolmogorov spectrum in the inertial-range. Regions where there are fluctu tions of the helicity density ($v \cdot \omega$) should have high levels of small-scale intermittency.

Numerical experiments [11,14] have been conducted to investigate these ideas on t role of helicity fluctuations. The two problems considered were the evolution of turbule channel flow and the Taylor-Green (TG) vortex flow [10]. For the channel flow data was e amined after the flow had reached a statistically steady state at a Reynolds number of 600 for the Taylor Green vortex flow data was collected at $R = 1500$ when the dissipation rate was well developed.

In a single realization, at a single time, the non-normalized probability density of t normalized helicity density $P(\cos\theta)$ is shown in Figure 5. In Figures 5a and b, condition sampling in regions were the dissipation was greater than 30% of the maximum was done f the channel and Taylor-Green vortex flow respectively. An essentially flat distribution su gests that there is no preferential arrangement of angle. However, Figures 5c and d show t probability for the conditionally sampled regions where dissipation is less than 5% of t maximum; there is a strong probability of v and ω being aligned. The helical structures ex where the dissipation is low.

Along with the numerical evidence for the presence of helical structures, there is the result [15,16] that purports to show that there exist a large variety of steady, helical Euler flows with chaotic streamlines. These flows are Beltrami or force free flows with their vorticity parallel to their velocity fields. More precisely, for any given streamline topology, there is a steady (possibly singular) Euler flow with the same topology. The argument is to consider a perfectly conducting, viscously dissipating magneto-hydrodynamic flow with zero initial velocity field and with the initial magnetic field chosen to have the same field line topology as the required streamline topology. As $t \to \infty$, this flow settles down to a motionless state in which $(\nabla \times B) \times B = \nabla p$ - identifying v with B and ω with $\nabla \times B$ gives the required steady Euler flow.

Recently, it has been argued [6] that, as a consequence of the streamlines being chaotic, there are regions of the flow that are dynamically stable to inviscid disturbances. Thus it is thought that an initial helical structure will break up in the regions where there are unstable (periodic) streamlines but in the regions where the *streamlines are chaotic, the helical* structure will persist. These inviscidly stable regions of chaotic streamlines are probably typically unstable to viscous disturbances.

In order to gain further understanding of the basic physics of the generation of small-scale turbulent flow *features, the TG vortex* is a nice model. This flow is that which develops in time from initial conditions that consist of excitation in basically a single Fourier mode. Because of nonlinear interaction, the flow becomes strongly three dimensional and develops excitation at all spatial scales. The TG vortex has been used to study such fundamental questions as the enhancement of vorticity by vortex line stretching, the approach to isotropy of the small scales, possible singular behavior of the Euler equations, formation of an inertial range and analysis of the geometry and intermittency of high-vorticity regions. The TG flow is advantageous for these studies because its special symmetry has allowed the development of numerical algorithms that are a *factor 64 more efficient in* both memory and storage than conventional periodic geometry spectral methods. For a three-dimensional flow, this factor 64 translates into a factor 4 increased range of spatial scales -- it is now possible to compute the TG vortex flow with 512^3 Fourier modes for each velocity component (or more than $4 \cdot 10^8$ effective degrees of freedom).

One of the more exciting results to emerge from our studies of the TG flow is the suggestion that viscosity may play an essential role in the development of small scale turbulence *and not just play a role in the dissipation of turbulent* kinetic energy. Indeed, we find that the development of the turbulent flow seems to require viscosity to induce instabilities of vortical structures in which the initial large-scale nonturbulent vorticity undergoes an explosive redistribution in space(see Figure 6). These viscosity induced instabilities are *probably* effective because viscosity allows vortex line reconnections prohibited in inviscid flow. Further study of viscosity induced instabilities should clarify the development of intermittent flow structures in turbulence.

5. Two-dimensional turbulence

Two-dimensional turbulence is a good testing ground for ideas on turbulence, first because it is unlikely to be more complicated than three-dimensional turbulence, and secondly because two-dimensional turbulence is likely to be approximately realized in many flows of geophysical importance. In addition, computations can be *performed with higher resolution* on flows in two dimensions than in three, so that numerical experiments can be used to discriminate between different theoretical turbulence models.

Two models which have been in apparent conflict for a number of years are the Batchelor-Kraichnan and the Saffman models for the high wavenumber behavior of the energy spectrum in fully-developed two-dimensional turbulence. Batchelor [17] and Kraichnan [?] independently proposed that the high wavenumber behavior of the spectrum would be governed by a cascade of the enstrophy, which is an inviscidly conserved quantity, to the smallest scales, where it would be dissipated viscously. Assuming that the enstrophy dissipa*tion rate tends to a constant value as the Reynolds number goes* to infinity, dimensional analysis gives a Kolmogorov-type power law decay for the energy spectrum E(k), which goes like k^{-3} as $k \to \infty$.

Shortly afterward, Saffman [19] argued that there was no particular reason why the enstrophy should cascade to the smallest scales, and proposed that viscosity would have very little effect on the structure of the flow. Instead, the large-scale flow would advect small-scale regions around the flow domain, and bring regions of different vorticity into close proximity. *The resulting flow would have large regions of smooth vorticity distribution separated* by comparatively narrow viscous layers across which the vorticity would jump abruptly. Geometric considerations then imply that the high- wavenumber spectrum has the form $E(k) \propto k^{-4}$ as $k \to \infty$ within the inertial range.

For a decade or so, there was no atmospheric data of sufficient quality, nor numerical simulations with enough resolution, to resolve the debate between the two theories. Recently however, Brachet *et al* [20] extended earlier computations [21] that showed a tendency for the Saffman theory to be correct at relatively *low Reynolds numbers and for the Batchelor-*Kraichnan ideas to hold at high Reynolds numbers. Brachet *et al* [20] performed very high resolution integrations of the Navier-Stokes equations at high R using random initial conditions for the velocity field and concluded that both Saffman and Batchelor-Kraichnan are correct, each for part of the time

Saffman's argument is correct for relatively short times after the initiation of the computation. *Figure* 7a shows the early-time evolution of the flow. Notice the relative motion of regions of piecewise smooth vorticity; *at these times the energy spectrum has the* k^{-4} *form* (see Figure 8). However, these regions retain their identity *only for* rather a short time as the flow evolves. The viscous layers separating different regions are rapidly stretched and contorted by the large-scale straining motion of the flow, and quickly develop a highly convoluted structure. At roughly the same time as the convolutions develop, the energy spectrum switches from k^{-4} asymptotic behavior to the Batchelor-Kraichnan k^{-3} form (see Figure 8). After the switch to the k^{-3} spectrum, the flow reaches an approximate dynamical equilibrium in which the vorticity contours are continually being stretched, convoluted, and reconnected by the large-scale motion with the small viscosity playing an essential role in the reconnection process (see Figure 7b).

6. *RNG Transport Models of Turbulence*

For the engineering design of aerodynamical and hydrodynamical shapes in turbulent shear flows, it is currently impractical, even on the most advanced available supercomputers, to solve the full Navier Stokes without approximation at large R. Because of the enormous range of scales in turbulent flows, the complete simulation of the turbulent flow would be extremely costly if not impossible even for one realization. For this reason, engineering calculations *of these flows are done*, and *probably will be done for some time, using Reynolds* averaged Navier Stokes equations (or some modification of these equations) with a turbulence model. The nature of the turbulence model is crucial to the success of these calculations. It

particularly important to have transport models that work well in the wall regions of the flow.

Recently, we have used dynamic renormalization group (RNG) methods to treat this problem [22]. The idea of the infrared RNG method is to use perturbation techniques similar to those used in the direct-interaction approximation [23] to eliminate all spatial scales smaller than the large eddies of the Navier Stokes equations. This is done perturbatively by eliminating narrow bands of wavenumbers from the dynamics, rescaling the resulting equations into the form of a k-ϵ transport model, and then repeating the process iteratively until all the required scales are removed.

The key approximations made in this procedure are as follows:

1. While the perturbation expansion is asymptotically exact for the elimination of an infinitesimally narrow band of wavenumbers at the ultraviolet end of the spectrum, it is not exact when iterated an infinite number of times to remove a finite band of wavenumbers. We neglect this iteration error (mostly on the grounds that similar types of approximations work well on other kinds of hard physics problems!).

2. The flow is assumed to be locally homogeneous and isotropic in pursuing the perturbation theory. In the neighborhood of walls, this restricts one to eliminating only those degrees of freedom small compared to the distance from the wall and the large eddies of the flow. It is also assumed that the retained wavenumbers and frequencies are negligible compared to those in the eliminated band so that suitable markovianization of the equations can be made.

Once these approximations are justified (or believed on the basis that they seem to give results that compare favorably with observations), it is possible to derive RNG closures for a variety of turbulence problems. If only those scales smaller than a finite-difference (or spectral) grid scale are removed by the RNG procedure, then one obtains a large eddy simulation model. The RNG large-eddy model has the advantages that it has built-in wall function behavior without making additional *ad hoc* approximations and that it generates a random force that drives the turbulence through its action in the buffer layer. If one applies the RNG procedure to multi-phase or chemically reacting flows [22], one obtains new forms of closure approximations that seem to fit well available data without further adjustment. Since data acquisition can be very difficult for these turbulent flows, the RNG procedure seems to have much appeal.

As an example of the RNG results, we give the equations here for the RNG form of the k-ϵ equations for pure kinetic turbulence. The resulting equations are:

$$\frac{Dk}{Dt} = \frac{\nu - 1}{\nu}\left(\frac{\partial u}{\partial y}\right)^2 - \bar{\epsilon} + \frac{\partial}{\partial y}\left(\alpha\nu\frac{\partial k}{\partial y}\right) \qquad (2)$$

$$\frac{D\bar{\epsilon}}{Dt} = a\frac{\nu - 1}{\nu}\left(\frac{\partial u}{\partial y}\right)^2 - Y + \frac{\partial}{\partial y}\left(\alpha\nu\frac{\partial\bar{\epsilon}}{\partial y}\right) \qquad (3)$$

$$\frac{\nu d\nu}{(\nu^3 + C - 1)^{1/2}} = \frac{1}{1.50}\, d\left(\frac{k}{\sqrt{\epsilon}}\right), \quad (C \approx 100) \qquad (4)$$

$$d\left(\frac{s}{\sqrt{\epsilon}}\right) = 0.2122\frac{d\nu}{(\nu^3 + C - 1)^{1/2}} \qquad (5)$$

$$d\left(\frac{Y}{\epsilon^{3/2}}\right) = 0.3216\frac{d\nu}{(\nu^3 + C - 1)^{1/2}} \qquad (6)$$

$$\left|\frac{\alpha - 1.2027}{0.2627}\right|^{0.6418}\left|\frac{\alpha + 2.2627}{3.2027}\right|^{0.3582} = \frac{\nu_0}{\nu} \qquad (7)$$

Some key results from these equations (in which the constants that appear are la... ly geometrical in character and not free parameters) are that the von Karman constant is 0... and the normalized turbulent kinetic energy level is $1/\sqrt{0.0080}$.

Finally, to illustrate the application of the RNG method to problems with comp... physics, we give some results for buoyantly driven convective shear flows. The key cha... from the above equations is that there is an inverse turbulent Prandtl numb... $\alpha_{eddy} = \frac{\kappa_{eddy}}{\nu_{eddy}}$, determined by the relation

$$\left|\frac{\alpha_{eddy} - 1.2027}{\alpha_0 - 1.2027}\right|^{0.6418}\left|\frac{\alpha_{eddy} + 2.2027}{\alpha_0 + 2.2027}\right|^{0.3582} = \frac{\nu_0}{\nu_{eddy}} \qquad (8)$$

where subscripts 0 indicate laminar quantities. *In a fully turbulent region, the inverse tu... bulent Prandtl number is asymptotically 1.2027*, in good agreement with the Reynol... Colburn analogy. Another key feature of the RNG method for buoyant flows is that the... a modified buoyancy force; *asymptotically, in fully turbulent unstable regions*, the RN... correction to the buoyancy force is to reduce it by a factor 0.27 from its laminar value. T... feature is due to small-scale turbulent mixing.

The resulting equations lead to impressive results for buoyant flows. In Fig. 9, we pl... the scaled velocity profile in stratified shear flow, for both stable and unstable stratificati... for the RNG transport approximation compared with experimental data. Then, in Fig. 1... we plot the heat transport as a function of Rayleigh number in Benard convection for t... RNG transport model and for the experimental data of Krishnamurti.

References

[1] Drazin, P.G., Reid, W.H. Hydrodynamic stability, Cambridge University Press, Cam-bridge 1981.

[2] Details and other references are given in Orszag, S.A., Patera, A.T., J. Fluid Mech., 128 (1983), 347.

[3] Goldhirsch, I., Orszag, S.A. An efficient method for computing the leading eigenvalues and eigenvectors of large asymmetric matrices, to be published (1986).

[4] Kleiser, L., Schumann, U. Laminar turbulent transition process in plane Poiseuille flow, in Proceedings of the Symposium in Spectral Methods (Philadelphia, PA, 1984), 141.

[5] Nishioka, M., Iida, S., Kanbayashi, S. An experimental investigation of the subcritical instability in plane Poiseuille flow, in Proceedings of the 10th Turbulence Symposium (Tokyo, 1978) 55.

[6] Bayly, B.J. Kinematic and dynamical properties of complex three-dimensional flows, Ph.D. thesis, Princeton University (1986).

[7] Fatnoh, P.C., Sherman, F.S., Corcos, G.M., J. Fluid Mech., 73 (1982), 215.

[8] Metcalfe, R., Orszag, S.A., Brachet, M.E., Menon, S., Riley, J. Secondary Instability of Free Shear Flows, submitted to J. Fluid Mech.

[9] Pierrehumbert, R.T., Widnall, S.E., J. Fluid Mech., 114 (1982), 59.

[10] Brachet, M.E., Meiron, D.I., Orszag, S.A., Nickel, B.G., Morf, R.H., Frisch, U., J. Fluid Mech., 130 (1982), 411 452.

[11] Pelz, R.B., Yakhot, V., Orszag, S.A., Shtilman, L., Levich, E. Velocity-Vorticity Patterns in Turbulent Flow, Phys. Rev. Lett., 54 (1985), 2505.

[12] Levich, E., Tsinober, A. On the role of helical structures in three dimensional turbulent flow, Phys. Lett., 93A (1983), 293 297.

[13] Tsinober, A., Levich, E. On the helical nature of three dimensional coherent structures in turbulent flows, Phys. Lett., 99A (1983), 321 324.

[14] Shtilman, L., Levich, E., Orszag, S.A., Pelz, R.B., Tsinober, A. On the role of helicity in complex fluid flows, Phys. Lett., 113A (1985) 32 37.

[15] Arnold, V.I. The asymptotic Hopf invariant and its application, in Proceedings of Summer School in Differential Equations, Erevan Armenian SSR Academy of Sciences, (1974).

[16] Moffatt, H.K. Magnetostatic equilibria in viscous, perfectly conducting fluid and analogous Euler flows of an incompressible fluid: I. Fundamentals, J. Fluid Mech., 159 (1985) 359-378.

[17] Batchelor, G.K. Phys. Fluids 12 (1969), 233.

[18] Kraichnan, R.H. Phys. Fluids 10 (1967), 1417.

[19] Saffman, P.G. Studies in Applied Math., 50 (1971), 377.

[20] Brachet, M.E., Sulem, P.L. Free decay of high Reynolds number, two-dimensional turbulence, in Ninth International Conference on Numerical Methods in Fluid Mechanics, Lecture Notes in Physics, 218 Springer (1985), 103.

[21] Orszag, S.A. in Fifth International Conference on Numerical Methods in Fluid Dynamics, Lecture Notes in Physics, 59, Springer (1977), 32.

[22] Yakhot, V., Orszag, S.A. Renormalization group analysis of turbulence I. Basic theory, J. Sci. Comp., 1 (1986) 1.

[23] Kraichnan, R.H., J. Fluid Mech., 5 (1959), 497.

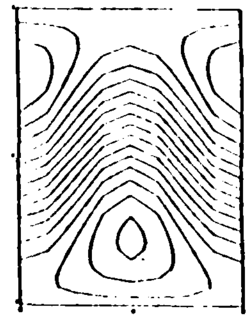

Figure 1 : Streamlines of the steady (stable) finite amplitude two-dimensional traveling wave for plane Poiseuille flow at R = 4000, plotted in the rest frame of the wave (from ref. [2]).

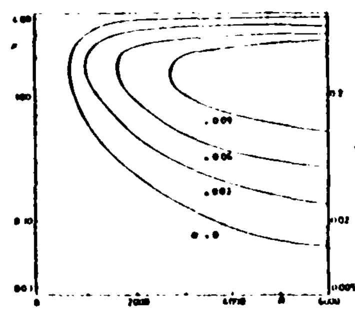

Figure 2 : Contours of constant growth rate (labelled by growth rate) as a function of R and the amplitude of the background two-dimensional nonlinear wave (see right-hand scale) (from ref. [8]).

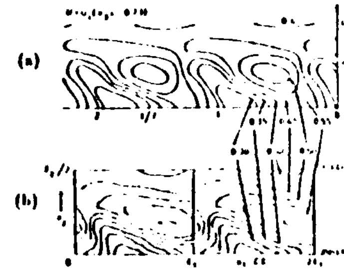

Figure 3 : Contours of x velocity in the (x,y) plane at the one spike stage in laboratory experiments of Nishioka et al. (a) and in the numerical simulation of Kleiser and Schumann (b) (from ref.

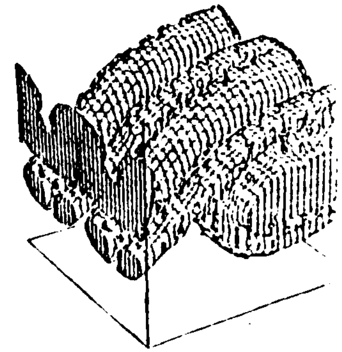

Figure 4 : A plot of the region of large vorticity in the secondary instability of a mixing layer flow (from ref. [8]). The ribs connecting the large rollers are regions of significant streamwise vorticity in which ω is nearly aligned with v

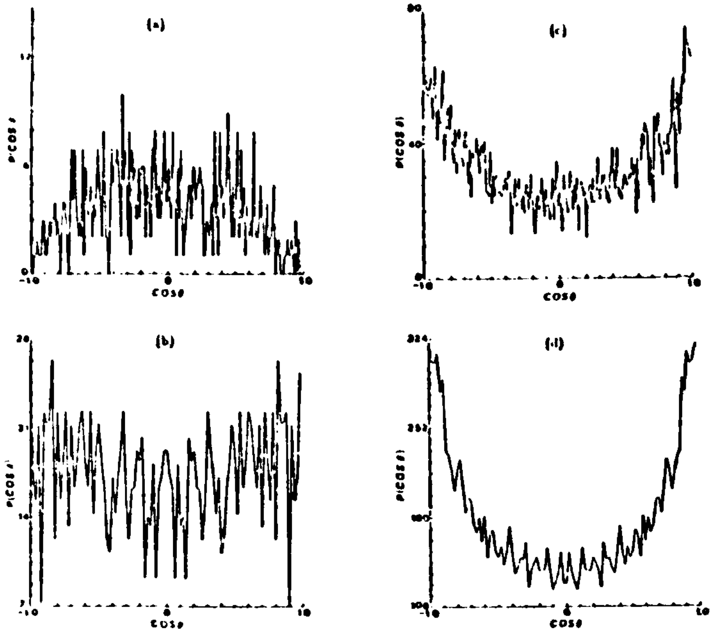

Figure 5 : The probability density for the distribution of the angle between velocity v and vorticity ω conditionally sampled in the region where dissipation is (a) greater than 30% of its maximum value in the outer part of the channel ($15 < z_+ < 100$), (b) greater than 30% of its maximum value in the Taylor Green vortex at t = 8.6. (c) less than 5% of its maximum value in the outer part of the channel ($15 < z_+ < 100$), (d) less than 5% of its maximum value in the Taylor-Green vortex at t = 8.6 (from ref. [11]).

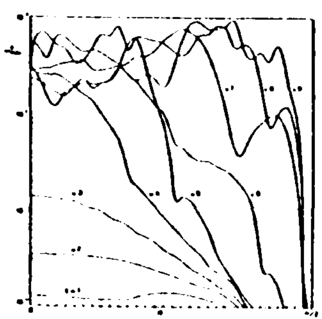

Figure 6 : A plot of the distribution of large vorticity regions in the TG vortex flow as a function of time t and distance l away from the side walls of the impermeable cube in which the flow takes place. Observe how vorticity explodes in towards the center of the cube between t = 4 and t = 8 (from ref. [10]).

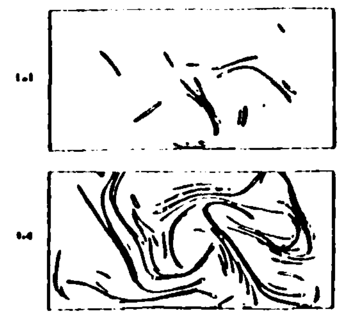

Figure 7 : Contours of squared vorticity gradient in a high resolution, two dimensional turbulence run (from ref. [18]). Notice that at t=1 the vortex gradient sheets are well separated from each other in contrast to t=4 when they are much more densely packed.

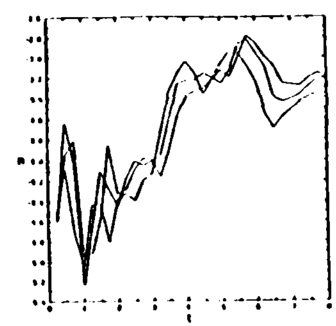

Figure 8 : The best fit to the inertial exponent, n, as a function of time for a high R, two-dimensional turbulence run (from ref. [18]). These results were obtained from a 1024^2 spectral code, fitting the results of the form $E(k) = ck^{-n(t)}$. The k^{-4} regime occurs near t ~ 4 when the inertial exponential flattening of the vortex gradient sheets is started by viscous effects.

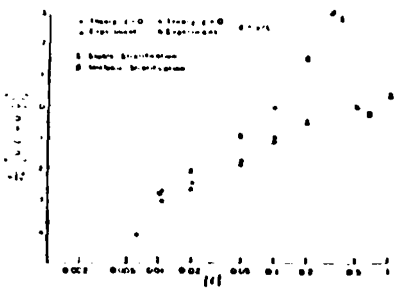

Figure 9 : A comparison between the RNG transport model predictions and experiment for the mean velocity profile in a stratified boundary layer for both stable and unstable stratification. Here the flow variables are scaled using Monin-Obukhov scaling.

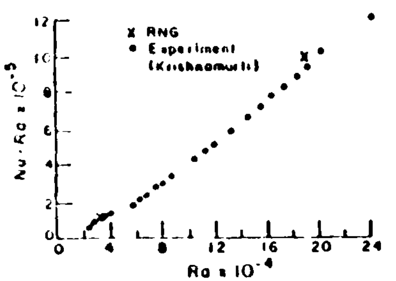

Figure 10 : A comparison between the RNG prediction and experiment for the heat flux in a Benard convection.

BOOTSTRAPPING IN TURBULENCE COMPUTATION

Joel H. Ferziger
Department of Mechanical Engineering
Stanford University
Stanford, CA USA 94305

1. Introduction

Classification schemes for methods for predicting turbulent fl- were presented by Kline et al. (1978) and Ferziger et al. (1981); tl scheme is given in Table 1. At each level in the scheme, a sin method or model is more broadly applicable than a method at the pr ceding levels. This allows data for one flow to be used to predi other flows, an advantage of obvious importance. The primary dis vantage of the higher levels is that they cost more than the preced levels; the data required to fix a model or correlation is also m difficult to acquire.

Table 1

Approaches to Turbulent Flow Prediction

1. Correlations
2. Integral Methods
3. One Point Closures
4. Two Point Closures
5. Large Eddy Simulation
6. Full Turbuence Simulation

The ability of a method to compute more detail and a wider ra of flows allows it to produce data required to test models at lo levels. Indeed, working engineers often use simulations made w sophisticated turbulence models to construct correlations for optimi ing designs; it is not unusual for engineers to move up and d through the levels (and from computation to experiment) in the des process.

The main goal of this paper is to demonstrate that it is possible to use full turbulence simulations (FTS) to study models large eddy simulation (LES) and to use both of these methods to t and develop one point closure turbulence models. This bootstrap procedure makes it possible, at least in principle, to use turbule simulations to predict turbulent flows without reference to expe mental data; this procedure is not recommended but the possibility interesting.

Reynolds Number Scaling of Cellular-Automaton Hydrodynamics

Steven A. Orszag and Victor Yakhot
Applied and Computational Mathematics, Princeton University, Princeton, New Jersey 08544
(Received 25 November 1985)

We argue that the computational requirements for presently envisaged cellular-automaton simulations of continuum fluid dynamics are much more severe than for solution of the continuum equations.

PACS numbers: 47.10.+g

It has recently been suggested[1,2] that cellular automata (CAs) [defined as discretely and locally linked, finite- (and few-) state machines] may be an effective way to compute complex fluid flows. These automata have the advantage that they may be simply and perhaps inexpensively constructed with use of specially designed parallel hardware. With suitable interaction rules, it has been argued,[1,2] the space-time average kinetic behavior of the CA system follows the incompressible Navier-Stokes dynamical equations. While the Navier-Stokes equations for continuum fluids can be calculated efficiently on parallel-architecture machines, it is probably easier to make efficient use of the parallel architecture with CAs. In this Letter, we wish to point out that there are some considerations that require resolution before these methods can be considered to be a viable alternative to traditional continuum mechanical methods for high-Reynolds-number fluid dynamics.

Let us compare the resolution and work requirements for a CA simulation of a high-Reynolds-number flow with those of direct numerical solution of the incompressible Navier-Stokes equations. It is well known[3,4] that, at Reynolds number N_{Re}, the Kolmogorov and Batchelor-Kraichnan theories of three- and two-dimensional equilibrium range dynamics, respectively, predict that the range of excited scales is of order $N_{\mathrm{Re}}^{3/4}$ and $N_{\mathrm{Re}}^{1/2}$ and the computational work required to calculate a significant time in the evolution of large-scale flow structures is of order N_{Re}^{3} and $N_{\mathrm{Re}}^{3/2}$ in three and two dimensions, respectively.

The suggested evolution rules for CAs to reproduce hydrodynamic behavior are based on conservation laws of mass, momentum, and energy. Dissipation is modeled through the thermalization of coherent hydrodynamic modes. Therefore, the lattice resolution of the CA calculation must be much finer than that of the hydrodynamic simulation, the latter requiring the retention of only those degrees of freedom describing motions on scales of the dissipation range or larger. Thus, the lattice spacing a must be smaller than the dissipation scale η in the turbulent fluid.

We now discuss some conditions that CA models should satisfy to describe high-Reynolds-number fluid flows. We present three successively more restrictive arguments that show that η/a must grow rapidly with Reynolds number.

Signal-to-noise ratio.—The hydrodynamic velocity in the CA simulation is calculated by subdividing the computational domain into cells with linear dimensions $\gg a$, averaging over the CAs within a (finite) cell, and smoothing (filtering) the resulting (noisy) velocity field. Thus, the hydrodynamic velocity at a point x is the (space-time) filtered velocity of the CAs in the cell C_x centered at x, $v_H(x) = \langle v(x) \rangle$, where the local velocity in C_x is

$$v(x) = \frac{1}{n} \sum_{i \in C_x} v_i, \tag{1}$$

where n is the number of occupied sites i within the cell. We assume that the possible velocity values at an occupied CA site are $v_i = \pm v_{\mathrm{th}}$ where v_{th} is the constant (thermal) velocity over the CA grid. At low Mach numbers, $v_H \ll v_{\mathrm{th}}$. In this case, the fluctuations in $v(x)$ are of order $n^{-1/2} v_{\mathrm{th}}$. In order that the hydrodynamic velocity found in this way may be a good representation of the continuum hydrodynamics, it is necessary that the noise $n^{-1/2} v_{\mathrm{th}}$ be small compared to the smallest significant hydrodynamic velocity. The smallest significant hydrodynamic velocity is the eddy velocity on scales of order of the dissipation scale η. In three dimensions, $\eta = O((\epsilon/\nu^3)^{-1/4})$ and the eddy velocity on the scale of η is $v_\eta = O((\epsilon\nu)^{1/4})$. Here ν is the viscosity and ϵ is the turbulent energy dissipation rate per unit mass. Thus, we require that the number of CA sites n within a cell of size η be at least

$$n \gg v_{\mathrm{th}}^2/(\epsilon\nu)^{1/2}. \tag{2}$$

Since $\epsilon = O(U^3/L)$ where U is the large-scale rms fluctuating velocity and L is the associated large-scale length of these velocity fluctuations, we find that $n \gg N_{\mathrm{Re}}^{1/2} M^2$, where $N_{\mathrm{Re}} = UL/\nu$ is the Reynolds number and $M = U/v_{\mathrm{th}}$ is the Mach number.[5] Since the number of cells of size η within a three-dimensional turbulent eddy of size L scales as $N_{\mathrm{Re}}^{9/4}$, the overall number of CA sites must increase at least as $N_{\mathrm{Re}}^{11/4}/M^2$.

Since the effective evolution time of the fluid system is L/U, while the time step on the CA lattice is a/v_{th}, it follows that the CA simulation requires at least L/aM steps in time. Since the computational work for each site update is of order 1, it follows that the CA simulation requires at least of order $(N_{Re}/M)^{11/3}$ work.

In summary, the above signal-to-noise considerations suggest the following lower-bound estimates for the computer storage S and work W for CA simulations of high–Reynolds number, low–Mach-number flows (where, for reference, we include the corresponding estimates for the continuum Navier-Stokes equations): for CA (2D),

$$S = N_{Re}^{3/2}/M^2, \quad W = N_{Re}^{9/4}/M^4;$$

for Navier-Stokes (2D),[6]

$$S = N_{Re}, \quad W = N_{Re}^{3/2};$$

for CA (3D),

$$S = N_{Re}^{11/4}/M^2, \quad W = (N_{Re}/M)^{11/3};$$

for Navier-Stokes (3D),[7]

$$S = N_{Re}^{9/4}, \quad W = N_{Re}^{3}.$$

Upper bound for the Reynolds number.—A more stringent condition on the Reynolds-number dependence of the minimal number of lattice sites in a CA simulation of hydrodynamics is found as follows. If the discrete velocity of the CAs is $\pm v_{th}$ (again, the thermal velocity or sound speed on the CA lattice) and the lattice spacing is a, then the kinematic viscosity ν on the lattice is at least of order va. For the CA to give a self-consistent hydrodynamic simulation, the viscosity determined on the "molecular" level must equal the viscosity governing the dissipation of the hydrodynamic modes. Thus the Reynolds number of the simulated fluid can be at most UL/ν or ML/a. Since the number N of CA sites in the lattice is of order $(L/a)^d$, where d is the dimension of space, we obtain the result that N must be at least of order $(N_{Re}/M)^d$. As above, the CA simulation of the flow requires at least L/aM steps in time. It follows that the CA simulation requires at least of order $(N_{Re}/M)^d$ memory and of order N_{Re}^{d+1}/M^{d+2} work.

These estimates for storage S and work W based on lower bounds for the effective viscosity on the lattice are of order

$$S = (N_{Re}/M)^2, \quad W = N_{Re}^3/M^4$$

for CA (2D),

$$S = N_{Re}, \quad W = N_{Re}^{3/2}$$

for Navier-Stokes (2D),

$$S = (N_{Re}/M)^3, \quad W = N_{Re}^4/M^5$$

for CA (3D),

$$S = N_{Re}^{9/4}, \quad W = N_{Re}^3$$

for Navier-Stokes (3D).

Hydrodynamic fluctuations.—The CA system will yield a self-consistent continuum hydrodynamic description only if the thermal energy fluctuations on hydrodynamic spatial scales are small compared to the energy of the hydrodynamic modes on corresponding length scales. If the "mass" of an occupied CA site is m, its energy is $d/2m v_{th}^2$ in d space dimensions. Then the fluctuation in total thermal energy over a cell with n occupied CAs is $\sqrt{n}\, m v_{th}^2$. (We note that in a CA with velocity states $\pm v_{th}$, energy fluctuations are proportional to density fluctuations.) The corresponding hydrodynamic energy within a cell of size η is $\rho\eta^3 v_H^2$, where v_H is the hydrodynamic velocity and ρ is the hydrodynamic density. In three dimensions, the dissipation scale is η and the associated hydrodynamic velocity is v_η. Also, the relation between m and ρ is $nm = \rho\eta^3$. Thus, for thermal fluctuations to be small, we must require that $n \gg N_{Re}/M^4$. In two dimensions, the corresponding result is $n \gg N_{Re}^2/M^4$.

This argument shows that the storage and work required for a self-consistent hydrodynamic description using CAs is of order

$$S = N_{Re}^3/M^4, \quad W = N_{Re}^{9/2}/M^7$$

for CA (2D),

$$S = N_{Re}, \quad W = N_{Re}^{3/2}$$

for Navier-Stokes (2D);

$$S = N_{Re}^{13/4}/M^4, \quad W = N_{Re}^{13/3}/M^{19/3}$$

for CA (3D),

$$S = N_{Re}^{9/4}, \quad W = N_{Re}^3$$

for Navier-Stokes (3D).

The CA models approximate fluids that are by their nature necessarily compressible. This means that an equation of state for pressure is needed. However, self-consistency requires that thermodynamic pressure fluctuations over dissipation scales be small. This latter condition leads to results identical to those just obtained by use of energy estimates. Indeed, it is known[8] that the rms thermodynamic pressure fluctuations in a volume η^3 are $(\rho k T c^2/\eta^3)^{1/2}$, where T is the temperature of the fluid and c is the sound speed. But the hydrodynamic pressure fluctuations over length scales of order η are of order $\rho(\epsilon\nu)^{1/2}$. Since $kT = m v_{th}^2$ and $c \approx v_{th}$, the previously given estimates apply.

We believe that these pessimistic estimates for high Reynolds numbers and low Mach numbers must be overcome before CAs can be an effective modeling tool for complex fluid flows. This can, in principle, be

done by averaging over the shortest scales $a \ll \eta$ in order to reduce the number of degrees of freedom.[9] However, it seems that this renormalization can be useful (in the context of local, few-bit, parallel computations) only if it does not generate nonlocal, complex interactions in the set of basic rules defining CAs. Unfortunately, we do not now understand why this kind of "turbulence transport" modeling should be either easier or more successful on the CA lattice than for the continuum equations or for molecular dynamics.

While the above estimates for CA simulations of turbulence are quite pessimistic, there may be cases in which CA simulations of turbulence may be effective. In a turbulent boundary layer, the local Reynolds number is $O(1)$ in the viscous sublayer and is modest within the buffer layer. A CA model could be effective in these regions in the modeling of turbulent burst formation and evolution. However, this application requires the development of three-dimensional CA models and suitable techniques to match the outer regions of the flow.

[1] U. Frisch, B. Hasslacher, and Y. Pomeau, Phys. Rev. Lett. 56, 1505 (1986).

[2] J. Salem and S. Wolfram, to be published.

[3] S. A. Orszag, J. Fluid Mech. 41, 363–386 (1970).

[4] J. R. Herring, S. A. Orszag, R. H. Kraichnan, and D. G. Fox, J. Fluid Mech. 66, 417–444 (1974).

[5] Notice that the Mach number is bounded in CA simulations of fluid dynamics. With allowed velocities of $\pm v_{th}$, $M \leq O(1)$, the upper limit being achieved when the CAs exhibit pure streaming, nonhydrodynamic motion.

[6] The Batchelor-Kraichnan theory suggests that there may be logarithmic corrections to these estimates.

[7] Intermittency effects may slightly change these estimates.

[8] L. D. Landau and E. M. Lifschitz, *Fluid Mechanics* (Pergamon, London, 1959), p. 529.

[9] A kind of renormalization using "pseudovertices" is suggested in Ref. 1. The idea is to introduce vertices on subhydrodynamic scales that are not kept track of explicitly. If this idea can be successfully implemented, it would reduce the computational storage requirements given above but apparently not the computational work. We are grateful to C. H. Bennett for this comment.

Reprinted from Journal of Scientific Computing

Vol. 1, No. 1, 1986
Printed in Belgium

Renormalization Group Analysis of Turbulence. I. Basic Theory

Victor Yakhot[1] and Steven A. Orszag[1]

Received May 14, 1986

We develop the dynamic renormalization group (RNG) method for hydrodynamic turbulence. This procedure, which uses dynamic scaling and invariance together with iterated perturbation methods, allows us to evaluate transport coefficients and transport equations for the large-scale (slow) modes. The RNG theory, which does not include any experimentally adjustable parameters, gives the following numerical values for important constants of turbulent flows: Kolmogorov constant for the inertial-range spectrum $C_K = 1.617$; turbulent Prandtl number for high-Reynolds-number heat transfer $P_t = 0.7179$; Batchelor constant $Ba = 1.161$; and skewness factor $\bar{S}_3 = 0.4878$. A differential K–$\bar{\varepsilon}$ model is derived, which, in the high-Reynolds-number regions of the flow, gives the algebraic relation $\nu = 0.0837 K^2/\bar{\varepsilon}$, decay of isotropic turbulence as $K = O(t^{-1.3307})$, and the von Karman constant $\kappa = 0.372$. A differential transport model, based on differential relations between K, $\bar{\varepsilon}$, and ν, is derived that is not divergent when $K \to 0$ and $\bar{\varepsilon}$ is finite. This latter model is particularly useful near walls.

KEY WORDS: Renormalization group; turbulence theory; inertial range; turbulence transport; Reynolds number; large eddy simulation; computational fluid dynamics.

1. INTRODUCTION

Turbulent flows occur in many circumstances, differing by geometry, driving mechanisms, and the physicochemical processes that take place within them. Perhaps the most distinguishing characteristic of high-Reynolds-number turbulent flows is their large range of excited space and time scales. It is well known (e.g., Landau and Lifshitz, 1982) that, in homogeneous

[1] Applied & Computational Mathematics and Mechanical & Aerospace Engineering, Princeton University, Princeton, New Jersey 08544

turbulence, dissipation scale eddies are of order $R^{3/4}$ times smaller than the energy containing eddies, where R is a (microscale) Reynolds number. In order to solve the Navier Stokes equations accurately for such a turbulent flow, it is necessary to retain order $(R^{3/4})^3$ spatial degrees of freedom. Also, since the time scale of significant evolution of turbulent flow is of the order of the turnover time of the energy-containing eddies, it is necessary to perform $R^{3/4}$ time steps to calculate a significant time evolution of the flow. Even if these calculations require only $O(1)$ arithmetic operations per time step, the requirement for computer storage would be $O(R^{9/4})$ and for computational work $O(R^3)$. In this case, even a mere doubling of the Reynolds number would require an order-of-magnitude improvement of computer capability. With this kind of operation and storage count, it is not likely that foreseeable advances in computers will allow the full simulation of turbulent flows at Reynolds numbers much larger than $R = O(100-1000)$ already achieved.

The second distinguishing characteristic of turbulence is the approximate universality of the properties of scales much smaller than the integral scale L in the flow. High-Reynolds-number turbulent flow is characterized by three different ranges of spatial scales:

1. For wavenumbers $k = O(\pi/L)$ the energy spectrum is strongly anisotropic and is not universal. The integral scale L reflects both the geometry of the flow and the physicochemical processes taking place on these scales.
2. At much smaller scales, with wavenumbers satisfying $\pi/L \ll k \ll k_d = R^{3/4}L^{-1}$, the velocity fluctuation spectrum $E(k)$ is nearly universal and is approximately given by the Kolmogorov energy spectrum:

$$E(k) = C_K \bar{\epsilon}^{2/3} k^{-5/3} \tag{1.1}$$

   with the Kolmogorov constant $C_K = 1.3-2.3$. Here $\bar{\epsilon}$ is the rate of energy dissipation per unit volume in the flow.
3. In the dissipation range, $k > O(k_d)$, the energy spectrum decreases exponentially with k.

The existence of the universal inertial range characterized by the Kolmogorov law (1.1) has been checked experimentally for a large variety of turbulent flows. The Kolmogorov law has been confirmed experimentally in fluid and gas shear flows, in atmospheric boundary layers and in the ocean, in hydromagnetic and bouyancy-influenced flows, in jets, and in turbulence behind a grid (e.g., Monin and Yaglom, 1975).

The universality of the small scales can be formulated dynamically as follows. Fluid motions are governed by the Navier Stokes equation

$$\frac{\partial \mathbf{v}}{\partial t} + (\mathbf{v}\cdot\nabla)\mathbf{v} = -\frac{1}{\rho}\nabla p + \nu_0 \nabla^2 \mathbf{v} \tag{1.2}$$

$$\nabla\cdot\mathbf{v} = 0 \tag{1.3}$$

and are subject to initial and boundary conditions. Here $\mathbf{v}(\mathbf{x}, t)$ is the fluid velocity, ρ is the density, p is the pressure, and ν_0 is the molecular kinematic viscosity. The inertial-range spectrum (1.1) does not depend directly on geometry or boundary conditions; geometry and boundary conditions do affect the structure of large scales as well as the value of $\bar{\epsilon}$ that appears in (1.1). Boundary conditions can be considered from the viewpoint of small scales as a source of energy injected into the large scales, which subsequently cascade to the small scales. Using the analogy with equilibrium statistical mechanics, in which small-scale fluctuations are independent of the details of the interaction of the system with a heat bath, we propose to replace (1.2) by the more general, but equivalent, equation

$$\frac{\partial \mathbf{v}}{\partial t} + (\mathbf{v}\cdot\nabla)\mathbf{v} = \mathbf{f} - \frac{1}{\rho}\nabla p + \nu_0 \nabla^2 \mathbf{v} \tag{1.4}$$

where $\mathbf{f}$ is a random force (noise) chosen to generate the velocity field described by the spectrum (1.1) in the limit of large wavenumber k.

It is important to emphasize that no initial and boundary conditions are needed in (1.4), since the fluid described by (1.4) is stirred by the force $\mathbf{f}$ so that a *statistically steady state with* $\mathbf{v} \neq 0$ *can be achieved. The relation* between the stirring force $\mathbf{f}$ and initial and boundary conditions will be discussed further below. Equation (1.4) is a model that is statistically equivalent to the original Eq. (1.2) in the inertial range. This *correspondence principle* is the basis for the RNG method discussed in this paper.

It is also known that Eq. (1.4) with the Gaussian random force defined by the wavevector frequency correlation

$$\langle f_i(\hat{k}) f_j(\hat{k}') \rangle = 2D_0 (2\pi)^{d+1} k^2 P_{ij}(\mathbf{k})\, \delta(\hat{k} + \hat{k}')$$

with

$$D_0 = \nu_0 k_B T/\rho$$

and

$$P_{ij}(\mathbf{k}) = \delta_{ij} - k_i k_j / k^2; \qquad \hat{k} = (\mathbf{k}, \omega) \tag{1.5}$$

describes both the static and dynamic properties of a fluid in thermal equilibrium independently of details of the fluid history and conditions on

its boundary (Landau and Lifshitz, 1982; Forster *et al.*, 1977). Here d is the dimension of space, k_B is Boltzmann's constant, and T is the temperature of the fluid.

On this basis, we may postulate that Eqs. (1.3) and (1.4) with a properly chosen random force provides a correct description of the small-scale motion of a wide class of turbulent flows. In the inertial range, solutions to Eqs (1.3) and (1.4) are statistically equivalent to solutions to the original Eqs. (1.2) and (1.3) with initial and/or boundary conditions. Equation (1.4) can be viewed as a general model describing small-scale properties of turbulent flow in the inertial range. This equation will be used for the development of turbulence models using the renormalization group method.

The present paper is organized as follows: The basic ideas of the renormalization group method are described in Section 2 following Forster *et al.* (1977). Modifications of this theory that enable us to evaluate the Kolmogorov constant as $C_K \approx 1.617$ are also described in this section. In Section 3, a subgrid-scale turbulence model is derived using the RNG method. It is shown that this subgrid model is very close to the model used by Deardorff (1970) in the high-Reynolds-number regions of turbulent channel flow far from walls.

In Section 4, the RNG procedure is applied to the evolution of a passive scalar in a turbulent flow. The results of this analysis include the prediction of the turbulent Prandtl number $P_t = 0.7179$ and the Batchelor constant $Ba = 1.161$ [see (4.3)]. In Section 5, the RNG method is used to derive turbulent transport approximations. The values of some basic constants of turbulent flows are found, *including the skewness factor* $S_3 = 0.4878$ and the von Karman constant $\kappa = 0.372$. The high-Reynolds-number version of the RNG form of the K-$\bar{\varepsilon}$ transport model is also derived in Section 5. It is shown that $\nu = 0.0837K^2/\bar{\varepsilon}$, where K and $\bar{\varepsilon}$ are the turbulent kinetic energy and mean dissipation rate, respectively. This K-$\bar{\varepsilon}$ model is very close to the algebraic two-equation K-$\bar{\varepsilon}$ models often used in turbulence modeling. This model also leads to the energy decay law $K = O(t^{-1.50})$ for homogeneous, isotropic turbulence. In Section 6, differential transport models are derived that are based on *differential* relations between K, ε, and ν. This model includes the important effects of destructive interference between molecular and eddy viscosities.

The results of this work, which are summarized in Section 7, are in good agreement with available experimental data. They give some hope that the RNG method may provide a rational, yet workable, basis for turbulence theory in a variety of circumstances. In following papers, we shall present applications of these RNG based turbulence closures.

2. RENORMALIZATION GROUP ANALYSIS OF FLUID DYNAMICS IN AN UNBOUNDED MEDIUM

2.1. Introductory Remarks and Basic Models

Renormalization group (RNG) methods were first developed in the context of quantum field theory. Wilson (1971) applied RNG ideas to the theory of critical phenomena and was able to solve the problem of the universality of critical exponents and the Kondo problem (Wilson and Kogut, 1974). In the mid-1970s, the theory of dynamic critical phenomena was developed. This theory deals with universal features of dynamics in the vicinity of the critical point (Hohenberg and Halperin, 1977). Dynamic RNG methods developed by Ma and Mazenko (1975) have been used by Forster *et al.* (1977) to investigate velocity fluctuations governed by the Navier-Stokes equation driven by a Gaussian random force. Their ideas have been developed by others (de Dominicis and Martin, 1979; Fournier and Frisch, 1978, 1983; Yakhot, 1981) to deal with the problem of hydrodynamic turbulence. In this section, we outline the basic ideas of the RNG method. The RNG method will be used in later sections to derive both turbulence transport equations for resolvable scales and subgrid models for large-eddy numerical simulations of turbulence.

Consider the Navier-Stokes Eqs. (1.4) for incompressible flow subject to the random force $\mathbf{f}(\mathbf{x}, t)$. Here we consider a random force specified by the two-point correlation:

$$\langle f_i(\mathbf{k}, \omega) f_j(\mathbf{k}', \omega') \rangle = 2D_0 k^{-y}(2\pi)^{d+1} P_{ij}(\mathbf{k})\, \delta(\mathbf{k} + \mathbf{k}')\, \delta(\omega + \omega') \quad (2.1)$$

where the parameter y is an arbitrary number. As mentioned in Section 1, the case $y = -2$ describes fluid in thermal equilibrium driven by thermal noise. Since we are interested in studying strongly nonequilibrium flows, we concentrate on the case $y > -2$.

We introduce the Fourier decomposition of the velocity fields with an ultraviolet cutoff $\Lambda = O(k_d)$

$$v_i(\mathbf{x}, t) = \int_{k < \Lambda} \frac{d\mathbf{k}}{(2\pi)^d} \int \frac{d\omega}{2\pi} v_i(\mathbf{k}, \omega) \exp(i\mathbf{k}\cdot\mathbf{x} - i\omega t) \quad (2.2)$$

The space-time Fourier-transformed equation of motion (1.4) is

$$v_l(\hat{k}) = G^0(\hat{k}) f_l(\hat{k}) - \frac{i\lambda_0}{2} G^0(\hat{k}) P_{lmn}(\mathbf{k}) \int v_m(\hat{q})\, v_n(\hat{k} - \hat{q}) \frac{d\hat{q}}{(2\pi)^{d+1}} \quad (2.3)$$

where

$$P_{lmn}(\mathbf{k}) = k_m P_{ln}(\mathbf{k}) + k_n P_{lm}(\mathbf{k})$$
$$G^0(\mathbf{k},\omega) = G^0(\hat{k}) = [-i\omega + \nu_0 k^2]^{-1} \quad (2.4)$$

Here we have introduced the formal parameter λ_0 $(=1)$ to facilitate the perturbation solution of (2.3) given below. Introducing the ultraviolet cutoff Λ in (2.2), we assume that the Fourier modes $\mathbf{v}(\hat{k})$ vanish when $k > \Lambda$. This assumption is quite plausible, at least for the forcing (2.1) with $y > 0$, since the modes $\mathbf{v}(\hat{k})$ corresponding to wavenumbers $k > O(k_d)$ are overdamped by the viscosity term in the equation of motion (2.3).

In principle, we can use the zeroth-order $(\lambda_0 = 0)$ solution of (2.3),

$$v_l^0(\hat{k}) = G^0(\hat{k})\, f_l(\hat{k}) \quad (2.5)$$

as the basis to construct the perturbation expansion of $\mathbf{v}$ in powers of λ_0. This problem has been solved formally by Wyld (1961) and Kraichnan (1961), although the resulting series is too complex to give very useful answers (see also Monin and Yaglom, 1975). However, it is less problematic to answer the following question: How are the long-wavelength modes $\mathbf{v}^<(\hat{k})$ belonging to the interval $0 < k < \Lambda e^{-r}$ affected by the short-wavelength modes $\mathbf{v}^>(\hat{k})$ from a narrow wavevector band near the ultraviolet cutoff $\Lambda e^{-r} < k < \Lambda$? This leads directly to the renormalization group method, which enables us, in some cases, to find the *infrared* $(k \to 0)$ asymptotics of correlations generated by the model (2.1)–(2.3).

2.2. Elimination of Small Scales

Following Ma and Mazenko (1975) and Forster *et al.* (1977), the RNG procedure consists of two steps. First, we write Eq. (2.3) in terms of the two components $\mathbf{v}^<$ and $\mathbf{v}^>$ of the velocity $\mathbf{v}$:

$$v_l(\hat{k}) = G^0(\hat{k})\, f_l(\hat{k}) - \frac{i\lambda_0}{2} G^0(\hat{k})\, P_{lmn}(\mathbf{k}) \int [v_m^<(\hat{q})\, v_n^<(\hat{k}-\hat{q})$$
$$+ 2v_m^<(\hat{q})\, v_n^>(\hat{k}-\hat{q}) + v_m^>(\hat{q})\, v_n^>(\hat{k}-\hat{q})]\, \frac{d\hat{q}}{(2\pi)^{d+1}} \quad (2.6)$$

In order to eliminate modes from the interval $\Lambda e^{-r} < q < \Lambda$, all terms $\mathbf{v}^>(\hat{q})$ in (2.6) should be removed by repeated substitution of (2.3) for $\mathbf{v}^>$ back into (2.6). *This generates an infinite expansion for* $\mathbf{v}^<$ *in powers of* λ_0 in which $\mathbf{v}^>$ does not formally appear.

Second, averages are taken over the part of the random force $\mathbf{f}^>$ belonging to the strip $\Lambda e^{-r} < q < \Lambda$. This procedure formally eliminates the modes $\Lambda e^{-r} < q < \Lambda$ from the problem. It can be shown readily that, after removing the modes $\Lambda e^{-r} < q < \Lambda$, the equation of motion for $\mathbf{v}^<$ can be written up to second order in λ_0 as

$$(-i\omega + \nu_0 k^2)\, v_l^<(\hat{k})$$
$$= f_l(\hat{k}) - \frac{i\lambda_0}{2} P_{lmn}(\mathbf{k}) \int G^0(\hat{q})\, G^0(\hat{k}-\hat{q})\, f_m^>(\hat{q})\, f_n^>(\hat{k}-\hat{q})\, \frac{d\hat{q}}{(2\pi)^{d+1}}$$
$$- \frac{i\lambda_0}{2} P_{lmn}(\mathbf{k}) \int v_m^<(\hat{q})\, v_n^<(\hat{k}-\hat{q})\, \frac{d\hat{q}}{(2\pi)^{d+1}}$$
$$+ 4\left(\frac{i\lambda_0}{2}\right)^2 2D_0 P_{lmn}(\mathbf{k}) \int |G^0(\hat{q})|^2\, G^0(\hat{k}-\hat{q})$$
$$\times P_{npq}(\mathbf{k}-\mathbf{q})\, P_{mp}(\mathbf{q})\, q^{-y}\, v_p^<(\hat{k})\, \frac{d\hat{q}}{(2\pi)^{d+1}}$$
$$+ O[(v^<)^3] \quad (2.7)$$

The second term on the right side of (2.7) is an induced random force, denoted by Δf_l, with zero mean if the forces are assumed to be statistically homogeneous.

Equation (2.7) is an approximation for $\mathbf{v}^<(\hat{k})$ that is valid in the limit $k \to 0$. It should be noted that, in addition to the terms accounted for in (2.7), *the scale elimination procedure introduces terms like*

$$\tfrac{1}{2}i P_{lmn}(\mathbf{k}) \int G^0(\hat{q})\, f_m^>(\mathbf{q})\, v_n^<(\mathbf{k}-\mathbf{q})$$

which we neglect, since they vanish after averaging over the force $\mathbf{f}^>$. It should be emphasized that the mean square of such terms does not vanish, but they go rapidly to zero when $k \to 0$. Another type of contribution generated by the scale elimination procedure and which is not taken into consideration in (2.7) is of the form

$$\lambda_0^3\, \delta\Gamma\, P_{lmn}(\mathbf{k}) \int v_m^<(\hat{q})\, v_n^<(\hat{k}-\hat{q})\, \frac{d\hat{q}}{(2\pi)^{d}}$$

where $\delta\Gamma$ is a "vertex" correction associated with the nonlinear term. It has been shown by Forster *et al.* (1977) that Galilean invariance implies that $\delta\Gamma = 0$ in the limit $k \to 0$.

In this work our goal is to assess the effect of small (and fast) eddies on the large (and slow) turbulent eddies. Thus, we are interested in the asymptotic description of the modes $v^<(\mathbf{k}, \omega)$ in the limit $k \to 0$ and $\omega \to 0$. On the basis of previous applications of the RNG method to other physical systems, we may expect that the resulting analysis is still reasonably accurate for finite $\mathbf{k}$, ω in the inertial range.

To begin the analysis of (2.7), let us evaluate the last term on the right side

$$R_l = -\lambda_0^2 \frac{2D_0}{(2\pi)^{d+1}} P_{lmn}(\mathbf{k}) \int^> |G^0(\hat{q})|^2 G^0(\hat{k} - \hat{q}) \times P_{n\mu\rho}(\mathbf{k} - \mathbf{q}) P_{m\rho}(\mathbf{q}) q^{-y} v_\rho^<(\hat{k})\, d\hat{q} \tag{2.8}$$

where the symbol $\int^>$ indicates integration over the band being removed

$$\int^> d\hat{q} = \int_{\Lambda_0 e^{-r} < q < \Lambda} d\mathbf{q} \int_{-\infty}^{\infty} d\Omega \tag{2.9}$$

where $\hat{q} = (\mathbf{q}, \Omega)$. Performing the frequency integration gives

$$R_l = -\lambda_0^2 \frac{2D_0\pi}{\nu_0(2\pi)^{d+1}} P_{lmn}(\mathbf{k}) \int^> \frac{P_{n\mu\rho}(\mathbf{k} - \mathbf{q}) P_{m\rho}(\mathbf{q}) q^{-y-2}\, d\mathbf{q}}{i\omega + \nu_0 q^2 + \nu_0 |\mathbf{k} - \mathbf{q}|^2} v_\rho^<(\hat{k}) \tag{2.10}$$

We shall evaluate (2.10) in the limit $\omega \to 0$ and $k \to 0$. Changing the integration variable by replacing $\mathbf{q} \to \mathbf{q} + \frac{1}{2}\mathbf{k}$ gives

$$R_l = -\lambda_0^2 \frac{2D_0\pi}{(2\pi)^{d+1}\nu_0} P_{lmn}(\mathbf{k}) \times \int^> \frac{P_{n\mu\rho}(\frac{1}{2}\mathbf{k} - \mathbf{q}) P_{m\rho}(\mathbf{q} + \frac{1}{2}\mathbf{k}) |\mathbf{q} + \frac{1}{2}\mathbf{k}|^{-y-2}\, d\mathbf{q}}{i\omega + 2\nu_0 q^2 + \nu_0 k^2/2} v_\rho^<(\hat{k}) \tag{2.11}$$

Neglecting terms that are $O(k^2)$ as $k \to 0$ in the integrand on the right side of (2.11) gives

$$R_l = -\frac{\lambda_0^2 2D_0\pi P_{lmn}(\mathbf{k})}{2(2\pi)^{d+1}\nu_0^2} \times \int^> q^{-2}|\mathbf{q} + \tfrac{1}{2}\mathbf{k}|^{-y-2}\{[k_\mu P_{n\rho}(\mathbf{q} - \tfrac{1}{2}\mathbf{k}) - q_\mu P_{n\rho}(\mathbf{q} - \tfrac{1}{2}\mathbf{k})] \times P_{m\rho}(\mathbf{q} + \tfrac{1}{2}\mathbf{k})\} v_\rho^<(\hat{k})\, d\mathbf{q} \tag{2.12}$$

It is easy to check that, to $O(k^2)$,

$$P_{n\rho}(\mathbf{q} - \tfrac{1}{2}\mathbf{k}) P_{m\rho}(\mathbf{q} + \tfrac{1}{2}\mathbf{k}) \simeq P_{mn}(\mathbf{q}) + \tfrac{1}{2}k_m q_n - \tfrac{1}{2}q_m k_n \tag{2.13}$$

Noting that $P_{lmn}(\mathbf{k}) = -P_{lnm}(\mathbf{k})$, we conclude that the $O(k)$ terms on the right side of (2.13) do not contribute to leading order in the integral (2.12). Thus,

$$R_l = -\frac{\lambda_0^2 D_0 P_{lmn}(\mathbf{k})}{2\nu_0^2(2\pi)^d} \times \int^> q^{-y-4}\left[k_\mu P_{n\rho}(\mathbf{q}) P_{m\rho}(\mathbf{q}) + q_\rho P_{mn}(\mathbf{q}) \frac{y+2}{2}\frac{k_s q_s}{q^2}\right] d\mathbf{q}\, v_\rho^<(\hat{k}) \tag{2.14}$$

The angular integration in (2.14) is easily caried out using the well-known relations

$$\int q_\alpha q_\beta\, d^d q = \frac{S_d}{d}\delta_{\alpha\beta} \int q^{d+1}\, dq \tag{2.15}$$

and

$$\int q_\alpha q_\beta q_\gamma q_\delta\, d^d q = \frac{S_d}{d(d+2)}(\delta_{\alpha\beta}\delta_{\gamma\delta} + \delta_{\alpha\gamma}\delta_{\beta\delta} + \delta_{\alpha\delta}\delta_{\gamma\beta}) \int q^{d+3}\, dq \tag{2.16}$$

where $S_d = 2\pi^{d/2}/\Gamma(d/2)$ is the area of a d-dimensional unit sphere. Using (2.15) and (2.16), we obtain

$$P_{lmn}(\mathbf{k}) k_\mu v_\rho^<(\hat{k}) \int^> P_{n\rho}(\mathbf{q}) P_{m\rho}(\mathbf{q}) q^{-y-4}\, d\mathbf{q} = k^2 v_l^<(\hat{k})\left[\frac{d-2}{d} + \frac{2}{d(d+2)}\right]\frac{e^{\epsilon r} - 1}{\epsilon} \tag{2.17}$$

where

$$\epsilon = 4 + y - d \tag{2.18}$$

Also, we find

$$\frac{y+2}{2} P_{lmn}(\mathbf{k}) \int^> q^{-y-4}\frac{q_\rho q_s k_s}{q^2} P_{mn}(\mathbf{q})\, d\mathbf{q}\, v_\rho^<(\hat{k}) = -\frac{y+2}{d(d+2)}\frac{e^{\epsilon r} - 1}{\epsilon} S_d k^2 v_l^< \tag{2.19}$$

Combining (2.17)–(2.19), the result is

$$R_l = -\frac{\lambda_0^2 D_0}{\nu_0^2 \Lambda^\epsilon}\frac{S_d}{(2\pi)^d}\frac{d^2 - d - \epsilon}{2(d+2)d}\frac{e^{\epsilon r} - 1}{\epsilon} k^2 v_l^< \tag{2.20}$$

This gives $R \approx \Delta\nu(k)k^2 \mathbf{v}^<(\hat{k})$, so the effect of this term is to modify the viscous term on the left side of (2.7).

We conclude that, in the limit $k \to 0$, $\omega \to 0$, the correction to the viscosity is given by

$$\Delta\nu(0) = A_d \frac{\lambda_0^2 D_0}{\nu_0^2 \Lambda^\epsilon} \frac{e^{(4+y-d)r} - 1}{4+y-d} \tag{2.21}$$

where

$$A_d = \bar{A}_d \frac{S_d}{(2\pi)^d}; \qquad \bar{A}_d = \frac{1}{2}\frac{d^2-d}{d(d+2)}; \qquad \epsilon = 4+y-d \tag{2.22}$$

Thus, the viscosity resulting from the elimination of the modes $v^>$ is

$$\nu_r = \nu_0\left(1 + A_d \bar{\lambda}_0^2 \frac{e^{(4+y-d)r} - 1}{4+y-d}\right) \tag{2.23}$$

where the dimensionless coupling constant $\bar{\lambda}_0$ is defined by

$$\bar{\lambda}_0 = \lambda_0 D_0^{1/2} / \nu_0^{3/2} \Lambda^{\epsilon/2} \tag{2.24}$$

Substituting this result into (2.7) gives the intermediate-state Navier-Stokes equations (without rescaling)

$$\begin{aligned} v_l^<(\hat{k}) &= G_r(\hat{k})(f_l + \Delta f) \\ &\quad - \frac{i\lambda_0}{2} G_r(\hat{k}) P_{lmn}(k) \int v_m^<(\hat{q}) v_n^<(\hat{k}-\hat{q}) \frac{d\hat{q}}{(2\pi)^{d+1}} \\ &\quad + O[(v^<)^3] \end{aligned} \tag{2.25}$$

where the intermediate-scale Green's function (propagator) is given by

$$G_r = (-i\omega + \nu_r k^2)^{-1}$$

with ν_r given by (2.23). Equation (2.25) is defined on the domain $0 < k < \Lambda e^{-r}$, unlike the original Navier-Stokes equation, which is defined on the larger interval $0 < k < \Lambda$.

2.3. Recursion Relations: Rescaling of the Variables

The next step of the RNG procedure, following Forster *et al.* (1977) and Ma and Mazenko (1975), consists in rescaling the variables according to

$$k = k' e^{-r}, \qquad \omega = \omega' e^{-\alpha(r)}, \qquad v^<(\mathbf{k}, \omega) = \xi v'(\mathbf{k}', \omega') \tag{2.26}$$

Thus, the new variable $\mathbf{k}'$ is defined on the same interval $0 < k' < \Lambda$ as the wavevector $\mathbf{k}$ in the original Navier-Stokes equation. In terms of the new variables, given by (2.26), the intermediate Navier-Stokes equation is

$$\begin{aligned} v_l'(\hat{k}') &= G_r(\hat{k}') f_l'(\hat{k}') - \frac{i\lambda(r)}{2} G_r(\hat{k}') P_{lmn}(\mathbf{k}') \\ &\quad \times \int v_m'(\hat{q}') v_n'(\hat{k}' - \hat{q}') \frac{d\hat{q}'}{(2\pi)^{d+1}} + \cdots \end{aligned} \tag{2.27}$$

where

$$G_r = [-i\omega + \nu(r)(k')^2]^{-1}$$

$$\mathbf{f}'(\hat{k}') = \mathbf{f}^<(\hat{k}) e^{\alpha(r)} \xi^{-1}(r) \tag{2.28}$$

$$\lambda(r) = \lambda_0 \xi(r) e^{-(d+1)r} \tag{2.29}$$

$$\nu(r) = \nu_r e^{\alpha(r) - 2r} \tag{2.30}$$

The correlation function characterizing the force $\mathbf{f}'(\hat{k}')$, given by expression (2.28), can be constructed readily using definition (2.1) and the new set of variables (2.26):

$$\langle f_i'(\mathbf{k}, \omega) f_j'(\mathbf{k}', \omega') \rangle = 2D'(2\pi)^{d+1} k^{-y} P_{ij}(\mathbf{k}) \delta(\mathbf{k} + \mathbf{k}') \delta(\omega + \omega') \tag{2.31}$$

with

$$D' = \frac{D_0 \exp[3\alpha(r) + (d+y)r]}{\xi^2} \tag{2.32}$$

Noting that the elimination of small scales does not influence D_0, we choose the function ξ in such a way that $D' = D_0$ at each step of the RNG procedure:

$$\xi = \exp\left[\frac{3}{2}\alpha(r) + \frac{d+y}{2} r\right] \tag{2.33}$$

The procedure described so far is formally exact in the limit $r \to 0$. To eliminate a finite band of $\mathbf{k}$ space, one can iterate the above procedure by eliminating step by step infinitesimally narrow wavenumber bands. The coupling constants generated in this way depend on r and satisfy the following differential recursion relations, which follow from (2.22)-(2.24), (2.29), and (2.30).

$$\frac{d\nu}{dr} = \nu(r)[z - 2 + A_d\bar{\lambda}^2] \qquad (2.34)$$

$$\frac{dD}{dr} = 0 \qquad (2.35)$$

$$\frac{d\lambda}{dr} = \lambda(r)\left[\frac{3}{2}z - 1 - \frac{d-y}{2}\right] \qquad (2.36)$$

Here we define z by

$$dx/dr = z$$

and the dimensionless expansion parameter $\bar{\lambda}$ is defined in terms of $\lambda(r)$, $\nu(r)$, and $D(r)$ as

$$\bar{\lambda}^2 = \lambda^2 D/\nu^3 \Lambda^{\varepsilon} \qquad (2.37)$$

The recursion relation for $\bar{\lambda}$ can be derived readily from (2.34)–(2.36):

$$d\bar{\lambda}/dr = \tfrac{1}{2}\bar{\lambda}(\varepsilon - 3A_d\bar{\lambda}^2) \qquad (2.38)$$

where $\varepsilon = 4 + y - d$.

Equation (2.38) implies that, if $\varepsilon < 0$, the effective coupling constant $\bar{\lambda} \to 0$ when $r \to \infty$. When $\varepsilon > 0$, $\bar{\lambda}$ tends to a fixed point $\bar{\lambda}^*$:

$$\bar{\lambda} \to \bar{\lambda}^* = (\varepsilon/3A_d)^{1/2} \quad \text{as} \quad r \to \infty \qquad (2.39)$$

according to the formula

$$\bar{\lambda}(r) = \bar{\lambda}_0 e^{\varepsilon r/2}\left[1 + \frac{3}{\varepsilon}A_d\bar{\lambda}_0^2(e^{\varepsilon r} - 1)\right]^{-1/2} \qquad (2.40)$$

At the fixed point $\bar{\lambda}^*$, the viscosity $\nu(r)$ becomes r independent if

$$z = 2 - \varepsilon/3 \qquad (2.41)$$

Treating ε as a small parameter, the value of $\bar{\lambda}$ should be evaluated in terms of the ε expansion with the parameter A_d calculated to the lowest order in ε. The accuracy and basis of this ε expansion will be discussed below.

2.4. Energy Spectrum

The expression (2.33) fully determines the scaling (2.26). Homogeneity relations can be constructed by demanding that the correlation functions computed from the original and reduced (renormalized) equations of motion be the same for all $k < \Lambda e^{-r}$:

$$(2\pi)^{d+1} V_{ij}(\mathbf{k},\omega) = \frac{\langle v_i(\mathbf{k},\omega)\, v_j(\mathbf{k}',\omega')\rangle}{\delta(\mathbf{k}+\mathbf{k}')\,\delta(\omega+\omega')}$$

$$= \xi^2 e^{[illegible]} \frac{\langle v_i(\mathbf{k}e^r, \omega e^{\alpha})\, v_j(\mathbf{k}'e^r, \omega' e^{\alpha})\rangle}{\delta(\mathbf{k}e^r + \mathbf{k}'e^r)\,\delta(\omega e^{\alpha} + \omega' e^{\alpha})} \qquad (2.42)$$

Noting (2.33) and that $\alpha = zr$ when z is constant gives the solution of (2.42) as

$$V_{ij}(k,\omega) = O[k^{[illegible]} F(\omega/k^z)] \qquad (2.43)$$

The energy spectrum can be evaluated from (2.43) as

$$E(k) = \mathrm{Tr}\, k^{d-1}\int V_{ij}(k,\omega)\frac{d\omega}{2\pi}$$

$$= O(k^{[illegible]}) = O(k^{[illegible]}) \qquad (2.44)$$

where we use expression (2.41) for z.

The asymptotic solution (2.44) has been derived from the theory that takes into account only terms up to $\bar{\lambda}^2$. This is justified in terms of the ε expansion. A remaining problem is that the nonlinear terms generated by the renormalization procedure have been neglected. This problem is addressed next.

2.5. Irrelevant Nonlinear Terms

The typical nonlinear contribution in the Navier–Stokes equation after the elimination of small scales is

$$v_l(\hat{k}) = \mathrm{NS} + \mu(r)\, G(\hat{k})\, P_{lmn}(\mathbf{k}) \int P_{n\ldots}(\mathbf{q})\, G(\hat{q})$$

$$\times v_m^<(q_1)\, v_n^<(\hat{q} - \hat{q}_1)\, v_\alpha^<(\hat{k} - \hat{q} - \hat{q}_1)\frac{d\hat{q}}{(2\pi)^{d+1}}\frac{d\hat{q}_1}{(2\pi)^{d+1}}$$

where NS symbolizes the terms in the Navier–Stokes equation taken into account in the RNG analysis given above. Performing the scale transformation (2.26), we find that

$$\mu(r) \approx \mu_0 \xi^2 e^{[illegible]} = \mu_0 e^{[illegible]} \qquad (2.45)$$

in the vicinity of the fixed point where relations (2.26)–(2.33) hold. It follows from (2.45) that, when $y < d$, the proportionality coefficient $\mu(r)$ tends exponentially to zero when $r \to \infty$, so that the new nonlinear contributions to the Navier–Stokes equation are *irrelevant*. This means in turn that the solution (2.43) is asymptotically exact in the limit $k \to 0$. On the other hand, if $y > d$, the theory diverges in the limit $k \to 0$, which is reflected in the growing importance of the nonlinearities generated by the elimination of small scales ($\mu \to \infty$ with $r \to \infty$). If $y = d$, it follows from (2.44) that

$$E(k) = O(k^{-5/3}) \qquad (2.46)$$

The result (2.46) shows that the fluid driven by the random force (2.1) with $y = d$ generates velocity correlations described, in the limit $k \to 0$, by the Kolmogorov law (2.46). The only problem is that, as seen from (2.45), the nonlinear terms generated by the procedure are marginal, i.e., they approach a finite nonzero value. This means that formula (2.46) is not an exact solution of the problem in the limit $k \to 0$, but is at the edge of the region of convergence ($y \to d^-$). One can hope that in this case the contributions from nonlinear operators are not too large, although the justification for this conclusion is weak. However, it is gratifying that the nonlinear operators with $y = d$ do not grow to infinity, so one can hope that they lead only to logarithmic corrections to (2.46), as in the theory of critical phenomena.

2.6. Renormalized Equation of Motion

The RNG method has allowed us to develop the equation of motion for the velocity field modes with $k \to 0$ averaged over the small scales $q > \Lambda e^{-r}$. The equation of motion at the fixed point is

$$\frac{\partial \mathbf{v}^<}{\partial t} + (\mathbf{v}^< \cdot \nabla)\mathbf{v}^< = \mathbf{f} - \frac{1}{\rho}\nabla p + \nu \nabla^2 \mathbf{v}^< \qquad (2.47)$$

where $\nu(r)$ is the solution of the recursion relation (2.34). It follows from (2.26) that, at the fixed point, the frequency scales as $\omega \approx k^z$. This implies, in turn, that the viscosity becomes k dependent (since $z = 2/3$ when $y = d = 3$). Indeed,

$$\omega = O(k^{2/3}) \approx \nu(k)k^2 \qquad (2.48)$$

so $\nu = O(k^{-4/3})$, which is a result well known from the theory of isotropic turbulence.

Note also that *in the derivation of* (2.47) we neglected the correction to the random force whose correlation function is proportional to k^2. In the limit $k \to 0$ this force is negligible in comparison with original forcing given by (2.1) with $y < -2$.

The major drawback of the RNG method in the formulation given here is that it does not provide the proportionality coefficients needed for simulations of real flows. Another problem with the method is that it deals with a fluid stirred by a random force with a given coefficient D_0. The latter problem is a major drawback, since in real flows the intensity of turbulent pulsations, which are proportional to D_0, has to be determined from the dynamics of the problem. In the next sections, we shall rework the RNG method described above to resolve some of these problems and to make the RNG technique suitable for the derivation of subgrid scale and transport turbulence models.

2.7. RNG Evaluation of the Kolmogorov Constant

It has been shown above that the elimination of the modes $\mathbf{v}^>(\hat{q})$ belonging to the band near the ultraviolet cutoff $\Lambda e^{-r} < q < \Lambda$ leads to the following corrections to viscosity at long space time scales:

$$\Delta\nu(0) = A_d \frac{\lambda_0^2 D_0}{\nu_0^2 \Lambda^\epsilon} \frac{e^{\epsilon r} - 1}{\epsilon} \qquad (2.49)$$

where

$$A_d = \bar{A}_d \frac{S_d}{(2\pi)^d}; \qquad \bar{A}_d = \frac{1}{2}\frac{d^2 - d}{d^2 + 2d}; \qquad \epsilon = 4 + y - d$$

and $S_d = 2\pi^{d/2}/\Gamma(d/2)$ is the area of the unit sphere in d dimensions. From now on we consider only the case $y = d$.

The elimination procedure described in the previous section is accurate in the limit $r \to 0$. We conclude that elimination of small scales with $\Lambda e^{-r} < q < \Lambda$ *does not affect either the coupling constant λ_0 or the forcing amplitude D_0*. The constancy of D_0 under this renormalization holds because, while the second term on the right side of Eq. (2.7) gives a zero-mean (averaged over $\mathbf{k}^>$) Gaussian random variable with correlation function proportional to k^2, this correction cannot be absorbed in the bare force (2.1), whose correlation function is proportional to k^{-y} ($y > -2$). Thus, $D = D_0$ and we must include a new random force with correlation function proportional to k^2 in the renormalized Navier–Stokes equations. The fact that λ_0 is not renormalized is a consequence of Gaussian invariance (Forster *et al.*, 1977).

It is also possible to eliminate a finite band of modes $\Lambda e^{-r} < q < \Lambda$ by iterating the above procedure of eliminating an infinitesimally narrow band of modes but not performing the rescaling procedure (2.26). The goal of this unscaled iteration procedure is to generate a renormalized viscosity coefficient $\nu = \nu(r)$ and coupling constant $\bar{\lambda} = \bar{\lambda}(r)$ while $D(r) = D_0$ and $\lambda(r) = \lambda_0$ still hold. While the elimination of an infinitesimal band of modes is justified by the use of second order perturbation solutions of the Navier-Stokes equations [or by comparing with the results of applying Kraichnan's (1959) direct-interaction approximation to this system], the result of the iteration procedure is no longer justifiable in this way. The nature of the errors incurred by the iteration procedure must be clarified later.

The functions $\nu(r)$ and $\bar{\lambda}(r)$ are most easily determined by taking the limit $r \to 0$ in (2.23) in order to obtain the differential equation

$$d\nu/dr = A_d \nu(r) \bar{\lambda}^2(r) \tag{2.50}$$

where

$$\bar{\lambda}^2(r) = \frac{\lambda_0^2 D_0}{\nu^3(r) \Lambda^{\varepsilon}} e^{\varepsilon r} \tag{2.51}$$

Since $\Lambda(r) = \Lambda e^{-r}$. Here we emphasize that the rescaling (2.26) is *not* done. The solution of (2.50)–(2.51) is

$$\nu(r) = \nu_0 [1 + \tfrac{3}{2} A_d \bar{\lambda}_0^2 (e^{\varepsilon r} - 1)/\varepsilon]^{1/3} \tag{2.52}$$

and

$$\bar{\lambda}(r) = \bar{\lambda}_0 e^{\varepsilon r/2} [1 + \tfrac{3}{2} A_d \bar{\lambda}_0^2 (e^{\varepsilon r} - 1)/\varepsilon]^{-1/2} \tag{2.53}$$

which coincides with (2.40) when $y = d$. In the limit $r \to \infty$, the parameter $\bar{\lambda}$ given by (2.53) approaches the fixed point

$$\bar{\lambda}^* = (4\varepsilon/3A_d)^{1/2} \quad (\varepsilon/3A_d)^{1/2} \tag{2.54}$$

It has been mentioned in the previous section that at the fixed point the coupling parameter (2.54) can be treated, from the point of view of the ε expansion, as a small parameter. Thus, in the zeroth order, neglecting the nonlinear term in the forced Navier-Stokes equation defined on the smaller domain $0 < k < \Lambda e^{-r}$, one has that the velocity field is determined by

$$v_i(\hat{k}) = G(\hat{k}) f_i(\hat{k})$$

where the renormalized propagator $G(\hat{k})$ is given by

$$G(\hat{k}) = [-i\omega + \nu(r)k^2]^{-1} \tag{2.56}$$

If only modes with wavenumbers larger than $\Lambda(r)$ are removed by renormalization, then (2.45) gives a k dependent viscosity in the limit $r \to \infty$:

$$\nu(k) = (\tfrac{3}{4} A_d D_0)^{1/3} k^{-4/3} \tag{2.57}$$

where we have set $\lambda_0 = 1$.

Equation (2.55) leads to the energy spectrum

$$\begin{aligned} E(k) &= \frac{1}{2} \frac{S_d k^{d-1}}{(2\pi)^{d+1}} \int_{-\infty}^{\infty} \mathrm{Tr}\, U_0(\mathbf{k}, \omega)\, d\omega \\ &= \frac{1}{2(\frac{3}{4} A_d)^{1/3}} \left(2D_0 \frac{S_d}{(2\pi)^d}\right)^{2/3} k^{-5/3} \\ &= 1.186 \left(2D_0 \frac{S_d}{(2\pi)^d}\right)^{2/3} k^{-5/3} \end{aligned} \tag{2.58}$$

Formula (2.58) has also been derived by Fournier and Frisch (1983). We remark that the numerical constants appearing in (2.58) and in later equations are evaluated at the fixed point to lowest order in ε. Thus, $\bar{A}_d$ in (2.22) is evaluated at $\varepsilon = 0$ as $\bar{A}_3 = 0.2$.

To derive the Kolmogorov constant for the inertial-range power spectrum we must relate D_0 in (2.58) to the mean rate of energy dissipation $\bar{\varepsilon}$. To do this we can use the solution (2.57) for $\nu(k)$ and the equation for energy balance following the calculation of Kraichnan (1971). Substituting the inertial range spectral law

$$E(k) = C_K \bar{\varepsilon}^{2/3} k^{-5/3} \tag{2.59}$$

into the energy balance equation in the inertial range gives [Kraichnan, 1971, Eq. (3.1); see also Leslie, 1972]

$$\frac{(3/8 \bar{A}_d)^{1/2}}{C_K^{3/2}} \left(\frac{2D_0 S_d/(2\pi)^d}{\bar{\varepsilon}}\right)^{1/2} = 0.1904$$

so

$$C_K = 1.496 \left(\frac{2D_0 S_d/(2\pi)^d}{\bar{\varepsilon}}\right)^{1/3} \tag{2.60}$$

Consistency between (2.59) with (2.60) and (2.58) requires that $\bar{\varepsilon}$ and D_0 be proportional, namely,

$$2D_0 S_d/(2\pi)^d = 1.594 \bar{\varepsilon} \tag{2.61}$$

Substituting (2.61) into (2.58) gives the energy spectrum

$$E_{RNG}(k) = 1.617\bar{\varepsilon}^{2/3}k^{-5/3} \qquad (C_K = 1.617) \tag{2.62}$$

The relation (2.61) will be used later in this paper to derive transport models.

3. RNG SUBGRID SCALE TURBULENCE MODEL FOR LARGE-EDDY SIMULATIONS

Using (2.61), we can rewrite the result (2.52) of the RNG theory in terms of the total mean dissipation rate $\bar{\varepsilon}$ as

$$\nu_r = \nu_0[1 + a\bar{\varepsilon}/\nu_0^3\Lambda^4(e^{4r} - 1)]^{1/3} \tag{3.1}$$

where $a = 1.594(\frac{3}{8}\bar{A}_d)^3 \approx 0.120$. The RNG subgrid scale turbulence model is derived as follows: Let $\bar{\Delta}$ be the computational mesh size and let $\Lambda_0 = \pi/\bar{\Delta}$ be the wavevector corresponding to the scale $\bar{\Delta}$. Our goal is to eliminate all scales $\Lambda_0 < k \le \Lambda$ from the problem. The corresponding *subgrid* model is given by (3.1) with the wavevector $\Lambda_0 = \Lambda e^{-r}$ expressed through $\bar{\Delta}$. However, it is customary to express the viscosity in terms of $\Delta = 2\bar{\Delta}$. Here, Δ is the width of a suitably chosen Gaussian filter. It is known from the theory of isotropic turbulence that the dissipation cutoff $k_d \approx \Lambda$ is not an independent parameter, but obeys the relation

$$k_d = \Lambda = \gamma(\bar{\varepsilon}/\nu_0^3)^{1/4}$$

where $\gamma \approx 0.2$ according to experimental data. Thus, relation (3.1) becomes

$$\nu = \nu_0\left[1 + H\left(\frac{a\bar{\varepsilon}}{(2\pi)^4\nu_0^3}\Delta^4 - C\right)\right]^{1/3} \tag{3.2}$$

where $C = a/\gamma^4$. Here, the Heaviside function, defined by $H(x) = x$ when $x > 0$ and $= 0$ otherwise, reflects the fact that $r > 0$ in (3.1).

Formula (3.2) express the renormalized viscosity in terms of $\bar{\varepsilon}$ and the filter length scale Δ. It is important that $\bar{\varepsilon}$ is a flow parameter that does not depend on the scale $\Lambda_0 = \Lambda e^{-r}$. This means that

$$\bar{\varepsilon} = \frac{\nu_0}{2}\left(\frac{\partial v_i}{\partial x_j} + \frac{\partial v_j}{\partial x_i}\right)^2 = \frac{\nu(r)}{2}\left(\frac{\partial v_i^<}{\partial x_j} + \frac{\partial v_j^<}{\partial x_i}\right)$$

so that $\bar{\varepsilon}$ can be expressed entirely through the *resolvable field* $\mathbf{v}^<$. This makes it possible to use formula (3.2) for large eddy simulations. Writing

$$\bar{\varepsilon} = \frac{\nu(r)}{2}\left(\frac{\partial v_i^<}{\partial x_j} + \frac{\partial v_j^<}{\partial x_i}\right)^2 \tag{3.3}$$

and substituting into (3.2), we obtain

$$\nu = \nu_0\left[1 + H\left(\frac{a\Delta^4}{2(2\pi)^4\nu_0^3}\nu\left(\frac{\partial v_i^<}{\partial x_j} + \frac{\partial v_j^<}{\partial x_i}\right)^2 - C\right)\right]^{1/3} \tag{3.4}$$

It follows that, when $a\Delta^4/2(2\pi)^4\nu_0^3 \gg C$,

$$\nu = c_s\Delta^2\left|\frac{\partial v_i^<}{\partial x_j} + \frac{\partial v_j^<}{\partial x_i}\right| \tag{3.5}$$

where $c_s^2 = a/2(2\pi)^4$, so that

$$c_s = 0.0062 \qquad \text{(RNG)}$$

Formula (3.5) is the well known Smagorinsky (1962) eddy viscosity, which has been widely used in large-eddy simulations. Deardorff (1970, 1971) was the first to use relation (3.5) for large eddy simulations of shear flows. Deardorff (1971) argued that $c_s \approx 0.005$ worked best. Moin and Kim (1981) performed their simulations of wall-bounded shear flows with $c_s \approx 0.003$. However, in order to prevent the turbulence in the wall region from decaying, Moin and Kim redefined the average dissipation $\bar{\varepsilon}$ as the *turbulent dissipation and separated effects of mean shear from the fluctuating shear as in a turbulence transport model*. They defined $\bar{\varepsilon}$ as

$$\bar{\varepsilon} = \tfrac{1}{2}\nu_0\langle(s_{ij} - \langle s_{ij}\rangle)^2\rangle \tag{3.6}$$

where

$$s_{ij} = \frac{\partial v_i^<}{\partial x_j} + \frac{\partial v_j^<}{\partial x_i}$$

and $\langle \; \rangle$ stands for the horizontal average over all scales. Moin and Kim *also neglected the effect of random forcing due to subgrid scale motions.* They pointed out that their calculated turbulent intensities were insensitive to variations of the constant in (3.5) by 40%. Thus, we conclude that the agreement between calculated and "experimental" data are rather good.

Although the renormalized equation of motion derived in this section is basically the same as that used far from the wall by Deardorff and others, it differs significantly in the wall region, where formula (3.5) is not valid. In the wall region the renormalized Eqs. (3.4) do not lead to a turbulent eddy viscosity proportional to Λ^2. Near the wall, the argument of $H(x)$ in (3.4) is negative, so $\nu = \nu_0$.

Relations (3.1) and (3.4) are, strictly speaking, valid at the fixed point or in the limit $r \to \infty$. However, we shall use these formulas for the calculation of turbulent flows in the entire interval $0 \leq r < \infty$. The nature of the errors incurred can be illustrated by the limit $r \to 0$:

$$\nu_r = \nu_0 + A_d \bar{\lambda}_0^2 \frac{e^{\epsilon r} - 1}{\epsilon}$$

which is asymptotically accurate [see (2.23)]. Thus, the result is accurate in both limits $r \to \infty$ and $r \to 0$. Equations (3.1) and (3.4) describe the smooth transition between these two asymptotic solutions.

3.1. Role of the Random Force

Another important feature of finite systems is the role of the random force generated by the elimination of small scales. This force is a zero-mean Gaussian force given by the second term on the right side of (2.7). The analytic expression for the correlation function of this force is

$$\langle f_i(\hat{k}) f_j(\hat{k}') \rangle = D'(2\pi)^{d+1} k^{-2} P_{ij}(\mathbf{k})\, \delta(\hat{k} + \hat{k}') \qquad (3.7)$$

where

$$D' = 2D_0^2 \lambda_0^2 \int \frac{d\hat{q}}{(2\pi)^{d+1}} P_{lmn}(\mathbf{k})\, P_{ln'}(\mathbf{k})\, P_{mm'}(\mathbf{q})\, P_{nn'}(\mathbf{k}-\mathbf{q})$$

$$\times q^{-d}|\mathbf{k}-\mathbf{q}|^{-d}|G^0(\hat{q})|^2 |G^0(\hat{k}-\hat{q})|^2 \qquad (3.8)$$

The integrals in (3.8) are readily evaluated, giving

$$D' = B_d \frac{D_0^2 \lambda_0^2}{\nu_0^3} \frac{e^{3r}}{\Lambda^8} \frac{1}{9} \qquad (d = 3)$$

$$B_d = \frac{1}{2} \frac{d^2 - 2}{d(d+2)} \frac{S_d}{(2\pi)^d} \qquad (3.9)$$

The recursion relation for $D'(r)$ is derived readily:

$$\frac{dD'}{dr} = B_d \frac{D_0}{\Lambda^4(r)} \bar{\lambda}^2(r) \qquad (3.10)$$

For the approximate evaluation of (3.10) we take the coupling constant $\bar{\lambda} = \bar{\lambda}_0$ at the fixed point and find, using $y = d$:

$$D' \approx \frac{4}{15} \frac{d^2 - 2}{d^2} \frac{2D_0 S_d/(2\pi)^d}{d \; \Lambda_0^4} (e^{4r} - 1)$$

or, in other words, introducing the dissipation cutoff k_d and the cutoff corresponding to the largest eliminated scales k_c, we have

$$D' \approx 1.594 \frac{4}{15} \frac{d^2 - 2}{d^2} \frac{\bar{\varepsilon}}{d\, k_d^4} \left[\left(\frac{k_d}{k_c} \right)^4 - 1 \right] \qquad (3.11)$$

Far from the wall, where $k_d/k_c \gg 1$, the induced noise is smaller than the stirring force if

$$\frac{4}{15} \frac{d^2 - 2}{d^2} \frac{\bar{\varepsilon}}{d\, k_c^4} k^2 \ll \frac{\bar{\varepsilon}}{k^3} \qquad (3.12)$$

and thus

$$(k/k_c)^5 \ll 1 \qquad (3.13)$$

This always holds when $k \ll k_c$. If, on the other hand, $k \approx k_c$, the induced noise is comparable with the stirring force and cannot be neglected. It is clear that the role of this noise is most important in the buffer region where $k_d \approx k_c$. Indeed, setting $k_d/k_c = O(1)$, we conclude that in the buffer layer the bare and induced noises are of the same order.

4. TURBULENT HEAT AND MASS TRANSPORT

In this section, we apply the renormalization group method developed above to the problem of the distribution of a scalar advected by a turbulent fluid. The method is a combination of the ideas developed in the works of Forster *et al.* (1977) and the approach described in Sections 2 and 3. Despite the fact that modeling of flows coupled to a scalar field is of much practical importance in the description of heat and mass transfer, previous analytic theories have not led to much quantitative success. A passive scalar is governed by the equation of motion

$$\partial T/\partial t + (\mathbf{v} \cdot \nabla) T = \chi_0 \nabla^2 T \qquad (4.1)$$

where the turbulent velocity $\mathbf{v}$ is the solution of the Navier Stokes equation.

To analyze advection of a passive scalar governed by (4.1), we assume that the random temperature field, mixed by a turbulent fluid, is isotropic at small scales and is independent of the integral scale L. According to the Kolmogorov (1941) theory, the dynamics of the scalar field at scales much smaller than L are characterized by $\bar{\varepsilon}$, ν, and χ_0, and the rate of dissipation $\bar{N}$ of fluctuations of T.

$$\frac{\partial}{\partial t}\frac{1}{2}\int T^2(\mathbf{x}, t)\,d\mathbf{x} = -\chi_0\int (\nabla T)^2\,d\mathbf{x} \equiv -\bar{N} \tag{4.2}$$

In the inertial range, transfer of T fluctuations dominates dissipation, so the spectrum depends only on $\bar{\varepsilon}$ and $\bar{N}$ (see Batchelor, 1959) and the inertial range scalar spectrum is

$$E_T(k) = Ba\,\frac{\bar{N}}{\bar{\varepsilon}^{1/3}}\,k^{-5/3} \tag{4.3}$$

Here the constant Ba is called the Batchelor constant.

Another milestone of phenomenological modeling is the idea, proposed by Reynolds and extended by Prandtl and Colburn, that in the limit of large Reynolds number R the distributions of velocity and of passive scalar are similar. This leads to the inference that, at large R, the eddy viscosity ν and eddy diffusivity χ are similar, so that

$$\alpha = P_t^{-1} = \chi/\nu \tag{4.4}$$

is nearly a constant. Here P_t is the turbulent Prandtl number. The near constancy of α in (4.4) has been confirmed experimentally in a variety of flows. The value $\alpha = 1.1$–1.4 ($P_t = 0.7$–0.9) has been widely used in engineering studies.

Repeating the argument presented in Section 1, we model small scales by adding a random force to the right side of the Navier Stokes equation. *To derive the renormalized equation of motion, we Fourier transform* (4.1) to obtain

$$T(\hat{k}) = -i\lambda_0' k_j g^0(\hat{k})\int v_j(\hat{q})\,T(\hat{k}-\hat{q})\,\frac{d\hat{q}}{(2\pi)^{d+1}} \tag{4.5}$$

together with the Navier Stokes equation

$$v_l(\hat{k}) = G^0(\hat{k})f_l(\hat{k}) - \frac{i\lambda_0}{2}P_{lmn}(\mathbf{k})G^0(\hat{k})\int v_m(\hat{q})\,v_n(\hat{k}-\hat{q})\,\frac{d\hat{q}}{(2\pi)^{d+1}} \tag{4.6}$$

Equations (4.5)–(4.6) are defined on the domain $\pi/L < k < k_d$, where L is the characteristic dimension of the system and k_d is the Kolmogorov's dissipation scale, $k_d \approx 0.2(\bar{\varepsilon}/\nu_0^3)^{1/4}$. The bare propagators $G^0(\mathbf{k}, \omega)$ and $g^0(\mathbf{k}, \omega)$ are defined by

$$G^0(\mathbf{k}, \omega) \equiv G^0(\hat{k}) = (-i\omega + \nu_0 k^2)^{-1} \tag{4.7}$$

$$g^0(\mathbf{k}, \omega) \equiv g^0(\hat{k}) = (-i\omega + \chi_0 k^2)^{-1} \tag{4.8}$$

Our goal is to eliminate modes $\mathbf{v}^>$ and $T^>$ belonging to the wavenumber strip $k_d e^{-r} \leq k \leq k_d$ and to derive an equation of motion for the modes $\mathbf{v}^<$ and $T^<$ belonging to the domain $\pi/L \leq k \leq k_d e^{-r}$.

It has been shown in Section 2 that the renormalized Navier Stokes equation after elimination of small scales is (2.25) with modified viscosity ν_r given by (2.23) and the random foce Δf induced by the small scale elimination procedure.

To develop the RNG procedure for Eq. (4.5), we rewrite it as

$$\begin{aligned} T(\hat{k}) = {} & -i\lambda_0' k_j g^0(\hat{k})\int v_j^<(\hat{q})\,T^<(\hat{k}-\hat{q})\,\frac{d\hat{q}}{(2\pi)^{d+1}} \\ & - i\lambda_0' k_j g^0(\hat{k})\int [v_j^<(\hat{q})\,T^>(\hat{k}-\hat{q}) \\ & + v_j^>(\hat{q})\,T^<(\hat{k}-\hat{q}) + v_j^>(\hat{q})\,T^>(\hat{k}-\hat{q})]\,\frac{d\hat{q}}{(2\pi)^{d+1}} \end{aligned} \tag{4.9}$$

To eliminate modes from the interval $k_d e^{-r} < k < k_d$, all terms $\mathbf{v}^>(\hat{k})$ and $T^>(\hat{k})$ should be removed as in Section 2. This introduces a formal expansion in powers of λ_0 and λ_0'. This procedure leaves the bare coupling constants λ_0 and λ_0' intact in accordance with the Galilean invariance of the equations of motion. Upon constructing the formal expansion for T in powers of λ_0 and λ_0' in which $\mathbf{v}^>$ and $T^>$ do not apear, one averages over the part of the random force $\mathbf{f}^>$ belonging to the strip $k_d e^{-r} < k < k_d$. This procedure formally eliminates the modes $\mathbf{v}^>$ and $T^>$ from the problem.

After removing the modes $k_d e^{-r} < k < k_d$, one can write the equation of motion for $T^<(\hat{k})$ up to the second order in λ_0' as

$$\begin{aligned} (-i\omega + \chi_0 k^2)\,T^<(\hat{k}) = {} & -i\lambda_0' k_j\int v_j^<(\hat{q})\,T^<(\hat{k}-\hat{q})\,\frac{d\hat{q}}{(2\pi)^{d+1}} \\ & - 2(\lambda_0')^2 D_0 T^< k_j k_m\int |G^0(\hat{q})|^2 g^0(\hat{k}-\hat{q})\,q^{-y}P_{jm}(\mathbf{q})\,\frac{d\hat{q}}{(2\pi)^{d+1}} \end{aligned} \tag{4.10}$$

When the second term on the right side of (4.10) is evaluated in the limit $k \to 0$, $\omega \to 0$ it can be identified as a correction to the bare diffusivity, namely

$$\Delta\chi = \frac{k_l k_n}{k^2} 2(\lambda_0)^2 D_0 \int |G^0(\hat q)|^2 g^0(\hat k - \hat q) P_{ln}(q) q^{-y} \frac{d\hat q}{(2\pi)^{d+1}} \quad (4.11)$$

As in Section 2, the integration in (4.11) is carried out over $\hat q = (\mathbf{q}, \omega)$, where $\Lambda_d e^{-r} < q < \Lambda_d$. For $k \to 0$, the result is

$$\Delta\chi = \frac{d-1}{d} A_d \frac{(\lambda_0)^2 \nu_0^2}{\chi_0 + \nu_0} \frac{e^{\epsilon r} - 1}{\epsilon} \quad (4.12)$$

where $A_d = S_d/(2\pi)^d$ and the effective dimensionless coupling constant is

$$\bar\lambda_0 = \lambda_0 D_0^{1/2} / \nu_0^{3/2} \Lambda_d^{\epsilon/2} \quad (4.13)$$

It may be shown that if $\lambda_0 = \bar\lambda_0 = 1$, one can set $\lambda(r) = \bar\lambda(r)$ at each step of the renormalization procedure. By iteration, it is possible to eliminate modes from the finite band $\Lambda_d e^{-r} < k < \Lambda_d$ generating the renormalized viscosity $\nu = \nu(r)$ and coupling $\lambda = \lambda(r)$. Taking $r \to 0$, one derives the differential equation for the renormalized diffusivity (with $d = 3$)

$$\frac{d\chi}{dr} = \frac{2}{3} A_3 \frac{\bar\lambda^2 \nu^2}{\chi(r) + \nu(r)} \quad (4.14)$$

where

$$\bar\lambda^2 = \frac{\lambda_0^2 D_0}{\Lambda_d^\epsilon} \frac{e^{\epsilon r}}{\nu^3(r)} \quad (4.15)$$

Using (2.50) and (4.14) gives

$$\frac{d\alpha}{dr} = \nu_r \bar\lambda^2 \left(\frac{2}{3\bar A_3} \frac{1}{1+\alpha} - \alpha \right) \quad (4.16)$$

where $\alpha = \chi(r)/\nu(r)$ and $\bar\lambda_3 = 1/5$.

Equation (4.16) may be solved exactly using (2.52) and (2.53), with the result

$$\left| \frac{\alpha - a}{\alpha_0 - a} \right|^{a/(a+b)} \left| \frac{\alpha + b}{\alpha_0 + b} \right|^{b/(a+b)} = \frac{1}{[1 + \frac{3}{4}\bar A_3 \bar\lambda_0^2 (e^{4r} - 1)]^{1/3}} \quad (4.17)$$

where

$$\begin{aligned} a &= \tfrac{1}{2}\{-1 + [1 + 4(d-1)/d\bar A_3]^{1/2}\} = \tfrac{1}{2}[-1 + (43/3)^{1/2}] \approx 1.3929 \\ b &= \tfrac{1}{2}\{1 + [1 + 4(d-1)/d\bar A_3]^{1/2}\} = \tfrac{1}{2}[1 + (43/3)^{1/2}] \approx 2.3929 \end{aligned} \quad (4.18)$$

Thus, with $d = 3$,

$$\left| \frac{\alpha - 1.3929}{\alpha_0 - 1.3929} \right|^{0.6321} \left| \frac{\alpha + 2.3929}{\alpha_0 + 2.3929} \right|^{0.3679} = \frac{\nu_0}{\nu} \quad (4.19)$$

In high Reynolds number, fully-developed turbulence where $\nu_0/\nu \to 0$, $\alpha \to 1.3929$ and the turbulent Prandtl number is $P_t = 0.7179$ ($P_t = \alpha^{-1}$).

The Batchelor constant Ba in (4.3) can be evaluated from the equations of motion at the fixed point using the modified Pao (1965, 1968) theory. The equation for the energy spectrum can be written in the vicinity of the fixed point as

$$\frac{\partial E(k,t)}{\partial t} = 2D_0 \frac{S_d}{(2\pi)^d} k^{-1} + T(k,t) - 2\chi k^2 E(k,t) \quad (4.20)$$

where now ν stands for the total viscosity derived using the RNG method. It is important to notice that, since $\bar\epsilon$ is proportional to D_0, no new dimensional parameters are involved in (4.25). The rate of nonlinear energy transfer from wavenumbers less than k to wavenumbers greater than k is

$$W(k) = \int_k^\infty \bar T(k', t)\, dk' \quad (4.21)$$

where

$$\bar T(k,t) = 2D_0 \frac{S_d}{(2\pi)^d} k^{-1} + T(k', t) \quad (4.22)$$

Following Pao (1965, 1968), we assume that the function $W(k)$ is k-independent in the inertial range and that the dimensionally correct prescription

$$W(k) = 2\gamma_p \bar\epsilon^{1/3} k^{5/3} E(k) \quad (4.23)$$

holds. In a statistically stationary state, Eq. (4.20) becomes

$$\frac{d}{dk} W(k) + 2\chi k^2 E(k) = 0 \quad (4.24)$$

Substituting (4.23) into (4.24) gives a differential equation for $E(k)$. The solution of this equation satisfying the condition

$$2\nu \int k^2 E(k)\, dk = \bar\epsilon$$

is

$$E(k) = C_K k^{-5/3} \varepsilon^{2/3} \exp\left(-\frac{3}{4\gamma_p} \varepsilon^{-1/3} \nu k^{4/3}\right) \tag{4.25}$$

with $C_K = 1/(2\gamma_p)$. In the inertial range, $W(k) = \bar{\varepsilon}$.

The Batchelor constant may be derived using Pao's formulation if we introduce the scalar transfer function $W_s(k)$, which satisfies

$$\frac{dW_s(k)}{dk} + 2\alpha\nu E_s(k) = 0 \tag{4.26}$$

Equation (4.26) with $\alpha = 1.3929$ follows from the steady state transport equation for the scalar. It follows from (4.24) and (4.26) that

$$\frac{dW(k)}{dW_s(k)} = \frac{E(k)}{\alpha E_s(k)} = \frac{C_K \bar{\varepsilon}}{\alpha \; Ba \; \bar{N}} \tag{4.27}$$

The differential Eq. (4.27) is solved by assuming that, in the inertial range, ε and N are constant, so that

$$W(k) = \frac{C_K \varepsilon}{\alpha \; Ba \; N} W_s(k) \tag{4.28}$$

Pao's theory in the inertial range gives

$$W_s(k) = N$$

so that we must require that

$$Ba = C_K/\alpha = 1.16 \tag{4.29}$$

This number is in good agreement with experimental data, $Ba \approx 1.2$–1.4 (see Monin and Yaglom, 1975).

5. RNG-BASED TURBULENCE TRANSPORT APPROXIMATIONS

Turbulence transport approximations can be constructed using the RNG in several ways. In this section, we begin by deriving an RNG based algebraic turbulence model. Let us assume that the integral scale $L = \pi/\Lambda_f$ corresponds to the largest fluctuating scales in the system. This means that $\mathbf{v}(k) = \mathbf{v}(k)$ is assumed to be nonfluctuating if $k < \Lambda_f$. Eliminating all modes from the interval $\Lambda_f < k < \Lambda$, we obtain the equation of motion governing the man velocity $\bar{\mathbf{v}} = \mathbf{V}$. The (turbulent) viscosity can be obtained from the relation (3.1),

$$\nu = \nu_0 \left[1 + H\left(\frac{3}{8}\bar{A}_d \frac{1.594\bar{\varepsilon}}{\nu_0^3 \Lambda_f^4} - C\right)\right]^{1/3} \tag{5.1}$$

The result (5.1) is derived by systematic averaging over the small-scale isotropic fluctuating velocity components. It may be argued that formula (5.1) is valid only for the description of isotropic homogeneous turbulence, since it does not include the effects of strong anisotropy. However, it has been shown (Sivashinsky and Yakhot, 1985; Yakhot and Sivashinsky, 1986; Bayly and Yakhot, 1986) that in some cases strongly anisotropic small scales are effectively decoupled from the man velocity field $\mathbf{V}$, so that (5.1) may still hold. The integral scale $L = \pi/\Lambda_f$ in (5.1) should be viewed as corresponding to the largest scale within the inertial range. This point will be considered in detail in the next section.

It is convenient to express Λ_f in (5.1) through more familiar and more easily observable properties of the flow. To do this, we compute the isotropic part of the turbulent energy K,

$$K = \int_{\Lambda_f}^{\infty} E(k)\, dk = \frac{3}{2} C_K \frac{\bar{\varepsilon}^{2/3}}{\Lambda_f^{2/3}}$$

$$= \frac{3}{2} 1.617 \left(\frac{3}{8}\bar{A}_d 1.594\right)^{1/3} \frac{\bar{\varepsilon}}{\nu \Lambda_f^2} = 1.195 \frac{\bar{\varepsilon}}{\nu \Lambda_f^2} \tag{5.2}$$

where we use

$$\nu = (\tfrac{3}{8}\bar{A}_d 1.594)^{1/3} (\bar{\varepsilon}/\Lambda_f^4)^{1/3} \tag{5.3}$$

which follows from (5.1). Eliminating Λ_f between (5.2) and (5.3) gives the turbulent viscosity expressed in terms of the energy K and dissipation rate ε.

$$\nu = c_\nu K^2/\bar{\varepsilon} \tag{5.4}$$

with $c_\nu = \frac{2}{3}(1.594 \frac{3}{8}\bar{A}_d)^{1/3}/C_K^2 \approx 0.0837$. This relation, which is usually called an algebraic K–$\bar{\varepsilon}$ model, has been widely used in turbulence modeling (Launder and Spalding, 1972; Reynolds, 1976; Launder *et al.*, 1975). The "experimentally" determined coefficient $c_\nu = 0.09$ is quite close to $c_\nu = 0.0837$ obtained here by the RNG method.

Relation (5.4) can be obtained by a somewhat different, although equivalent, calculation. Let us write the total turbulent energy density as

$$K = \frac{1}{2VT}\int v^2(\mathbf{x}, t)\, d^3x\, dt \qquad (5.5)$$

where V and T are the (large) space and time extents of the flow. Introducing the Fourier decomposition (2.2) gives

$$K = \frac{1}{2}\int v_i(\hat{q})\, v_i(\hat{k} - \hat{q})\, \frac{d\hat{q}}{(2\pi)^4} \qquad (k \to 0, \omega \to 0) \qquad (5.6)$$

Here $k \to 0$ stands for $k \to k_{min} \sim \Lambda_f$, where Λ_f is the smallest wavevector at which the system dynamics is isotropic.

To evaluate (5.6), we rewrite the integral in terms of the decomposition into the $\mathbf{v}^>$ and $\mathbf{v}^<$ components.

$$2K = \int v_i^<(\hat{q})\, v_i^<(\hat{k} - \hat{q})\, \frac{d\hat{q}}{(2\pi)^4} + 2\int v_i^>(\hat{q})\, v_i^<(\hat{k} - \hat{q})\, \frac{d\hat{q}}{(2\pi)^4}$$
$$+ \int v_i^>(\hat{q})\, v_i^>(\hat{k} - \hat{q})\, \frac{d\hat{q}}{(2\pi)^4} \qquad (5.7)$$

where the integration in the last term on the right is carried out over the interval $k_d e^{-r} \le k \le k_d = \Lambda$. To leading order in λ_0, the expression (5.7) is

$$2K \approx \int v_i^<(\hat{q})\, v_i^<(\hat{k} - \hat{q})\, \frac{d\hat{q}}{(2\pi)^4} + Q^> = Q^< + Q^> \qquad (5.8)$$

where

$$Q^> = 2D_0 \int |G^0(\hat{q})|^2\, P_{ii}(\mathbf{q})\, q^{-y}\, \frac{d\hat{q}}{(2\pi)^4} \qquad (y = d = 3) \qquad (5.9)$$

The integral $Q^>$ is evaluated as

$$Q^> = \frac{2D_0 S_d/(2\pi)^d}{\nu_0 \Lambda^2}\, \frac{e^{2r} - 1}{2} \qquad (5.10)$$

It follows from (5.7)–(5.10) that the kinetic energy can be decomposed into the part due to components $v^<$ and an additional contribution $Q^>$ that takes into account eliminated modes from the interval $k_d e^{-r} < k < k_d$.

The result (5.10) can be iterated as done earlier in this paper. Replacing ν_0 and Λ by $\nu(r)$ and $\Lambda(r)$, we have that the differential relation for $Q(r)$ is simply

$$\frac{dQ}{dr} = \frac{2D_0}{\nu(r)\, \Lambda(r)^2}\, \frac{S_d}{(2\pi)^d}$$
$$= \frac{2D_0}{\nu_0 \Lambda^2}\, \frac{S_d}{(2\pi)^d}\, \frac{e^{2r}}{[1 + \frac{3}{2}\bar{A}_d \lambda_0^2 (e^{4r} - 1)]^{1/3}} \qquad (5.11)$$

The recursion relation (5.11) is easily integrated in the limit of fully developed turbulence $\frac{3}{2}\bar{A}_d \lambda_0^2 e^{4r} \gg 1$. Integrating up to the scale Λ_f gives

$$Q = \frac{3}{2}\, \frac{2D_0 S_d/(2\pi)^d}{\nu \Lambda_f^2} \qquad (5.12)$$

Substituting (5.12) into (5.8) and keeping in mind that $Q^< \to 0$ when $k \to \Lambda_f$, we obtain

$$K \approx \frac{3}{4}\, \frac{2D_0 S_d/(2\pi)^d}{\nu \Lambda_f^2} \qquad (5.13)$$

so that

$$K = 1.195\bar{\varepsilon}/\nu \Lambda_f^2$$

which is identical to (5.2). Note that it follows by eliminating $\bar{\varepsilon}$ from (5.2) and (5.4) that

$$10\nu^2 \Lambda_f^2 = K \qquad (5.14)$$

The algebraic model (5.4) is valid only in the strongly turbulent regions of the flow. To account for the low-Reynolds-number parts of the flow, the recursion relation (45.11) must be integrated everywhere, including regions where $\frac{3}{2}\bar{A}_d \lambda_0^2 e^{4r} \approx O(1)$. This gives the differential transport model that is derived in the next section.

In the above discussion, we have given the basic steps of the averaging procedure that will be used to derive transport models. The basic idea of the method is summarized as follows: To obtain the mean of any nonlinear term in the velocity field, say Y, we compute $Y(k)$ in the limit $k \to 0$. This is done by repetitive averaging over shells in wavevector space $\Lambda e^{-r} \le k \le \Lambda$ using the Navier–Stokes equation to remove unwanted modes. Eliminating all modes from the interval $\Lambda_f < k < \Lambda$ leads to the evaluation of Y.

To illustrate the procedure again, we shall compute the skewness factor S_3, defined as

$$-S_3 = \overline{(\partial v_1/\partial x_1)^3}/[\overline{(\partial v_1/\partial x_1)^2}]^{3/2} \equiv A/B^{3/2} \qquad (5.15)$$

First we calculate

$$A = \overline{(\partial v_i/\partial x_j)^3}$$

$$= -i\int q_i Q_j (k - q - Q)_i\, v_j(\hat{q})\, v_i(\hat{Q})\, v_j(\hat{k} - \hat{q} - \hat{Q})\, \frac{d\hat{q}\, d\hat{Q}}{(2\pi)^{2d+2}} \qquad (5.16)$$

in the limit $k \to 0$.

Decomposing the velocity field into $\mathbf{v}^<$ and $\mathbf{v}^>$ components, we rewrite (5.16) as

$$A = A^< - i\int q_i Q_j (k - q - Q)_i (a + b + c + d + e + f + g)\, \frac{d\hat{q}\, d\hat{Q}}{(2\pi)^{2d+2}} \qquad (5.17)$$

where the seven terms a–g are given by

$$\begin{aligned} a &= v_j^>(\hat{q})\, v_i^>(\hat{Q})\, v_j^<(\hat{k} - \hat{q} - \hat{Q}) \\ b &= v_j^>(\hat{q})\, v_i^<(\hat{Q})\, v_j^>(\hat{k} - \hat{q} - \hat{Q}) \\ c &= v_j^<(\hat{q})\, v_i^>(\hat{Q})\, v_j^>(\hat{k} - \hat{q} - \hat{Q}) \\ d &= v_j^<(\hat{q})\, v_i^<(\hat{Q})\, v_j^>(\hat{k} - \hat{q} - \hat{Q}) \\ e &= v_j^<(\hat{q})\, v_i^>(\hat{Q})\, v_j^<(\hat{k} - \hat{q} - \hat{Q}) \\ f &= v_j^>(\hat{q})\, v_i^<(\hat{Q})\, v_j^<(\hat{k} - \hat{q} - \hat{Q}) \\ g &= v_j^>(\hat{q})\, v_i^>(\hat{Q})\, v_j^>(\hat{k} - \hat{q} - \hat{Q}) \end{aligned} \qquad (5.18)$$

and

$$A^< = -i\int q_i Q_j (k - q - Q)_i\, v_j^<(\hat{q})\, v_i^<(\hat{Q})\, v_j^<(\hat{k} - \hat{q} - \hat{Q})\, \frac{d\hat{q}\, d\hat{Q}}{(2\pi)^{2d+2}} \qquad (5.19)$$

We have to evaluate (5.17), eliminating modes $\mathbf{v}^>$ from the problem using the Navier–Stokes equation. Averaging over the random force $\mathbf{f}^>$, we find the following contribution from expression a of (5.18) to the integral (5.17):

$$\begin{aligned} A_a = {} & -2D_0 \int q_i Q_j (k - q - Q)_i \\ & \times [\,|G^0(\hat{q} + \hat{Q})|^2\, G^0(\hat{q})\, P_{imn}(\mathbf{q})\, P_{jn}(\mathbf{q} + \mathbf{Q}) \\ & \times |\mathbf{q} + \mathbf{Q}|\; v_l^<(\hat{Q})\, v_m^<(\hat{k} - \hat{Q}) \\ & - |G^0(\hat{q})|^2\, G^0(-\hat{q} - \hat{Q})\, P_{imn}(\mathbf{q} + \mathbf{Q})\, P_{jn}(\mathbf{q}) \\ & \times q\; v_l^<(\hat{Q})\, v_m^<(\hat{k} - \hat{Q})]\, \frac{d\hat{q}\, d\hat{Q}}{(2\pi)^{2d+2}} \end{aligned} \qquad (5.20)$$

The frequency integration is performed readily:

$$\begin{aligned} A_a = {} & -\frac{\pi}{\nu_0^2}\, 2D_0 \int \frac{q_i Q_j (k - q - Q)_i}{q^2 + |\mathbf{q} + \mathbf{Q}|^2}\, [\, P_{imn}(\mathbf{q})\, P_{jn}(\mathbf{q} + \mathbf{Q})\, |\mathbf{q} + \mathbf{Q}| \\ & - P_{imn}(\mathbf{q} + \mathbf{Q})\, P_{jn}(\mathbf{q})\, q\,]\, v_l^<(\hat{Q})\, v_m^<(\hat{k} + \hat{Q})\, \frac{d\mathbf{q}\, d\hat{Q}}{(2\pi)^{2d+1}} \end{aligned} \qquad (5.21)$$

It is clear that the expression in the square brackets in the integrand of (5.21) goes to zero when $Q \to 0$. Thus, we have to expand the integrand of (5.21) in powers of the small ratio $Q/q < 1$ and retain the first nonvanishing contribution. This can be done conveniently if we shift the variables in (5.21) by replacing $\mathbf{q} \to \mathbf{q} - \mathbf{Q}/2$ and let $k \to 0$. Thus,

$$\begin{aligned} A_a = {} & \frac{2\pi D_0}{\nu_0^2} \int \frac{(q - Q/2)_i\, Q_j (q + Q/2)_i}{2q^2 + \frac{1}{2}Q^2} \\ & \times \Big[\, P_{imn}\Big(\mathbf{q} - \frac{\mathbf{Q}}{2}\Big)\, P_{jn}\Big(\mathbf{q} + \frac{\mathbf{Q}}{2}\Big)\Big|\mathbf{q} + \frac{\mathbf{Q}}{2}\Big| \\ & - P_{imn}\Big(\mathbf{q} + \frac{\mathbf{Q}}{2}\Big)\, P_{jn}\Big(\mathbf{q} - \frac{\mathbf{Q}}{2}\Big)\Big|\mathbf{q} - \frac{\mathbf{Q}}{2}\Big|\,\Big]\, v_l^<(\hat{Q})\, v_m^<(\hat{k} - \hat{Q})\, d\mathbf{q}\, d\hat{Q} \end{aligned}$$

After simple algebra we obtain

$$A_a = -\frac{2\pi D_0}{\nu_0^2} \int q_i^2 Q_j Q_n P_{imn}(q)\, P_{jn}(\mathbf{q})\, q\; v_l^<(\hat{Q})\, v_m^<(\hat{Q})\, \frac{d^d q\, q\hat{Q}}{(2\pi)^{2d+1}} \qquad (5.22)$$

The angular integration in (5.22) leads to $A_a = 0$ when $d = 2$ and, when $d = 3$,

$$A_a = -\frac{5}{210}\, \frac{2D_0 S_3}{(2\pi)^3}\, \frac{1}{\nu_0^2 \Lambda^2}\, \frac{e^{2r} - 1}{2} \int Q_i^2 [v_i^<(\hat{Q})]^2\, \frac{d\hat{Q}}{(2\pi)^{d+1}} \qquad (5.23)$$

It can be shown that the contributions from the terms a, b, and c to the integral in (5.17) are all equal to (5.23) and that d, e, f, and g do not contribute to (5.17) in the lowest order of the ε expansion. Thus

$$A = A^< - \frac{15}{210}\, \frac{2D_0 S_3}{(2\pi)^3}\, \frac{1}{\nu_0^2 \Lambda^2}\, \frac{e^{2r} - 1}{2} \int Q_i^2 [v_i^<(\hat{Q})]^2\, \frac{d\hat{Q}}{(2\pi)^{d+1}} \qquad (5.24)$$

The relation (5.24) can be easily iterated if we notice that, for $d = 3$,

$$\nu \int Q_i^2 [v_i^<(\hat{Q})]^2\, \frac{d\hat{Q}}{(2\pi)^{d+1}} = \bar{\varepsilon}_i = \frac{1}{15}\bar{\varepsilon} \qquad (5.25)$$

is independent of r. The result for A is

$$A = A^{<}(r) - \frac{15}{210}\bar{\varepsilon}_1 \int_0^r \frac{2D_0 S_3 e^{2r}\,dr}{(2\pi)^3 \Lambda^2 \nu^3(r)} \tag{5.26}$$

This result for A is best evaluated by rewriting it as

$$A = A^{<}(r) - \frac{15}{210}\bar{\varepsilon}_1 \int_0^{\infty} \frac{2D_0 S_3}{(2\pi)^3} \frac{e^{2r}\,dr}{\Lambda^2 \nu^3(r)}$$
$$+ \frac{15}{210}\bar{\varepsilon}_1 \frac{2D_0 S_3}{(2\pi)^3 \Lambda_0^2} \int_r^{\infty} \frac{2D_0 S_3}{(2\pi)^3} \frac{e^{2r}\,dr}{\Lambda^2 \nu^3(r)} \tag{5.27}$$

It follows from (5.27) that, in high Reynolds-number, fully-developed turbulence,

$$A^{<} = -\frac{15}{420}\frac{2D_0 S_d}{(2\pi)^d}\frac{\bar{\varepsilon}_1}{\nu^3 \Lambda_f^2} = -\frac{1}{420}\frac{2D_0 S_d}{(2\pi)^d}\frac{\bar{\varepsilon}}{\nu^3 \Lambda_f^2} \tag{5.28}$$

Next we compute

$$B = \int q_i^2 v_i(\hat{q})\, v_i(\hat{k} - \hat{q}) \frac{d\hat{q}}{(2\pi)^{d+1}} \tag{5.29}$$

in the limit $k \to 0$. It is easy to show that, to the lowest order in λ_0,

$$B = B^{<} + \int q_i^2 |G^0(\hat{q})|^2 P_{ii}(\mathbf{q})\, 2D_0 q^{-d} \frac{d\hat{q}}{(2\pi)^4} \tag{5.30}$$

The integration in (5.30) leads to the result

$$B = B^{<} + \frac{1}{15}\frac{2D_0 S_d}{(2\pi)^d}\frac{r}{\nu_0} \tag{5.31}$$

Iterating the procedure, we find that, in regions where $\nu \gg \nu_0$,

$$B^{<} = \frac{1}{20}\frac{2D_0 S_d/(2\pi)^d}{\nu} \tag{5.32}$$

Combining (2.61), (5.28), and (5.32) gives

$$S_3^{<}(r) = -\frac{A^{<}}{(B^{<})^{3/2}} = 0.1336\left(\frac{2D_0 S_d/(2\pi)^d}{\nu^3 \Lambda_f^4}\right)^{1/2} \tag{5.33}$$

At the fixed point, (2.51)–(2.54) give with $d = 3$

$$\frac{2D_0}{\nu^3 \Lambda_f^4}\frac{S_d}{(2\pi)^d} = \frac{8}{3\bar{\lambda}_d} = 13.333 \tag{5.34}$$

so that

$$\bar{S}_3^{<}(r) = 0.4878 \tag{5.35}$$

We see that $S_3^{<}(r)$ is independent of r, so that $\bar{S}_3^{<}(r) = \bar{S}_3 = 0.4878$ in the limit $r \to 0$. This result is in good agreement with the experimental values of the skewness factor $S_3 = 0.4$–0.6 (see Section 7).

It should also be mentioned that the RNG result that $\bar{S}_3 = 0$ in two-dimensional isotropic turbulent flow is an exact result (Herring *et al.*, 1974).

5.1. Energy Equation

The result (5.4) shows that, within the framework of the present RNG theory, the total viscosity is entirely determined by two characteristics of turbulent flow: the kinetic energy K and the dissipation rate $\bar{\varepsilon}$. Now we apply the RNG method to derive the equation governing the kinetic energy K. The equation of motion for $K(\mathbf{x}, t)$ follows directly from the Navier–Stokes equation (Tennekes and Lumley, 1972; Monin and Yaglom, 1975)

$$\frac{\partial K}{\partial t} + (\bar{\mathbf{v}} \cdot \nabla) K = P - D - \frac{\partial}{\partial x_i} p v_i + \nu_0 \frac{\partial^2 K}{\partial x_i^2} \tag{5.36}$$

Here $\mathbf{v} = \bar{\mathbf{v}} + \mathbf{v}'$, where $\bar{\mathbf{v}} = \langle \mathbf{v} \rangle$ is the (local) average velocity, $K = \frac{1}{2}\langle v'^2 \rangle$, the production term P is given in terms of the eddy viscosity ν_T as

$$P = \frac{\nu_T}{2}\left(\frac{\partial \bar{v}_i}{\partial x_j} + \frac{\partial \bar{v}_j}{\partial x_i}\right)^2 \equiv 2\nu_T \bar{S}_{ij}^2 \tag{5.37}$$

and

$$D = \nu_0 (\partial v_i'/\partial x_j)^2 \tag{5.38}$$

Our goal is to evaluate the mean value of $\overline{K(\mathbf{x}, t)}$, defined as

$$\bar{K} = \int_0^T dt \int_V K(\mathbf{x}, t)\, d^3x = K(\mathbf{k}, \omega) \qquad (k \to 0, \omega \to 0) \tag{5.39}$$

To evaluate (5.39), we Fourier transform (5.36):

$$K(\hat{k}) = G^0(\hat{k})[P(\hat{k}) - D(\hat{k})] - i\lambda_0 k_i G^0(\hat{k}) \int v_i(\hat{q}) K(\hat{k} - \hat{q}) \frac{d\hat{q}}{(2\pi)^4}$$

$$- i\lambda_0 k_i G^0(\hat{k}) \int p(\hat{q}) v_i(\hat{k} - \hat{q}) \frac{d\hat{q}}{(2\pi)^4} \tag{5.40}$$

In (5.40), the expression for the Fourier transform $p(\hat{k})$ of the pressure is obtained easily from the Navier Stokes equation and the incompressibility condition as

$$p(\hat{k}) = -\frac{k_l k_m}{k^2} \int v_l(\hat{q}) v_m(\hat{k} - \hat{q}) \frac{d\hat{q}}{(2\pi)^4} \tag{5.41}$$

We observe that, except for the last term on the right side, (5.40) is precisely the equation for a passive scalar K with "molecular diffusivity" $\chi_0 = \nu_0$ and "force" $P - D$. The renormalization-group procedure for such an equation has already been developed in Section 4.

Our concern now is to evaluate the role of the pressure velocity correlation in the turbulent diffusion of kinetic energy K. To do this we decompose modes into their $<$ and $>$ components and express the last contribution to the right side of (5.40) as

$$Y_k = -i\lambda_0 k_i G^0(\hat{k})$$

$$\times \int [p^<(\hat{q}) v_i^<(\hat{k} - \hat{q}) + p^<(\hat{q}) v_i^>(\hat{k} - \hat{q}) + p^>(\hat{q}) v_i^<(\hat{k} - \hat{q})$$

$$+ p^>(\hat{q}) v_i^>(\hat{k} - \hat{q})] \frac{d\hat{q}}{(2\pi)^4} \tag{5.42}$$

with

$$p^>(\hat{q}) = -\lambda_0 \frac{q_\alpha q_\beta}{q^2} \int [v_\alpha^<(\hat{Q}) v_\beta^<(\hat{q} - \hat{Q}) + 2v_\alpha^<(\hat{Q}) v_\beta^>(\hat{q} - \hat{Q})$$

$$+ v_\alpha^>(\hat{Q}) v_\beta^>(\hat{q} - \hat{Q})] \frac{d\hat{Q}}{(2\pi)^4} \tag{5.43}$$

All contributions to (5.40) up to λ_0^2 can be obtained by substitution of (5.43) into (5.42). Elimination of the modes $v^>(k)$ from the interval $k_d e^{-r} < k < k_d$ is carried out using the zeroth order solution of the Navier Stokes equation with subsequent averaging over the part of the random force acting in the domain $k_d e^{-r} < k < k_d$.

All contributions to the equation of motion (5.40) stemming from (5.42) (5.43) can be classified into two types of terms:

$$Y_k^0 = \lambda_0^2 k_i \int \frac{q_\alpha q_\beta}{q^2} v_\alpha^>(\hat{Q}) v_\beta^>(\hat{q} - \hat{Q}) v_i^<(\hat{k} - \hat{q}) \frac{d\hat{Q}\, d\hat{q}}{(2\pi)^8}$$

$$\approx k_i \int \frac{q_\alpha q_\beta}{q^2} |G^0(\hat{Q})|^2 P_{\alpha\beta}(Q)\, \delta(\mathbf{q}) \frac{d\hat{q}}{(2\pi)^4} v_i^<(k) \equiv 0 \tag{5.44}$$

and

$$Y_k^1 = \lambda_0^2 k_i \int \frac{q_\alpha q_\beta}{q^2} v_\alpha^>(\hat{Q}) v_i^>(\hat{k} - \hat{q}) v_\beta^<(\hat{q} - \hat{Q}) \frac{d\hat{Q}\, d\hat{q}}{(2\pi)^8}$$

$$\approx \lambda_0^2 k_i \int \frac{q_\alpha q_\beta}{q^2} P_{\alpha i}(\mathbf{k} - \mathbf{q})\, |\mathbf{k} - \mathbf{q}|^{-y} |G^0(\hat{k} - \hat{q})|^2 v_\beta(\hat{k}) = O(k^3) \tag{5.45}$$

and can be neglected in the limit $k \to 0$. Thus, the pressure velocity correlations do not contribute to the equation of motion for K to second order in the coupling parameter, which is considered small in terms of the ϵ expansion.

Recalling the results of Section 4 for the RNG description of a passive scalar, it follows from (5.40) that the RNG equation for mean turbulent kinetic energy is

$$\frac{\partial K}{\partial t} + (\bar{v} \cdot \nabla) K = P - D + \frac{\partial}{\partial x_i} \alpha_K \nu \frac{\partial K}{\partial x_i}$$

where the "turbulent Prandtl number" α_K is found from the algebraic relation

$$\left|\frac{\alpha_K - 1.3929}{0.3929}\right|^{0.63} \left|\frac{\alpha_K + 2.3929}{3.3929}\right|^{0.37} = \frac{\nu_0}{\nu_T} \tag{5.46}$$

which is just (4.19) for the case $\chi_0 = \nu_0$. Here the turbulent viscosity ν_T is given by (3.2) (3.3).

At this level of approximation, the dissipation $D \approx \bar{\epsilon}$. For the production term that involves the unknown Reynolds stress $\bar{v}_i\bar{v}_j$, one can use different types of closures, including

$$P \approx 2\nu_T \bar{S}_{ij}^2 \tag{5.47}$$

$$P \approx 0.3K(2\bar{S}_{ij}^2)^{1/2} \tag{5.48}$$

Thus the K equation is

$$\frac{\partial K}{\partial t} + (\bar{v}\cdot\nabla)K = \frac{\nu_T}{2}\left(\frac{\partial v_i}{\partial x_j} + \frac{\partial v_j}{\partial x_i}\right)^2 - \bar{\varepsilon} + \frac{\partial}{\partial x_i}\alpha_k \nu_T \frac{\partial K}{\partial x_i} \qquad (5.49)$$

or

$$\frac{\partial K}{\partial t} + (\bar{v}\cdot\nabla)K = 0.3(2S_{ij}^2)^{1/2} - \bar{\varepsilon} + \frac{\partial}{\partial x_i}\alpha_k \nu \frac{\partial K}{\partial x_i} \qquad (5.50)$$

Next we need to derive an equation governing the turbulent dissipation $\bar{\varepsilon}$.

5.2. Equation for the Dissipation Rate

The mean dissipation rate is defined in general by

$$\bar{\varepsilon} = \tfrac{1}{2}\nu_0\overline{(\partial v_i/\partial x_j + \partial v_j/\partial x_i)^2} = \varepsilon(\hat{k}) \qquad (\hat{k}\to 0) \qquad (5.51)$$

It can be argued that strongly anisotropic fluctuations of the velocity field do not contribute to turbulent diffusivity (Sivashinsky and Yakhot, 1985; Bayly and Yakhot, 1986; Yakhot and Sivashinsky, 1986). Thus, we are interested in evaluating the isotropic part of the dissipation, defined as

$$\bar{\varepsilon} = \nu_0\overline{(\partial v_i/\partial x_j)^2} = \varepsilon(\hat{k}) \qquad (\hat{k}\to 0) \qquad (5.52)$$

To evaluate (5.52), we write the equation of motion for

$$\varepsilon(\mathbf{x}, t) = \nu_0[\partial v_i(\mathbf{x}, t)/\partial x_j]^2 \qquad (5.53)$$

Taking the time derivative of (5.52) and using the Navier–Stokes equation, we find

$$\frac{\partial \varepsilon}{\partial t} = 2\nu_0 \frac{\partial v_i}{\partial x_j}\frac{\partial}{\partial x_j}\left[\left(-v_l\frac{\partial v_i}{\partial x_l} - \frac{\partial p}{\partial x_i} + \nu_0\frac{\partial^2 v_i}{\partial x_l^2}\right)\right] \qquad (5.54)$$

or

$$\frac{\partial \varepsilon}{\partial t} = -2\nu_0\frac{\partial v_i}{\partial x_j}\frac{\partial v_l}{\partial x_j}\frac{\partial v_i}{\partial x_l} - v_l\frac{\partial \varepsilon}{\partial x_l} + \nu_0\frac{\partial^2 \varepsilon}{\partial x_l^2} - 2\nu_0^2\left(\frac{\partial^2 v_i}{\partial x_j \partial x_l}\right)^2 \qquad (5.55)$$

To derive the equation of motion for $\varepsilon(\mathbf{x}, t) \to \varepsilon(k, t)$ in the limit $k \to 0$, we take the Fourier transform of (5.55)

$$\varepsilon(\hat{k}) = -ig_\varepsilon^0 k_l \int v_l(\hat{q})\,\varepsilon(\hat{k}-\hat{q})\frac{d\hat{q}}{(2\pi)^4} - Y_\varepsilon^1(\hat{k}) - Y_\varepsilon^2(\hat{k}) - Y_\varepsilon^3(\hat{k}) \quad (5.56)$$

where

$$Y_\varepsilon^1 = 2\nu_0^2 g_\varepsilon^0 \int q_l(k-q)_j q_l(k-q)_j v_i(\hat{q})\,v_i(\hat{k}-\hat{q})\frac{d\hat{q}}{(2\pi)^4} \qquad (5.57)$$

$$Y_\varepsilon^2 = -2i\nu_0 g_\varepsilon^0 k_l \int q_j(k-q)_j v_l(\hat{q})\,p(\hat{k}-\hat{q})\frac{d\hat{q}}{(2\pi)^4} \qquad (5.58)$$

$$Y_\varepsilon^3 = -2i\nu_0 g_\varepsilon^0 \int q_j Q_l(k-q-Q)_j v_i(\hat{q})\,v_l(\hat{Q})\,v_i(\hat{k}-\hat{q}-\hat{Q})\frac{d\hat{Q}\,d\hat{q}}{(2\pi)^8} \qquad (5.59)$$

and the bare propagator is

$$g_\varepsilon^0 = (-i\omega + \chi_\varepsilon^0 k^2)^{-1} \qquad (5.60)$$

Here $\chi_\varepsilon^0 = \nu_0$ is the bare diffusivity of the dissipation rate ε.

To eliminate small scales from the problem, we decompose the velocity $\mathbf{v}$ and the scalar field ε into the two components $\mathbf{v}^<$ and $\mathbf{v}^>$ and $\varepsilon^<$ and $\varepsilon^>$, respectively. Thus,

$$\begin{aligned}\varepsilon(k) = -ig_\varepsilon^0 k_l \int\Big[& v_l^>(\hat{q})\,\varepsilon^<(\hat{k}-\hat{q}) + v_l^<(\hat{q})\,\varepsilon^>(\hat{k}-\hat{q}) + v_l^>(\hat{q})\,\varepsilon^>(\hat{k}-\hat{q}) \\ &+ v_l^<(\hat{q})\,\varepsilon^<(\hat{k}-\hat{q})\Big]\frac{d\hat{q}}{(2\pi)^4} - Y_\varepsilon^1 - Y_\varepsilon^2 - Y_\varepsilon^3 \end{aligned} \qquad (5.61)$$

and

$$\begin{aligned} Y_\varepsilon^1 = 2\nu_0^2 g_\varepsilon^0 \int & q_l(k-q)_j q_l(k-q)_j \\ &\times[2v_i^>(\hat{q})\,v_i^<(\hat{k}-\hat{q}) + v_i^>(\hat{q})\,v_i^>(\hat{k}-\hat{q})]\frac{d\hat{q}}{(2\pi)^4} + (Y_\varepsilon^1)^< \end{aligned} \qquad (5.62)$$

$$\begin{aligned} Y_\varepsilon^2 = -2i\nu_0 g_\varepsilon^0 k_l \int & q_j(k-q)_j \\ &\times[v_l^<(\hat{q})\,p^>(\hat{k}-\hat{q}) + v_l^>(\hat{q})\,p^<(\hat{k}-\hat{q}) \\ &+ v_l^>(\hat{q})\,p^>(\hat{k}-\hat{q})]\frac{d\hat{q}}{(2\pi)^4} + (Y_\varepsilon^2)^< \end{aligned} \qquad (5.63)$$

$$\begin{aligned} Y_\varepsilon^3 = -2i\nu_0 g_\varepsilon^0 \int & q_j Q_l(k-q-Q)_j \\ &\times(a+b+c+d+e+f+g)\frac{d\hat{Q}\,d\hat{q}}{(2\pi)^8} + (Y_\varepsilon^3)^< \end{aligned} \qquad (5.64)$$

where we have introduced the notation $Y(v^<) \equiv Y^<$. The expression (5.64) for Y_i^1 involves seven contributions:

$$\begin{aligned} a &= v_i^>(\hat{q})\, v_i^>(\hat{Q})\, v_i^<(\hat{k}-\hat{q}-\hat{Q}) \\ b &= v_i^>(\hat{q})\, v_i^>(\hat{Q})\, v_i^>(\hat{k}-\hat{q}-\hat{Q}) \\ c &= v_i^>(\hat{q})\, v_i^<(\hat{Q})\, v_i^>(\hat{k}-\hat{q}-\hat{Q}) \\ d &= v_i^<(\hat{q})\, v_i^>(\hat{Q})\, v_i^<(\hat{k}-\hat{q}-\hat{Q}) \\ e &= v_i^<(\hat{q})\, v_i^<(\hat{Q})\, v_i^>(\hat{k}-\hat{q}-\hat{Q}) \\ f &= v_i^>(\hat{q})\, v_i^<(\hat{Q})\, v_i^<(\hat{k}-\hat{q}-\hat{Q}) \\ g &= v_i^<(\hat{q})\, v_i^>(\hat{Q})\, v_i^>(\hat{k}-\hat{q}-\hat{Q}) \end{aligned} \tag{5.65}$$

The elimination of the modes $\mathbf{v}^>$ and $\varepsilon^>$ from (5.61)–(5.65) is carried out as above: all modes $\varepsilon^>$ in (5.62)–(5.65) are eliminated using (5.61) and the modes $\mathbf{v}^>$ are eliminated using the Navier–Stokes equation. This generates an infinite expansion in powers of the Reynolds number. Next, averages are taken over the random force for $k_d e^{-r} < k < k_d$. The resulting equation does not include the modes $\mathbf{v}^>$ and $\varepsilon^>$. The results are calculated to the second order in the coupling parameter $\bar{\lambda}$.

The integral term in (5.61) is similar to the equation for a passive scalar ε. The RNG scale elimination procedure for a passive scalar has been described above in detail. Thus the sole effect of the second, third, and fourth terms within the integral on the right side of (5.61) is to generate a correction to the bare diffusivity:

$$\delta\chi_c = \frac{d-1}{d}\frac{2D_0 S_d}{(2\pi)^d}\frac{1}{v_0(\chi_i^0 + v_0)\Lambda_0^4}\frac{e^{4r}-1}{4} \tag{5.66}$$

It is easy to show that the contribution of the pressure velocity correlation term (5.63) is equal to zero to second order in $\bar{\lambda}_0$. This agrees with the conclusion of Hanjalić and Launder (1972).

It remains to evaluate (5.62) and (5.64). After elimination of the modes from the interval $\Lambda e^{-r} < k < \Lambda$, the expression for Y_i^1 can be written as

$$Y_i^1 = (Y_i^1)^< + y_1 + y_2 + 2\frac{2D_0 S_d}{(2\pi)^d} v_0 \Lambda^2 \frac{1-e^{-(2+d-y)r}}{2+d-y} \tag{5.67}$$

where

$$y_1 = 4v_0^2 D_0 \int q_i q_j (k-q)_i (k-q)_j G^0(\hat{q})\, G^0(\hat{k}-\hat{q})\, |G^0(\hat{q}-\hat{Q})|^2$$
$$\times P_{\alpha\beta}(\mathbf{q})\, P_{\gamma\delta}(\mathbf{k}-\mathbf{q})\, P_{\beta\delta}(\mathbf{q}-\mathbf{Q})\, |\mathbf{q}-\mathbf{Q}|^{-y}\, v_\alpha^<(\hat{Q})\, v_\gamma^<(\hat{k}-\hat{Q})\, \frac{d\hat{q}\, d\hat{Q}}{(2\pi)^{2d+2}} \tag{5.68}$$

and

$$y_2 = -8v_0^2 D_0 \int |G^0(\hat{k}-\hat{q})|^2\, G^0(\hat{q}-\hat{Q})\, G^0(\hat{q})[\mathbf{q}\cdot(\mathbf{k}-\mathbf{q})]^2$$
$$\times P_{\alpha\beta}(\mathbf{q})\, P_{\beta\delta}(\mathbf{q}-\mathbf{Q})\, P_{\gamma\delta}(\mathbf{q})\, q^{-y}\, v_\alpha^<(\hat{Q})\, v_\gamma^<(\hat{k}-\hat{Q})\, \frac{d\hat{q}\, d\hat{Q}}{(2\pi)^{2d+2}} \tag{5.69}$$

Here $\Lambda e^{-r} < q < \Lambda$ and the wavevectors $\mathbf{Q}$ and $\mathbf{k}$ belong to the interval $\Lambda_f < k < \Lambda e^{-r}$, so that $Q/q < 1$ and $k/q < 1$. We are interested in the limit $k \to 0$. After the frequency integration is performed, (5.68) becomes

$$y_1 = -\frac{8\pi}{v_0} D_0$$
$$\times \int \frac{[\mathbf{q}\cdot(\mathbf{k}-\mathbf{q})]^2 P_{\alpha\beta}(\mathbf{q})\, P_{\gamma\delta}(\mathbf{k}-\mathbf{q})\, P_{\beta\delta}(\mathbf{q}-\mathbf{Q})\, |\mathbf{q}-\mathbf{Q}|^{-d-y}}{(q^2 + |\mathbf{k}-\mathbf{q}|^2)(q^2 + |\mathbf{q}-\mathbf{Q}|^2)}$$
$$\times v_\alpha^<(\hat{Q})\, v_\gamma^<(\hat{k}-\hat{Q})\, \frac{d\mathbf{q}}{(2\pi)^{d+1}}\, \frac{d\hat{Q}}{(2\pi)^{d+1}} \tag{5.70}$$

and

$$y_2 = -\frac{8\pi}{v_0} D_0$$
$$\times \int \frac{[\mathbf{q}\cdot(\mathbf{k}-\mathbf{q})]^2 P_{\alpha\beta}(\mathbf{q})\, P_{\beta\delta}(\mathbf{q}-\mathbf{Q})\, P_{\gamma\delta}(\mathbf{q})\, q^{-d-y}}{|\mathbf{k}-\mathbf{q}|^2(|\mathbf{k}-\mathbf{q}|^2 + |\mathbf{q}-\mathbf{Q}|^2)(|\mathbf{k}-\mathbf{q}|^2 + q^2)}$$
$$\times v_\alpha^<(\hat{Q})\, v_\gamma^<(\hat{k}-\hat{Q})\, \frac{d_q}{(2\pi)^{d+1}}\, \frac{d\hat{Q}}{(2\pi)^{d+1}} \tag{5.71}$$

The integrations over the wavevector $\mathbf{q}$ in (5.70) and (5.71) can be carried out if we expand the integrands in powers of $Q/q < 1$ and $k/q < 1$. Second-order terms in Q/q produce corrections proportional to $\int Q^2 v^2(\hat{Q})\, d\hat{Q} = O[\varepsilon(k)]$ in the limit $k \to 0$. The fourth-order terms proportional to $k^2 \int Q^2 v^2(\hat{Q})\, d\hat{Q} = O[k^2 \varepsilon(k)]$ give rise to additional corrections to diffusivity that *must* be taken into account. Thus, expanding the integrands in (5.70) and (5.71) in powers of Q/q and k/q, we obtain to second order in $\bar{\lambda}$ $(d = 3)$

$$y_1 = 0.217\frac{2D_0 S_d}{(2\pi)^d}\frac{\bar{\varepsilon}}{v_0^2 \Lambda^2}\frac{e^{2r}-1}{2}$$
$$-\frac{d-1}{d}\frac{2D_0 S_d}{(2\pi)^d}\frac{\bar{K}}{v}\varepsilon - 0.18\frac{2D_0}{v_0^2 \Lambda^4}\frac{e^{4r}-1}{4}k^2\varepsilon \tag{5.72}$$

$$Y_e^3 = -0.250\,\frac{2D_0S_d}{(2\pi)^d}\frac{\bar{\varepsilon}}{\nu_0^2\Lambda^2}\frac{e^{2r}-1}{2} + \frac{d-1}{d}\frac{2D_0S_d}{(2\pi)^d}\frac{K}{\nu}\varepsilon + 0.18\,\frac{2D_0}{\nu_0^2\Lambda^4}\frac{e^{4r}-1}{4}k^2\bar{\varepsilon} \tag{5.73}$$

It is interesting that the correction to the diffusivity of ε from the term Y_e^3 vanishes because the last terms in (5.72) and (5.73) cancel each other identically.

To eliminate small scales from (5.64)–(5.65) we use a procedure similar to the one developed to evaluate the skewness $\bar{S}_3$. It is easy to show that to second order in λ_0^2, contributions to (5.63) coming from the terms c, d, e, f, and g vanish. It is an elementary, although tedious, calculation to show that

$$Y_e^3 = (Y_e^3)^< + \frac{d-2}{d+2}\frac{2D_0S_d}{(2\pi)^d}\frac{\varepsilon}{\nu_0^2\Lambda^2}\frac{e^{2r}-1}{2} + i\frac{d-2}{d(d+2)}\frac{2D_0S_d}{(2\pi)^d}\frac{1}{\nu_0^2\Lambda^2}\frac{e^{2r}-1}{2} \times \int Q_j v_i^<(\hat{Q})\, v_i^<(\hat{q})\, v_j^<(\hat{k}-\hat{q}-\hat{Q})\,\frac{d\hat{Q}\,d\hat{q}}{(2\pi)^{2d+2}} \tag{5.74}$$

In the case of isotropic, homogeneous turbulence, the last term in (5.74) vanishes. If $\nabla v \neq 0$, this term is responsible for the production of the dissipation rate $\bar{\varepsilon}$. For now, let us neglect this term and substitute (5.66), (5.72), and (5.74) into (5.60). The result is

$$\varepsilon(\hat{k}) = -ig_\varepsilon k_j\int v_j(\hat{q})\,\varepsilon(\hat{k}-\hat{q})\,\frac{d\hat{q}}{(2\pi)^{d+1}} - Y_e^1 - Y_e^2 - Y_e^3 + g_\varepsilon\left[\left(0.217 + \frac{d-2}{d+2} - 0.250\right) \times \frac{2D_0S_d}{(2\pi)^d}\frac{\varepsilon}{\nu_0^2\Lambda^2}\frac{e^{2r}-1}{2} - 2\frac{2D_0S_d}{(2\pi)^d}\nu_0\Lambda^2\frac{(1-e^{-2r})}{2} + P\right] \tag{5.75}$$

where P stands for the production term, which will be considered below. The propagator g_ε in (5.75) is

$$g_\varepsilon = [-i\omega + (\chi_\varepsilon^0 + \delta\chi_\varepsilon)k^2]^{-1} \tag{5.76}$$

and $\delta\chi_\varepsilon$ is given by (5.65). Equation (5.75) is defined on the interval $\Lambda_f < k < \Lambda e^{-r}$.

The functions $Y_\varepsilon^{(1-3)}$ in (5.75) are those in (5.56)–(5.58) but with $v^<$, g_ε, and ν replacing v, g_ε^0, and ν_0, respectively. This renormalization procedure can now be iterated. The result is

$$\bar{\varepsilon} = -ig_\varepsilon k_j\int \bar{v}_j(q)\,\varepsilon(\hat{k}-\hat{q})\,\frac{d\hat{q}}{(2\pi)^{d+1}} - ag_\varepsilon\frac{2D_0S_d}{(2\pi)^d} + bg_\varepsilon\frac{2D_0S_d\bar{\varepsilon}}{(2\pi)^d} + g_\varepsilon\bar{P} \tag{5.77}$$

where the parameters a and b are determined from the recursion relations derived from (5.75):

$$\frac{da}{dr} = -2\nu(r)\,\Lambda^2(r) \tag{5.78}$$

$$\frac{db}{dr} = -\left(-0.033 + \frac{d-2}{d+2}\right)\frac{1}{\nu^2(r)\,\Lambda^2(r)} \tag{5.79}$$

and

$$g_\varepsilon = [-i\omega + \alpha_\varepsilon(r)\,\nu k^2]^{-1} \tag{5.80}$$

The inverse Prandtl number α_ε is defined by (4.19) with $\alpha_0 = 1$ [so $\alpha_\varepsilon = \alpha_k$ given by (5.46)].

The recursion relations (5.78) and (5.79) can be solved in the limit of high Reynolds number when $r \to r_c$. Using (2.52), one obtains the result

$$a = 3\nu\Lambda^2 \tag{5.81}$$

and

$$b = \frac{3}{2}\left(-0.033 + \frac{d-2}{d+2}\right)\frac{1}{\nu^3\Lambda^2} \tag{5.82}$$

Thus, the equation of motion governing the mean dissipation rate $\bar{\varepsilon}$ is

$$\frac{D\bar{\varepsilon}}{Dt} = \bar{P} - 3\nu\Lambda_f^2\frac{2D_0S_d}{(2\pi)^d} + 0.2505\,\frac{\bar{\varepsilon}}{\nu^3\Lambda_f^2}\frac{2D_0S_d}{(2\pi)^d} + \frac{\partial}{\partial x_i}\alpha_\varepsilon\nu\frac{\partial\bar{\varepsilon}}{\partial x_i} \tag{5.83}$$

Using (2.61), (5.2), and (5.14) to eliminate D_0, Λ_f, and ν, we obtain the dissipation equation

$$\frac{D\bar{\varepsilon}}{Dt} = \bar{P} - 1.7215\,\frac{\bar{\varepsilon}^2}{K} + \frac{\partial}{\partial x_i}\alpha_\varepsilon\nu\frac{\partial\bar{\varepsilon}}{\partial x_i} \tag{5.84}$$

For homogeneous turbulence, (5.84) with $\bar P = 0$ and the energy equation

$$DK/Dt = -\bar\varepsilon \tag{5.85}$$

show that homogeneous isotropic turbulence decays at high Reynolds number like

$$K = K_1(t - t_0)^{-1/0.7215} = K_1(t - t_0)^{-1.39} \tag{5.86}$$

for suitable constants t_0, K_1. This result agrees well with experimental data (Monin and Yaglom, 1975).

To evaluate the production term $\bar P$, let us consider the last term on the right side of (5.74). In the case of shear turbulence $\nabla\bar v \neq 0$, so the major contribution to the integral in (5.74) comes from wavevectors corresponding to the largest scales in the system. Examination of the structure of this Fourier integral shows that it is given by

$$\bar P = -\frac{d-2}{d(d+2)}\frac{2D_0S_d}{(2\pi)^d}\frac{e^{2r}-1}{2}\frac{\tau_{ij}(\mathbf{k})}{\nu_0^2\Lambda^2}\frac{\partial\bar v_i}{\partial x_j} \tag{5.87}$$

where $\tau_{ij}(\mathbf{k})$ is the contribution to the Reynolds stress $-\overline{v_iv_j}$ at wavenumber $\mathbf{k}$. This relation can be iterated if we note that a calculation similar to that used to derived (5.2) shows that $\tau_{ij}(\mathbf{k}) \sim \nu(r)\Lambda^2(r)$ is proportional to $\bar\varepsilon$, so it is independent of r in the inertial range. Thus,

$$\frac{d\bar P}{dr} = -\frac{d-2}{d(d+2)}\frac{1}{\nu^3\Lambda^4}\frac{2D_0S_d}{(2\pi)^d}\nu\Lambda^2\tau_{ij}\frac{\partial\bar v_i}{\partial x_j} \tag{5.88}$$

Noting that, to leading order in λ_0, we may assume that $\tau_{ij}(\mathbf{k})$ is statistically sharp at Λ_f, we obtain

$$\bar P = -\frac{d-2}{d(d+2)}\frac{2D_0S_d/(2\pi)^d}{\nu^2\Lambda_f^2}\bar\tau_{ij}\frac{\partial\bar v_i}{\partial x_j} \tag{5.89}$$

in the high Reynolds number limit. Using (2.61) and (5.14) to eliminate D_0, ν, and Λ_f, we conclude

$$\bar P = 1.063\frac{\bar\varepsilon}{K}\bar\tau_{ij}\frac{\partial\bar v_i}{\partial x_j} \tag{5.90}$$

Thus, the high Reynolds number version of the ε equation is

$$\frac{D\bar\varepsilon}{Dt} = -1.063\frac{\bar\varepsilon}{K}\bar\tau_{ij}\frac{\partial\bar v_i}{\partial x_j} - 1.7215\frac{\bar\varepsilon^2}{K} + \frac{\partial}{\partial x_i}\alpha_\varepsilon\nu\frac{\partial\bar\varepsilon}{\partial x_i} \tag{5.91}$$

As a consistency check, notice that it follows from (5.74) and (5.89) that

$$Y_i^3(k\to 0) = 2\nu_0(\overline{\partial v_i/\partial x_j})(\overline{\partial v_j/\partial x_l})(\overline{\partial v_l/\partial x_i})$$
$$= O[(d-2)/(d+2)] = 0 \tag{5.92}$$

when $d = 2$. It can be shown directly that $Y_i^3 = 0$ when $d = 2$, using the incompressibility condition $\nabla\cdot\mathbf{v} = 0$.

The result (5.91) allows us to calculate the von Karman constant. We express all parameters in wall coordinates

$$y_+ = \frac{yu_*}{\nu_0};\quad u_*^2 = \frac{\tau_w}{\rho};\quad v_+ = \frac{v}{u_*};\quad K_+ = \frac{K}{u_*^2};\quad \bar\varepsilon_+ = \frac{\bar\varepsilon\nu_0}{u_*^4};\quad \nu_+ = \frac{\nu}{\nu_0}$$

where τ_w is the wall shear stress. Consider a boundary layer in which all parameters are functions of the distance to the wall only. We use the simple version of the closure:

$$\bar\tau_{ij} = -\nu\left(\frac{\partial\bar v_i}{\partial x_j} + \frac{\partial\bar v_j}{\partial x_i}\right) \tag{5.93}$$

In a stationary state, Eqs. (5.49) and (5.91) in the region where K is constant (in wall coordinates) give

$$\nu_+\left(\frac{\partial v_+}{\partial y_+}\right)^2 - \varepsilon_+ = 0 \tag{5.94}$$

and

$$1.063\frac{\varepsilon_+}{K_+}\nu_+\left(\frac{\partial v_+}{\partial y_+}\right)^2 - 1.7215\frac{\varepsilon_+^2}{K_+} + \frac{\partial}{\partial y_+}\alpha\nu_+\frac{\partial\varepsilon_+}{\partial y_+} = 0 \tag{5.95}$$

Using (5.93) in wall coordinates, the Navier-Stokes equations are simply

$$1 - \frac{y_+}{R_*} = \nu_+\frac{\partial v_+}{\partial y_+} \tag{5.96}$$

so $\nu_+\,\partial v_+/\partial y_+ = 1$ when $y_+/R_* \ll 1$. Using this, we obtain

$$\varepsilon_+ = 1/\nu_+ \tag{5.97}$$

so that, using (5.4),

$$K_+ = 3.4159 \tag{5.98}$$

Substituting (5.97) and (5.98) and $\alpha_0 = 1.3929$ into (5.95) gives

$$v = \kappa y_+ \tag{5.99}$$

with the von Karman constant

$$\kappa = \left(\frac{1.7215}{1.3929} \cdot \frac{1.063}{3.416}\right)^{1/2} \approx 0.372 \tag{5.100}$$

Thus it follows from (5.96) that

$$v_+ = 2.688 \ln y_+ + c \tag{5.101}$$

6. DIFFERENTIAL TRANSPORT MODEL

The high Reynolds number version of the algebraic K–ϵ model derived in this work is given by relations (5.4), (5.48), (5.49), and (5.83). It is clear from (5.83) that in low-Reynolds number flow regions where $K \to 0$ the algebraic model is poor because of uncertainty of terms of the type ϵ/K. To derive a model valid in both high- and low-Reynolds number regions of the flow we must solve *the RNG differential recursion relations introduced in* Section 5. The results for this differential transport model presented here have been obtained with the collaboration of Dr. A. Yakhot.

Let us first solve Eq. (5.11) for the function $Q = 2K$:

$$2\frac{dK}{dr} = 1.594\frac{\epsilon}{v(r)\Lambda^3(r)} = \frac{\bar{\epsilon}e^{3r}}{v(r)\Lambda^2} \tag{6.1}$$

or

$$\frac{dK}{d[1/\Lambda^4(r)]} = \frac{1.594}{4}\frac{\bar{\epsilon}}{v} \tag{6.2}$$

From (2.52) and (5.2) we obtain

$$d\frac{1}{\Lambda^4} = \frac{3}{2\Upsilon}\frac{\hat{v}^2\, d\hat{v}}{(\frac{1}{4}\Lambda_d^4 1.5994\epsilon/v_0^3)^{1/2}} \tag{6.3}$$

where

$$\hat{v} = v/v_0 \tag{6.4}$$

and

$$\Upsilon = (\hat{v}^3 + C - 1)^{1/2} \tag{6.5}$$

Substituting (6.3)–(6.5) into (6.2) gives

$$d\frac{K}{\bar{\epsilon}^{1/2}} = 1.7288 v_0^{1/2}\frac{\hat{v}\, d\hat{v}}{\Upsilon} \tag{6.6}$$

The differential relation (6.6) expresses the total viscosity v in terms of the kinetic energy K and the mean dissipation rate ϵ. When $v/v_0 \gg 1$, the solution to (6.6) is identical to the algebraic model (5.4).

The low Reynolds number modification of the equation for the mean dissipation rate $\bar{\epsilon}$ can be written as

$$\frac{D\bar{\epsilon}}{Dt} = P - \bar{a} + \bar{b} + \frac{\partial}{\partial x_i}\alpha_\epsilon v \frac{\partial \bar{\epsilon}}{\partial x_i} \tag{6.7}$$

where the functions P, $\bar{a}$, and $\bar{b}$ are derived from the following relations

$$P = 0.08889\frac{K}{v}\bar{\epsilon}_{ij}\frac{\partial v_i}{\partial x_j} \tag{6.8}$$

and

$$d\frac{\bar{a}}{\bar{\epsilon}^{3/2}} = -0.8267\frac{\hat{v}^3\, d\hat{v}}{v_0^{1/2}\Upsilon^3} \tag{6.9}$$

$$d\frac{\bar{b}}{\bar{\epsilon}^{3/2}} = -0.5764\frac{d\hat{v}}{v_0^{1/2}\Upsilon} \tag{6.10}$$

Equation (6.8) is a direct consequence of expressions (5.14) and (5.4). The differential relations (6.9) and (6.10) can be obtained readily from (5.78)–(5.79) using the procedure (6.1)–(6.6). Detailed derivations and applications of this differential model will be published elsewhere.

7. DISCUSSION

The RNG method developed here is based on a number of ideas. First, there is the *correspondence principle*, which can be stated as follows. A turbulent fluid characterized in the inertial range by scaling laws can be described *in this inertial range* by a corresponding Navier–Stokes equation in which a random force generates velocity fluctuations that obey the scaling of the inertial range of the original unforced system. The dynamical equation with the random force is the basis for the systematic elimination of small scales and calculation of the renormalized transport coefficients.

Second, the RNG procedure is, strictly speaking, valid only in the asymptotic limits of $\hat{k} \to 0$ and $R \to \infty$ in which the scaling relations are

derived in the vicinity of the fixed point. What are the limits of validity of the RNG procedure? It is known from experimental data that the properties of turbulent fluids are approximately independent of the width of the inertial range if the Reynolds number is large enough. We believe that the *results of the RNG* fixed point calculations can be aplied to any fluid that demonstrates Kolmogorov-like scale-invariant behavior in some range of the wavevectors and frequencies. This situation resembles the theory of critical phenomena in the sense that the critical exponents computed at the fixed point are approximately valid in the vicinity of the critical point when $|(T - T_c)/T_c| \ll 1$ (where T_c is the critical temperature).

The major drawback of the theory presented here is that, according to (2.45), the higher nonlinearities generated by the RNG procedure are marginal, i.e., they do not exponentially go to zero when the iteration *parameter* $r \to \epsilon$. As discussed in Section 2, we can hope that these terms produce small logarithmic corrections to the results derived here. It is interesting that the same kind of problem arises in the derivation of the hydrodynamic equations from molecular dynamics by the small-scale elimination procedure. It is well known (Dorfman, 1975; Wood, 1975) that the so-called super-Burnett coefficients, which are neglected in the Navier-Stokes equation, are weakly divergent, while the molecular viscosity computed in terms of time-correlation functions is finite. These weakly divergent coefficients are not known to upset the results of classical hydrodynamics based on the Navier-Stokes equation. We can hope that the marginality of the nonlinear terms generated by the RNG method are unimportant. Of course, this hope does not have a solid theoretical basis, so the value of the RNG method should perhaps best be judged by comparison of its predictions with experiments.

The magnitude of the Kolmogorov constant calculated here, $C_K = 1.617$, agrees with experimental data. However, measurements of C_K do not allow an unambiguous interpretation of experimental data. The most widely accepted value for C_K is $C_K \approx 1.4$–1.7. Similarly, the value of the turbulent Prandtl number derived here, $P_t = 0.7179$, is close to $P_t = 0.7$–0.9 accepted in the engineering literature (Landau and Lifshitz, 1982; Monin and Yaglom, 1975).

The RNG calculation for the skewness factor S_3 gives $\bar{S}_3 = 0.4878$. Experimental data on $\bar{S}_3$ are quite scattered. Frenkiel *et al.* (1979) reported $\bar{S}_3 = 0.47$–0.48 and $\bar{S}_3 = 0.41$–0.44 measured in water and wind tunnels, respectively. The measurements of Antonia *et al.* (1984) in a plane jet showed $\bar{S}_3 = 0.43$. It must be mentioned, however, that the masurements of Wyngaard and Tennekes (1970) in an atmospheric boundary layer showed that, as the Reynolds number increased, the skewness factor $\bar{S}_3$ grew from $\bar{S}_3 \approx 0.6$ to $\bar{S}_3 \approx 1$. It is possible that the Reynolds number dependence is due to large-scale anisotropy effects, which are quite strong in the planetary boundary layer measurements. The role of the anisotropy on measurements of $\bar{S}_3$ has been discussed by Antonia *et al.* (1984).

The RNG derivation of the transport model given in Section 5 deserves more discussion. *The RNG procedure is based on the elimination of* small scales, which are assumed to be isotropic. The fact that such a grossly simplified picture of turbulence leads to a K-$\bar{\epsilon}$ model with $\nu = \nu_t K^2/\bar{\epsilon}$, $c_\nu = 0.0837$, and the von Karman constant $K = 0.372$ deserves comment. Two basic questions that may be asked are: First, why does turbulence modeling based on oversimplified models give reasonable results? Second, why is it widely found in the engineering literature that more sophisticated schemes, such as third-order closure models, do not lead to substantial improvement over existing K-$\bar{\epsilon}$ models? The second question may be *understood on the basis of the present theory. Higher-order nonlinear contributions* are asymptotically unimportant and lead to small corrections to the results based on the second-order closures.

The first question is much more difficult to answer. Existing schemes do not take into account the strongly anisotropic eddies that dominate the wall layer. It is well known from experimental data and direct numerical simulations that the turbulent energy distribution in a channel flow has a pronounced maximum very close to the wall, namely at $y_+ \approx 13$–18. In this region, the turbulent viscosity, defined as $\nu_t = \overline{v_x v_y}/(\partial \bar{v}_x/\partial y)$, is very small. On the other hand, far from the wall, the turbulent intensity is much lower, but the turbulent viscosity is $\nu_t \approx 0.008 R_*$, which is many orders of magnitude larger than molecular viscosity. The inevitable conclusion is that not all turbulent eddies interact with mean flow and, consequently, not all eddies contribute to turbulent viscosity. The same effect is found in studies of the relaminarization of turbulent channel flow in a strong magnetic field. It can be shown that, if the magnetic field is large enough, turbulent channel flow becomes strongly anisotropic and the velocity profile and the friction coefficient approach those of laminar flow. The total turbulent intensity, however, remains quite high. It seems that strongly anisotropic scales may not interact with the mean flow.

The interaction of small-scale flows with large-scale perturbations has been studied analytically by Sivashinsky and Yakhot (1985), Yakhot and Sivashinsky (1986), and Bayly and Yakhot (1986). It has been shown that if the small-scale flow is sufficiently anisotropic, it either decouples from the large-scale flow or gives its energy to the large eddies. Only when small scales are sufficiently isotropic do they increase the dissipation of large scales and thus give rise to a positive turbulent viscosity. The wall region of the channel or pipe flow is dominated by strongly anisotropic structures (streaks) which do not interact directly with the mean flow and thus do not

contribute to turbulent viscosity. Thus, it is possible for the maximum of turbulent kinetic energy to be located where the turbulent viscosity is close to zero. The weak coupling of strongly anisotropic scales to the mean motion may be the reason for the success of turbulence modeling based on the elimination of isotropic eddies from the inertial range dynamics and for the apparent success of RNG methods for turbulence.

REFERENCES

Antonia, R A, Chambers, A J, and Anselmet F (1984) *Phys Chem Hydrodyn* 5, 368
Batchelor G (1959) *J Fluid Mech* 5, 113
Bayly B, and Yakhot V (1986) *Phys Rev A* in press
Deardorff J W (1970) *J Fluid Mech* 41, 453
Deardorff J W (1971) *J Comp Phys* 7, 120
De Dominicis C and Martin P C (1979) *Phys Rev A* 19, 419
Dashen R (1975) In Cohen E G D (ed) *Fundamental Problems in Statistical Mechanics*, North Holland, Amsterdam
Forster D, Nelson D, and Stephen M (1977) *Phys Rev A* 16, 732
Fournier J P and Frisch U (1978) *Phys Rev A* 17, 747
Fournier J P and Frisch U (1983) *Phys Rev A* 28, 1000
Frenkiel F N, Klebanoff, P, and Huang T T (1979) *Phys Fluids* 22, 1606
Hanjalic K and Launder, B E (1972) *J Fluid Mech* 52, 609
Herring J R, Orszag, S A, Kraichnan R H, and Fox D G (1974) *J Fluid Mech* 66, 417
Hohenberg P C and Halperin B I (1977) *Rev Mod Phys* 49, 435
Kolmogorov A N (1941) *Dokl Akad Nauk SSSR* 30, 299
Kraichnan R H (1959) *J Fluid Mech* 5, 497
Kraichnan R H (1961) *J Math Phys* 2, 124
Kraichnan R H (1971) *J Fluid Mech* 47, 525
Landau L, and Lifshitz, E M (1982) *Fluid Mechanics*, Pergamon, New York
Launder, B E and Spalding D B (1972) *Mathematical Models of Turbulence*, Academic Press, New York
Launder B E, Reece G J, and Rodi, W (1975) *J Fluid Mech* 68, 537
Leslie D C (1973) *Developments in the Theory of Turbulence* Clarendon Press, Oxford
Ma S K and Mazenko G (1975) *Phys Rev B* 11, 4077
Moin P and Kim J (1982) *J Fluid Mech* 118, 341

Monin, A S, and Yaglom, A M (1975) *Statistical Fluid Mechanics*, Vol 2, MIT Press Cambridge, Massachusetts
Orszag, S, and Patera, A (1981) *Phys Rev Lett* 47, 832
Pao, Y H (1965) *Phys Fluids* 8, 1063
Pao, Y H (1968) *Phys Fluids* 11, 1371
Reynolds, W C (1976) *Ann Rev Fluid Mech* 8, 183
Sivashinsky, G, and Yakhot, V (1985) *Phys Fluids* 28, 1040
Smagorinsky, J (1963) *Monthly Weather Rev* 91, 99
Tennekes, H, and Lumley, J L (1972) *A First Course in Turbulence*, MIT Press Cambridge Massachusetts
Wilson, K G (1971) *Phys Rev B* 4, 3174
Wilson, K G, and Kogut J (1974) *Phys Rep* 12C, 77
Wood, W W (1975) In Cohen, E G D (ed), *Fundamental Problems in Statistical Mechanics* North Holland, Amsterdam
Wyld, H W (1961) *Ann Phys* 14, 143
Wyngaard, J C, and Tennekes, H (1970) *Phys Fluids* 13, 1962
Yakhot, V (1981) *Phys Rev A* 23, 1486
Yakhot, V, and Sivashinsky, G (1986) *Phys Rev A*, submitted

Printed by the St Catherine Press Ltd, Tempelhof 41, Bruges, Belgium

END

11-87

DTIC